Eindhoven University of Technology

MASTER

Controlled evaporation and condensation of liquids

Vernooij, J.

Award date:
2020

TECHNICAL UNIVERSITY EINDHOVEN

MASTER THESIS

Controlled evaporation and condensation of liquids

Author:
J. Vernooij

Supervisor:
ir. V. Murali
prof. dr. A.A. Darhuber

R-2040-A

*A thesis submitted in fulfillment of the requirements
for the degree of Master of science*

in the group

Fluids and Flows

November 16, 2020

ii

TECHNICAL UNIVERSITY EINDHOVEN

Abstract

This report investigates the influence of several parameters on the process of inkjet printing, with the focus on the occurring of condensation at unwanted places. To investigate this, the influence of the temperature difference between evaporating liquid and its surroundings is measured. Also measured is the influence of the distance between evaporating liquid and place of condensation, as well as for the gas flow velocity, which is used to transfer solvent vapor out of the system before it condenses. For these parameters the focus is on the two liquids, ethylene glycol and toluene.

At first the trajectory of the jetted droplet is calculated in order to establish the influence of the gas flow on the displacement of the droplet when it lands, in respect to the position where it was jetted. Larger distances, or smaller droplets are causes for large displacements of the droplet, which could indicate in accuracy of the printed droplet. A higher gas flow velocity could also result in large displacements.

Secondly a way of tracking condensation is investigated. The measuring of condensation, using light interference techniques works on a experimental setup without external gas flow. However data does not immediately seem to match with the simulation. Relations between the temperature difference and rate of condsation, as well as relations between distance in-between the liquid and place of condensation and the condensation rate are made, which seem to be correct in the simulations.

Next, the place of condensation is determined by tracking the distance between the start of the liquid and the point of transition between non-condensation and condensation. This transition point depends on the earlier mentioned variables such as temperature, distance and gas flow and almost perfectly agrees with analytical theory in case of the two dimensional models. The experimental setup, now with external air flow turns out to give a lot of difficulties regarding temperature and gas flow consistency. Due to these difficulties, only the influence of the gas flow velocity is investigated in the experimental setup. Although the results of the model and the experiment are different, they both give a clear linear relation between the transition point and the gas flow velocity, with agrees which the theory.

Last, the influence of the gas flow on the liquid layer height was investigated in order to prevent liquid being moved before it evaporates, which is unwanted as it causes inaccuracies in the printed structure. Relations between the normalized volume of moved liquid by the gas flow and the Vernooij number were found. The Vernooij number is defined as a dimensionless number which presents the ratio between the gas flow velocity and the evaporation rate of the liquid layer.

Acknowledgements

Contents

List of Figures

List of Tables

List of Abbreviations

CR	Condensation Rate
EG	Ethylene Glycol
RH	Relative Humidity
Tol	Toluene
TP	Transition Point

Physical Constants

Gravitational acceleration	$g = 9.806\,65\,\text{m} \cdot \text{s}^{-2}$
Universal gas constant	$R_u = 8.314\,462\,618\,153\,24\,\text{J} \cdot \text{K}^{-1} \cdot \text{mol}^{-1}$
Ambient Pressure	$p_{amb} = 100\,000\,\text{Pa}$
Ambient Temperature	$T_{amb} = 298.15\,\text{K}$

List of Symbols

β	Coefficient of volume expansion	K^{-1}
γ	Surface tension	$N \cdot m^{-1}$
μ	Dynamic viscosity	$kg \cdot m^{-1} \cdot s^{-1}$
ρ	Density	$kg \cdot m^{-3}$
$\underline{\underline{\sigma}}$	Stress tensor	Pa
$\underline{\underline{\tau}}$	Viscous stress tensor	Pa
c	Concentration	$mol \cdot m^{-3}$
C_p	Heat capacity	$J \cdot kg^{-1} K^{-1}$
D	Diffusion coefficient	$m^2 \cdot s^{-1}$
d	Droplet displacement	m
H	Height printhead / distance between evaporating liquid and place of condensation / height channel	m
h_n	Heat transfer coefficient	$W \cdot m^{-2} \cdot K^{-1}$
h	Liquid layer height	m
k	Thermal difussivity	$J \cdot s^{-1} \cdot m^{-1} \cdot K^{-1}$
L	Latent heat of vaporization	$J \cdot kg^{-1}$
L_c	Entrance length concentration	m
L_{char}	Characteristic length	m
M	Molar Mass	$kg \cdot mol^{-1}$
$\vec{n}$	Normal vector of a boundary/interface	1
p	Pressure	Pa
$\mathcal{R}$	Reaction rate	$mol \cdot m^{-3}$
R_e	Reynolds number	1
R_s	Specific gas constant	$J \cdot kg^{-1} \cdot K^{-1}$
T	Temperature	K
$\vec{u}$	Velocity field	$m \cdot s^{-1}$
$\vec{u}_{Jet,0}$	Jet velocity	$m \cdot s^{-1}$
U_{max}	Maximum velocity of the flow profile	$m \cdot s^{-1}$
$Vernooij$	Vernooij number	1

Chapter 1

Introduction

1.1 Süss MicroTec SE

The idea for the project originally came from the company Süss MicroTec SE, formerly Meyer Burger, in Eindhoven. This company manufactures equipment for industrial inkjet printing of functional materials.

1.2 Problem

The origin of the project lies in an issue encountered by the inkjet printer at Süss MicroTec SE. Inkjet printing uses small droplets mainly composed of an organic solvent. After the droplet is placed at the right position, the solvent evaporates, leaving the dissolved functional material. These left functional material often create structures of sizes around $20\mu m$. The average volume of a droplet printed lies in the region of $6pL$. When printing at high speeds, high volume and longer times, considerable quantities of solvent need to evaporate. In that case the evaporated solvent will start to condense in colder places. These droplets can then fall on the substrate and cause unwanted defects. This has to be prevented and thus the air with the evaporated solvent has to be taken away before the evaporated solvent has the change to condense in places where it is unwanted. For this a dry air flow is used. The velocity of this air flow can not be too high, as it might distort the printed features, whereas a too low velocity will not get rid the solvent vapor quickly enough. Other factors do also play a role, such as the distance between the liquid and the place of condensation, temperature differences and liquid properties. All of these are to be investigated to determine how to prevent unwanted condensation.

1.3 Research

In order to investigate the problem, numerical simulations were done and also experiments. Both experiment consist of at least two situations. One is a more simple approach, consisting of measuring the condendsation on a glass plate that is placed on a beaker with heated liquid. In the other one an air flow is added to remove the liquid vapor and to control the temperature of possible condensation locations. For the simulations, there are 3 other areas of investigation. One is the influence of several parameters of the trajectory and eventual landing spot of the jetted droplet. A second simulation is there to make sure that a certain temperature is really uniform after a certain time of heating up a liquid. This in order to prevent inaccuracies when comparing models to experiments. A last simulation is designed to investigate the influence of a gas flow on the layer height of the liquid due to viscous stress. A printed droplet can not be moved by the gas flow in the time between landing and

the solvent being fully evaporated. Therefore a model was designed to investigate the influence of either the evaporation and the gas flow velocity on this matter.

Chapter 2

Theory

2.1 Vapor transport by convection and diffusion

In order to describe the diffusion of a certain species through a media, the convection-diffusion equation is used (Socolofsky and Jirka, 2004),

$$\frac{\partial c}{\partial t} = \nabla \cdot (D \nabla c) - \nabla \cdot (\vec{u} c) + \mathcal{R} \tag{2.1}$$

With c being the concentration of the species, D the diffusion coefficient, $\vec{u}$ the velocity and $\mathcal{R}$ the reaction rate.

2.1.1 Evaporation flux

For this report, diffusion limited evaporation is assumed (Popov, 2005) . To describe the evaporation flux in a diffusion limited evaporation system, it is desired to look at the concentration that flow's away (or towards in case of condensation) the liquid-gas interface. Looking from the point of the interface, the evaporation flux can be described by Fick's Law,

$$J = -D \nabla c \cdot \hat{n}, \tag{2.2}$$

with D the diffusion coefficient and c the concentration.

2.1.2 Diffusion Coefficient

The diffusion coefficient of a liquid vapor in air is not constant. The temperature dependence can play a big role, as the liquid molecules tend to have more motion when experiencing higher temperatures. This temperature dependence can be given by

$$D(T) = D_{T_{ref}} \left(\frac{T}{T_{ref}} \right)^{1.5} \tag{2.3}$$

(Chen et al., 2018) (Carle et al., 2016)

2.1.3 Latent heat of vaporization

When a liquid changes state to a gas, this costs heat. This heat is called the latent heat of vaporization (Persaud, 2005). The same heat that is lost when evaporating, is gained when vapor condenses to a liquid. The heat flux, due to the loss of win of latent heat is then given by

$$q_{vap} = L \cdot \dot{m} \tag{2.4}$$

, with L the heat of vaporization $\left[\frac{J}{kg}\right]$ and $\cdot m$ the mass flux of the evaporating or condensing liquid or vapor per unit area $\left[\frac{kg}{sm^2}\right]$.

2.2 Heat transfer equation

To describe the heat transfer in a system, a modified version of the energy balance equation is used (Welty et al., 2008),

$$\rho C_p \frac{\partial T}{\partial t} + \rho C_p \vec{u} \cdot \nabla T + \nabla \cdot \vec{q} = Q \tag{2.5}$$

with

$$\vec{q} = -k\nabla T. \tag{2.6}$$

Here ρ is the density, C_p the heat capacity at constant pressure, T the temperature, $\vec{u}$ the velocity field, Q a collection term of all the heat sources and k the thermal conductivity.

2.2.1 Temperature continuity

At a boundary between two different solids, liquids and gases, without any heat sources or sinks, a temperature continuity is in place. This means that neither the temperature, nor the heat flux can make a jump at the boundary. For two substances, for now called 1 and 2, at the interface the following has to hold,

$$T_1|_{interface} = T_2|_{interface} \tag{2.7}$$

$$k_1 \nabla T_1|_{interface} = k_2 \nabla T_2|_{interface} \tag{2.8}$$

2.2.2 Newton's law of cooling

A specific way of describing the heat loss or gain of a system is Newton's law of cooling. This law states that the rate of heat loss is directly proportional to the temperature difference between the system and its surroundings (Bergman et al., 2007). This then translates into the equation

$$\vec{q} = -h_n(T_{surface} - T_{sur}) \tag{2.9}$$

, with $\vec{q}$ the heat flux, h_n the heat transfer coefficient, $T_{surface}$ the temperature of a surface or boundary and T_{sur} the temperature of the surroundings. The heat transfer coefficient h_n can be different for different kind of heat losses, for example, the value for free convection will be lower than the one for forced convection with high velocities, as that transfers heat away or to the system much faster.

2.2.3 Evaporation or condensation

In the case of condensation or condensation temperature continuity is not the case. As shown in section 2.1.3, evaporation costs heat, whereas condensation produces heat. This heats disturbs the continuity in the heat flux given in equation 2.8. This will then become

$$(k_1 \nabla T_1|_{interface} - k_2 \nabla T_2|_{interface}) - q_{vap} = 0 \tag{2.10}$$

, with q_{vap} the heat flux from equation 2.4. Note that the sign changes when talking about either evaporation or condensation.

2.3 Navier-Stokes

2.4 Compressible Flow

The compressible flow is defined by the Navier Stokes equation, which is a specific form of the Cauchy momentum equation, which describes the conservation of momentum in any continuum (D.J.Acheson, 1990):

$$\frac{D\vec{u}}{Dt} = \frac{1}{\rho}\nabla \cdot \underline{\underline{\sigma}} + \vec{F} \tag{2.11}$$

with $\vec{u}[m/s]$ the flow velocity, $t[s]$ the time, $\rho[kg/m^3]$ the density, $\underline{\underline{\sigma}}[Pa]$ the stress tensor and $\vec{F}[m/s^2]$ the acceleration due to body forces. $\underline{\underline{\sigma}}$ is composed of a viscous part and a pressure part,

$$\rho\frac{D\vec{u}}{Dt} = -\nabla p + \nabla \cdot \underline{\underline{\tau}} + \vec{F} \tag{2.12}$$

With p the pressure, $\underline{\underline{\tau}}$ the stress tensor and F the force per unit volume. The viscous part of the stress tensor is described as (G.K.Batchelor, 1967):

$$\underline{\underline{\tau}} = \mu(\nabla\vec{u} + (\nabla\vec{u})^T) - \frac{2}{3}\mu(\nabla \cdot \vec{u})\underline{\underline{I}} \tag{2.13}$$

, with μ the dynamic viscosity. Eventually, combining equation 2.12 and 2.13 will give the following result for the Navier-Stokes equation for a compressible liquid:

$$\rho\frac{\partial\vec{u}}{\partial t} + \rho(\vec{u} \cdot \nabla)\vec{u} = \nabla \cdot \left[-p\vec{I} + \mu(\nabla\vec{u} + (\nabla\vec{u})^T) - \frac{2}{3}\mu(\nabla \cdot \vec{u})\underline{\underline{I}} \right] + \vec{F} \tag{2.14}$$

and

$$\frac{\partial\rho}{\partial t} + \nabla \cdot (\rho\vec{u}) = 0. \tag{2.15}$$

2.4.1 Incompressible flow

An incompressible flow means that the liquid is not compressed, resulting in a uniform density, (G.K.Batchelor, 1967)

$$\frac{1}{\rho}\nabla p = \nabla\frac{p}{\rho}, \tag{2.16}$$

and also

$$\nabla \cdot \vec{u} = 0 \tag{2.17}$$

This then results in the following form of the Navier-Stokes equation (G.K.Batchelor, 1967)

$$\frac{\partial\vec{u}}{\partial t} + (\vec{u} \cdot \nabla)\vec{u} - \frac{\mu}{\rho}\nabla^2\vec{u} = -\nabla\frac{p}{\rho} + \vec{g}, \tag{2.18}$$

with $\vec{g}$ the gravitational acceleration.

2.4.2 Marangoni flow

At the interface between two liquid, or a gas and a liquid, the surface tension does not have to be uniform. A non-uniform surface tension can be the result of temperature differences. A non-uniform surface tension induces a discontinuity in the shear stress on that interface. This discontinuity in the shear stress can result in a surface tension driven flow, which is called a Marangoni flow (Darhuber, 2017a). Given an interface in the x-direction, this discontinuity at an interface between a liquid and a gas is given by (the z direction is perpendicular to the interface direction)

$$\left(\mu_{gas}\frac{\partial u_{x,gas}}{\partial z} - \mu_{liq}\frac{\partial u_{x,liq}}{\partial z}\right) + \frac{\partial\gamma}{\partial x} = 0 \tag{2.19}$$

, with γ the surface tension of the liquid-gas interface. s

2.5 Partial pressure

The partial pressure of a gas is the pressure of a component of a gas mixture, if that component would be the only gas in the volume occupied by the mixture. The total pressure of the mixture is then determined by Dalton's law (Dalton, 1802),

$$p_{total} = \sum_{i=1}^{n} p_i \tag{2.20}$$

for n different components in the gas mixture. An important note is that Dalton's law only accounts for non-reacting gases in a mixture.

2.5.1 Saturated vapor pressure

The partial pressure of vapor that is a part of a gas mixture, is also called the vapor pressure. This value is obtained when the vapor is in thermal equilibrium with its condensed phase, meaning that if the partial pressure of a vapor is at the saturated vapor pressure, an equal amount of liquid is evaporating and condensing. The value for this saturated vapor pressure is temperature and composition dependent. This temperature relation can be described by the Antoine equation (Antoine, 1888),

$$log_{10}p = A - \frac{B}{C+T}, \tag{2.21}$$

with p the saturated vapor pressure and T the temperature of the vapor. Depending on the source of the Antoine coefficients A, B and C, equation 2.21 can be adjusted to fit the units of the pressure and the temperature. The source of this report (Yaws, 2015) uses $mmHg$ as unit for the pressure and *Celsius* for the temperature. This alters equation 2.21 to

$$log_{10}(\frac{p}{133.322}) = A - \frac{B}{C+(T-273.15)}, \tag{2.22}$$

with p, the pressure in Pa and the Temperature in K.

2.6 Ideal gas law

The ideal gas law can be written as,

$$pV = nR_uT, \tag{2.23}$$

with p the pressure of the gas, V the volume, n the amount of mole of gas, R_u the universal gas constant and T the temperature. The equation can also be rewritten into an equation with the density and the specific gas constant of a certain gas,

$$p = \rho R_s T, \tag{2.24}$$

with ρ the density of the gas and R_s the specific gas constant of the gas. Further more, the ideal gas law also holds for each component of a mixture of ideal gases. In that case equation 2.24 becomes

$$p_i = \rho_i R_s T, \tag{2.25}$$

with p_i and ρ_i the partial pressure and the density of that mixture component alone.

2.7 Condensation

In order to establish condensation, the concentration a liquid in the air has to be higher than the saturated concentration for that temperature. This concentration is directly correlated with the saturated vapor pressure from equation 2.21. From this equation, in combination with equation 2.23 gives a relation between the saturated concentration and the saturated vapor pressure.

$$c_{sat} = \frac{p_{sat}}{R_u T} \left[\frac{mol}{m^3} \right] \tag{2.26}$$

At this value of the concentration, an equal amount of liquid is evaporating, as it is condensing. Higher concentrations mean that there is a surplus of concentration, resulting is more condensation, which equals a net condensation rate. Note that the saturated concentration is temperature dependent, meaning that cooling down, without adding any liquid vapor, can also lead to condensation, even though the concentration stays equal. This is because the 'critical' concentration is getting lower. A higher vapor concentration in the gas phase would also mean the concentration could go over the saturation limit, meaning condensation could happen.

2.7.1 Fog formation

Condensation is happening when the concentration is higher than its saturated concentration. However, this is true for a vapor in contact with a (mostly colder) surface. Eventually there is then also a liquid layer present on the surface, to make sure that the balance between condensation and evaporation can be kept. However, mid air, there can also be a surplus of vapor. This can be because of a non-isothermal gas, or a high concentration gradient. It can be possible to form fog then, however, to form fog, small particles, nuclei, have to be in the air for the vapor to condens on. Simulation wise the fog formation is left out of the picture, as in the experiments this fog formation did not seem to be happening significantly.

2.8   Entrance Length, transition point

The entrance lenght of a flow-driven system describes the distance it takes for a certain fixed boundary conditions, to develop throughout the whole . For instance a flow through a channel where both sides have the same temperature, different from the temperature of the flow at the entrance of the channel. A few units of length into the channel, the temperature at the centre of the channel will be close to the termpature at the sides of the channel. This distance is then called the entrance length. The same can be done with concentration, where the incoming flow has zero concentration of a certain vapor. On both sides this vapor is evaporating in to the gas flow. Somewhere along the flow this vapor concentration will also reach the centre of the gas flow. Figure 2.1 shows such a channel with its set concentration values at the top and bottom boundary. For the experiments done in this report, only half of the domain is actually used, as there is only liquid on the bottom boundary. However, if gravity is neglected, figure 2.1 is symmetrical and can thus be used to calculate an estimate of the entrance length.
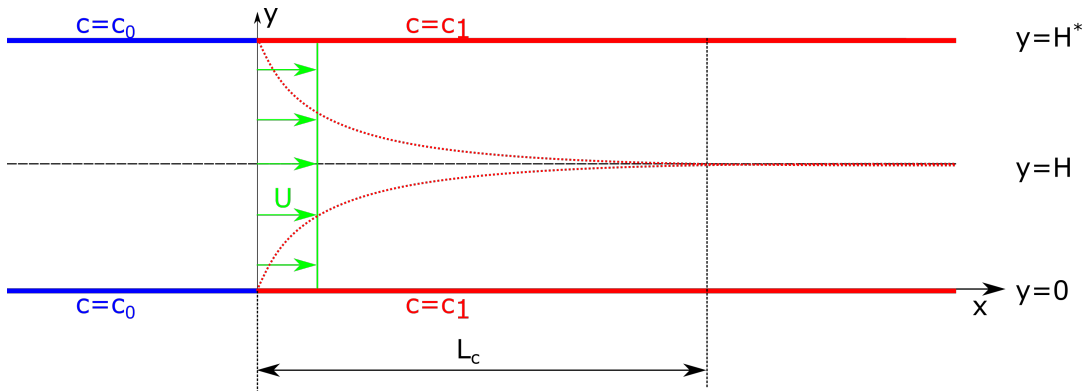
FIGURE 2.1: Entrance length L_c of the concentration in a channel, with H^* being the height of the channel. The dotted lines represent the development of the vapor concentration rich layer.

$x = L_c$ is defined as the point where there is enough concentration at $y = H$ to condense. Note that in this derivation, a two-sided system is used, with concentration constraints at both sides. Later on in the report, the channel used is only half the height, meaning there is a layer with a bottom boundary set with a concentration constraint. The top boundary will then be the line at $y = H$, which is exactly at half the height of the channel in this derivation. If a steady state is assumed, without any reactions and a constant diffusion coefficient, equation 2.1 simplifies to

$$D\nabla^2 c = \nabla \cdot (\vec{u}c) \tag{2.27}$$

If a uniform flow in the x direction is assumed, $\vec{u} = (U, 0)$, equation 2.27 can be written as

$$D\left(\frac{\partial^2 c}{\partial x^2} + \frac{\partial^2 c}{\partial y^2}\right) = U\frac{\partial c}{\partial x} \tag{2.28}$$

A dimensionless variable is introduced for the concentration,

$$\theta = \frac{c - c_1}{c_0 - c_1}. \tag{2.29}$$

This variable θ describes how much the concentration relatively differs from the end-concentration c_1. So

$$\begin{aligned} \theta(x < 0) &= 1 \\ \theta(x > 0, y = 0 \text{ or } y = H^*) &= 0 \end{aligned} \tag{2.30}$$

Equation 2.28 can then be written as

$$D\left(\frac{\partial^2\theta}{\partial x^2} + \frac{\partial^2\theta}{\partial y^2}\right) = U\frac{\partial\theta}{\partial x} \tag{2.31}$$

It is assumed that the main way of concentration transport in the flow direction is convective, meaning the $L_c \gg H^*$. To find the point where condensation starts, an estimation is made for the terms in 2.31.

$$\begin{aligned} \frac{\partial^2\theta}{\partial x^2} &\sim \frac{1}{L_c{}^2} \\ \frac{\partial^2\theta}{\partial y^2} &\sim \frac{1}{H^{*2}} \\ \frac{\partial\theta}{\partial x} &\sim \frac{1}{L_c} \end{aligned} \tag{2.32}$$

Given that $L_c \gg H^*$, this reduces to

$$L_c \sim \frac{UH^{*2}}{D} \sim \frac{UH^2}{D} \tag{2.33}$$

Note that $H^* = 2H$.

Next is the temperature dependency. For this, several temperature dependent factors will be neglected, like the diffusion coefficient dependency of the temperature, difference in inflow temperature and the heating up of the flow in the channel. The temperature is only used to estimate the saturated concentration and therefore define θ from equation 2.35. It will turn out that this estimation is sufficient and gives a general idea of how the temperature influences the entrance length. To say something about the temperature influences the entrance length, equation 2.31 is used. Assuming $L_c \gg H^*$, it can be said that $\frac{\partial^2\theta}{\partial x^2} \ll \frac{\partial^2\theta}{\partial y^2}$ due to the fact that diffusion in the flow direction is neglected. This means that equation 2.31 reduces to

$$D\frac{\partial^2\theta}{\partial y^2} = U\frac{\partial\theta}{\partial x} \tag{2.34}$$

A solution for this is (Darhuber, 2012)

$$\theta(x, y) = \frac{4}{\pi}\sin\left(\pi\frac{y}{2H}\right)\exp\left(-\pi^2\frac{1}{Pe_H 4H}x\right), \tag{2.35}$$

with the Peclet number

$$Pe_H = \frac{UH}{D}. \tag{2.36}$$

In order to find where the condensation starts, the definition of the $x = L_c$ and $y = H$ is defined by θ. Equation 2.29 gives the general value for θ, assuming the flow does not contain any solvent vapor, i.e. $c_0 = 0$. c_1 is defined by the temperature of the bottom, because that determines the saturated vapor concentration of the bottom

part of the channel, as shown in equation 2.26. The same goes for the top boundary of the real experiment (so $y = H$, and not $y = H^*$). With all this, equation 2.35 becomes

$$\frac{c_{Sat}(T_{y=H}) - c_{Sat}(T_{y=0})}{-c_{Sat}(T_{y=0})} = \frac{4}{\pi} \exp \left(\frac{-\pi^2}{4} \frac{1}{HPe_H} L_c \right). \tag{2.37}$$

Rewriting this gives

$$L_c = -\frac{4}{\pi^2} HPe_H \cdot \ln \left(\frac{\pi}{4} \frac{cSat(T_{y=H}) - cSat(T_{y=0})}{-cSat(T_{y=0})} \right) \tag{2.38}$$

2.9   Density

2.9.1   Density in incompressible flow

To couple the concentration of the vapor evaporated into a gas, the Temperature and its density, a combination of the ideal gas law and Dalton's Law is used. The total density of a gas mixture can be derived by adding the densities of the individual mixture components,

$$\rho_{total} = \sum_{i=1}^{n} \rho_i, \tag{2.39}$$

for n different components. In the case of one liquid evaporating into dry air, this simplifies to

$$\rho_{gas} = \rho_{air} + \rho_{vap}. \tag{2.40}$$

ρ_{air} can then be derived from equation 2.24,

$$\rho_{air} = \frac{p_{air}}{R_{air}T}, \tag{2.41}$$

with p_{air} the partial pressure of the dry air and R_{air} the specific gas constant of the dry air. The same can be done for the density of the solvent vapor, which concludes to

$$\rho_{vap} = \frac{p_{vap}}{R_{vap}T}. \tag{2.42}$$

For the next step, equation 2.23 is used in the following form,

$$p = \frac{n}{V} R_u T = c R_u T, \tag{2.43}$$

with c the concentration of the liquid vapor in the gas in $\frac{mol}{m^3}$. This means the partial pressure of the liquid vapor can be described as

$$p_{vap} = c_{vap} R_u T. \tag{2.44}$$

Dalton's Law 2.20 stated that the total pressure of the gas is equal to the sum of the partial pressures. This means that the partial pressure of the dry air can be described by

$$p_{air} = p_{gas} - p_{vap} = p_{gas} - c_{vap} R_u T \tag{2.45}$$

This leaves the density of the gas mixture to

$$\rho_{gas} = \frac{p_{gas} - c_{vap} R_u T}{R_{air}T} + \frac{c_{vap} R_u T}{R_{vap}T} = \frac{p_{gas}}{R_{air}T} + c_{vap} R_u \left(\frac{1}{R_{vap}} - \frac{1}{R_{air}} \right) \tag{2.46}$$

2.9.2   Density in compressible flow

In a compressible flow, the density is a variable that is solved for. Therefore, equation 2.46 can not be used to couple the liquid vapor concentration with the density of a gas. Another way to do this is to couple it via the specific gas constant of the gas. The value of the concentration can be given by

$$c = \frac{p}{R_u T} \tag{2.47}$$

The value of the specific gas constant of any gas can be calculated by,

$$R_s = \frac{R_u}{\overline{M}} [J \cdot K^{-1} \cdot kg^{-1}] \tag{2.48}$$

with $\overline{M}$ begin the mean molar mass of the mixture. This can then be expressed by

$$\overline{M} = \sum \chi_i M_i, \tag{2.49}$$

with χ_i the molar fraction of a mixture component and M_i the molar weight of the mixture component.

$$p = p_{air} + p_{vap} \tag{2.50}$$

$$c_{gas} = c_{air} + c_{vap} \tag{2.51}$$

p_{air} and p_{vap} are the partial pressures of respectively the air and the vapor. In order to calculate the mass fraction, the following equation is used,

$$\chi_i = \frac{c_i}{c_{total}} = \frac{c_i}{c_{gas}} = \frac{c_i}{c_{air} + c_{vap}}. \tag{2.52}$$

The concentration of the air will be calculated by the ideal gas law, saying

$$c_{air} = \frac{p_{vap}}{R_u T}, \tag{2.53}$$

with R_u the universal gas constant of and T the temperature. With equation 2.50, this can be rewritten to

$$c_{air} = \frac{p - p_{vap}}{R_u T}. \tag{2.54}$$

p_{vap} can then again be rewritten with the ideal gas law, to

$$p_{vap} = c_{vap} R_u T \tag{2.55}$$

Combining equations 2.52 and 2.54 gives

$$\chi_{vap} = \frac{c_{vap}}{\frac{p}{R_u T}} = \frac{c_{vap} R_u T}{p} \tag{2.56}$$

$$\chi_{air} = \frac{p - c_{vap} R_u T}{p} \tag{2.57}$$

Combining this with equations 2.48, 2.49, 2.56 and 2.57 gives

$$R_s = R_u \left(\frac{p}{c_{vap} R_u T M_{vap} + p M_{air} - c_{vap} R_u T M_{air}} \right) \tag{2.58}$$

2.10   Slip Velocity

A gas flowing over a liquid layer can induce motion of the liquid layer. If those velocities become large enough to move liquid before it is evaporated, this can cause problems when the functional part of the ink are moved before the solvent is totally evaporated, so therefore it is desired to know how big this effect is for a given flow. For the flow in either the liquid or the gas phase, a Couette flow is assumed. Assuming a Couette flow will already give a good approximation about the order of magnitudes of the flow velocities. Figure 2.2 shows the geometry. It is assumed that $t_{liq} << H$, meaning the distance between the middle of the gas flow and the gas-liquid interface is $0.5H$. The flow is described as $\vec{u} = (u_x(y), 0, 0)$.
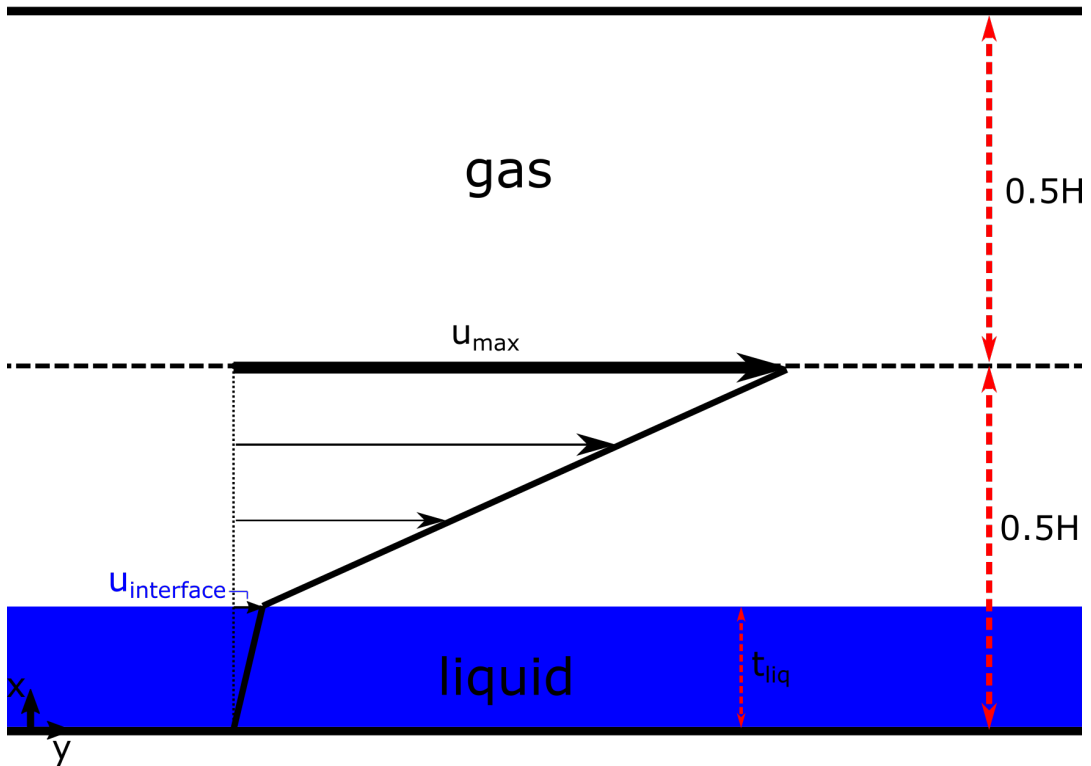
FIGURE 2.2: Slip velocity geometry

A Couette flow means

$$\frac{\partial^2 u_x}{\partial y^2} = 0,\qquad(2.59)$$

which then means that

$$\frac{\partial u_x}{\partial y} = C.\qquad(2.60)$$

At the gas-liquid interface, the shear stress is continuous in the absence of Marangoni effects, so (Darhuber, 2017b),

$$\mu_{liq}\frac{\partial u_{x,liq}}{\partial y} = \mu_{gas}\frac{\partial u_{x,gas}}{\partial y}.\qquad(2.61)$$

If the bottom of the liquid layer is at rest, in combination with a no-slip condition at the bottom wall, we have $u_x(y = 0) = 0$. Combining this with equation 2.60 gives

the velocity at the interface as

$$u_{interface} = \int_0^{t_{liq}} \frac{\partial u_{x,liq}}{\partial y} dx = t_{liq} \cdot \frac{\partial u_{x,liq}}{\partial y}. \tag{2.62}$$

Filling this in in equation 2.61 gives

$$u_{interface} = t_{liq} \frac{\mu_{gas}}{\mu_{liq}} \frac{\partial u_{x,gas}}{\partial y}. \tag{2.63}$$

Combining equation 2.60 with the fact that is was assumed that $t_{liq} << H$, it can be stated that

$$\frac{\partial u_{x,gas}}{\partial y} = \frac{U_{max} - u_{interface}}{\frac{1}{2}H}, \tag{2.64}$$

with U_{max} being the maximum velocity of the gas flow in the middle of the channel with height H. Filling in the results of equation 2.64 in equation 2.63 and rewriting it results in

$$u_{interface} = t_{liq} \frac{\mu_{gas}}{\mu_{liq}} \frac{U_{max}}{\frac{1}{2}H + t_{liq} \frac{\mu_{gas}}{\mu_{liq}}} \tag{2.65}$$

2.11 Lubrication equation

To describe the behaviour of a thin liquid film in contact with a solid and a gas phase, the lubrication equation is used. This equation is then described by (Wedershoven, 2017)

$$\frac{\partial h}{\partial t} + \frac{\partial}{\partial x}\left(-\frac{h^3}{3\mu_{liq}}\frac{\partial P}{\partial x} + \frac{h^2}{2\mu_{liq}}\tau\right) = -\frac{J}{\rho} \tag{2.66}$$

with

$$P = -\gamma\frac{\partial^2 h}{\partial x^2} + \rho g h \tag{2.67}$$

and

$$\tau = \mu_{gas}\frac{\partial u_{gas}}{\partial y}. \tag{2.68}$$

Variables are the height of the liquid layer h, the dynamic viscosity μ of either the liquid (*liq*) or the gas phase above the layer (*gas*), the evaporation flux J, from equation 2.2. ρ is the density of the liquid, γ the surface tension, g the gravitational acceleration. Note this is the lubriacation equation for a liquid layer stretching in only one dimension (x-direction). The height is in the y-direction.

2.12 Drag force on a liquid sphere

If an object travels a liquid medium, the drag force can be given by the Stokes drag, assuming the Reynolds number is sufficiently low (Darhuber, 2017c). The Reynolds number is defined as (Sommerfield, 1908)

$$R_e = \frac{\rho U L_{char}}{\mu}, \tag{2.69}$$

with R_e the Reynolds number, ρ the density of the fluid, U the flow velocity, L_{char} the characteristic length and μ the dynamic viscosity. The drag force on a liquid sphere,

generated by a stationary or moving gas, can then be given by (Leal, 1992)

$$F_{drag} = 4\pi\mu_{gas}(U_{gas} - U_{sphere})R_{sphere}C \tag{2.70}$$

with correction term

$$C = \frac{3(\lambda + 2)}{2(\lambda + 1)}, \lambda = \frac{\mu_{liq}}{\mu_{gas}}. \tag{2.71}$$

With μ_{gas} and μ_{liq} the dynamic viscosities of the liquid (sphere) and the gas (surroundings), U_{gas} the velocity of the gas flow in the direction that is investigated, U_{sphere} the velocity of the sphere in the direction investigated and R_{sphere} the radius of the sphere. However, when using a liquid going through a gas flow, the correction term C, is close to $\frac{3}{2}$. Filling this in in equation 2.70 gives the normal Stokes drag equation (Stokes, 1851)

$$F_{drag} = 6\pi\mu_{gas}(U_{gas} - U_{sphere})R_{sphere}, \tag{2.72}$$

due to the large ratio between the viscosity of air and liquid (in the cases used in this report).

2.13   Vernooij number

When a (gas) flow goes over an evaporating liquid layer, it is possible for the flow to move the liquid significantly before it is evaporated. This can have unwanted effects when inkjet printing technology is used. For inkjet printing to work, the solvent has to evaporate at the sport is is printed on, otherwise the functional material can be displaced before the liquid is dried out. To look at this phenomenon a model is constructed to investigate the influence of the gas flow on the liquid layer height, within the same geometry of figure 2.2. To describe the relation between the gas flow and the evaporation rate, a dimensionless number is constructed as

$$Vernooij = \frac{U_{flow,interface}}{EvapRate}. \tag{2.73}$$

$U_{flow,interface}$ is the horizontal velocity due to the air flow at the liquid-gas interface. Section 2.10 showed that an air flow going over a liquid layer induced a velocity at the liquid-air interface, parallel to the gas flow. The evaporation rate is defined as if the concentration gradient in the gas flow channel is constant, meaning

$$EvapRate = \left|\frac{J}{\rho}\right| \cdot M_{liq} = \frac{D}{\rho}\left|\frac{\partial c}{\partial y}\right| \cdot M_{liq} = \frac{D}{\rho}\left|\frac{c_{top} - c_{bottom})}{H}\right| \cdot M_{liq} = \frac{D}{\rho}\frac{c_{Sat}(T)}{H} \cdot M_{liq}, \tag{2.74}$$

with $c_{Sat}(T)$ being the saturated concentration from equation 2.26. Note that this holds, assuming that on the top of the channel there is no liquid and $H \gg t_{liq}$, with t_{liq} being the height of the liquid layer.

2.14   Light interference measurement of layer thickness

In this report, an important measurement is the determination of the condensed layer thickness. This has to be done from the other side of the glass, due to physical constraints in the experimental setup, as show in figure 2.3. It can be seen that the layer that has to be measured is on the other side of the glass, in respect to the

lens objective of the microscope. In order to determine the layer thickness, the interferometric pattern of the light of the microscope is used. When the wavelength of the light is known, the background light is reduced to a minimum and the glass is thin enough, the growth of the layer can be deduced from the intensity of the light measured by the microscope.
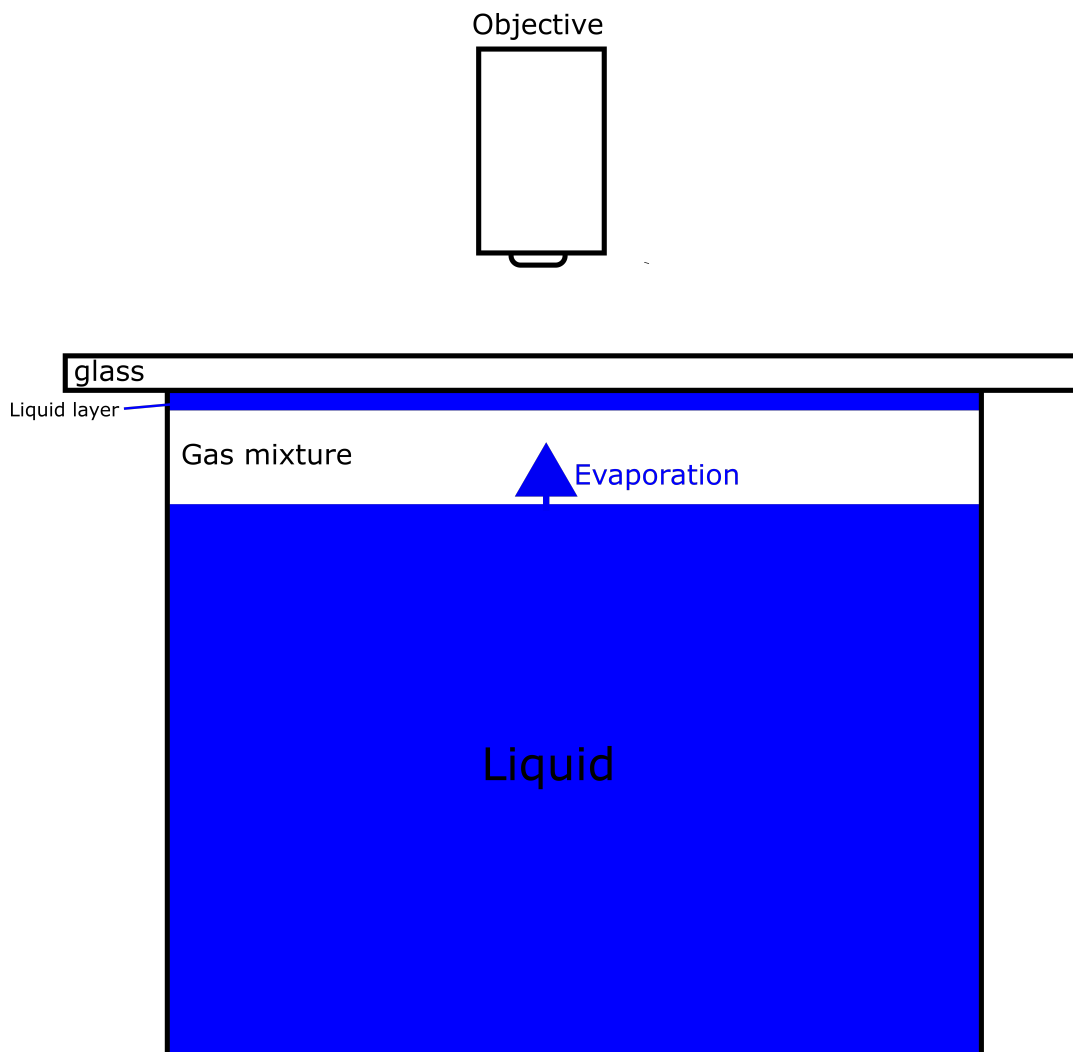
FIGURE 2.3: Drawing of the experimental setup for measuring the condensated layer thickness.

Figure 2.4 shows the light that is reflected by the interface between the condensated liquid layer and the air in the beaker. There are of course other places where the light can be reflected, but this interface is the interestings part and furthermore, it gives a big enough difference in intensity to be noticed. Figure 2.4 shows the situation without a liquid layer. If the glass is kept at the same position, the phase of this light will remain the same. When the liquid layer start growing, light will also be reflected by the liquid-gas interface. The figure shows the situation when the liquid thickness is a quarter of the wavelength of the light inside the liquid (2). At this point, the reflected wave is completely out of phase with the wave that is reflected by the glass-liquid interface. Due to superposition (Fowles, 1975), the intensity of the light captured by the microscope will be at a relative minimum, whereas in situation (3), with a liquid layer thickness of half the wavelength of the light, the intensity will
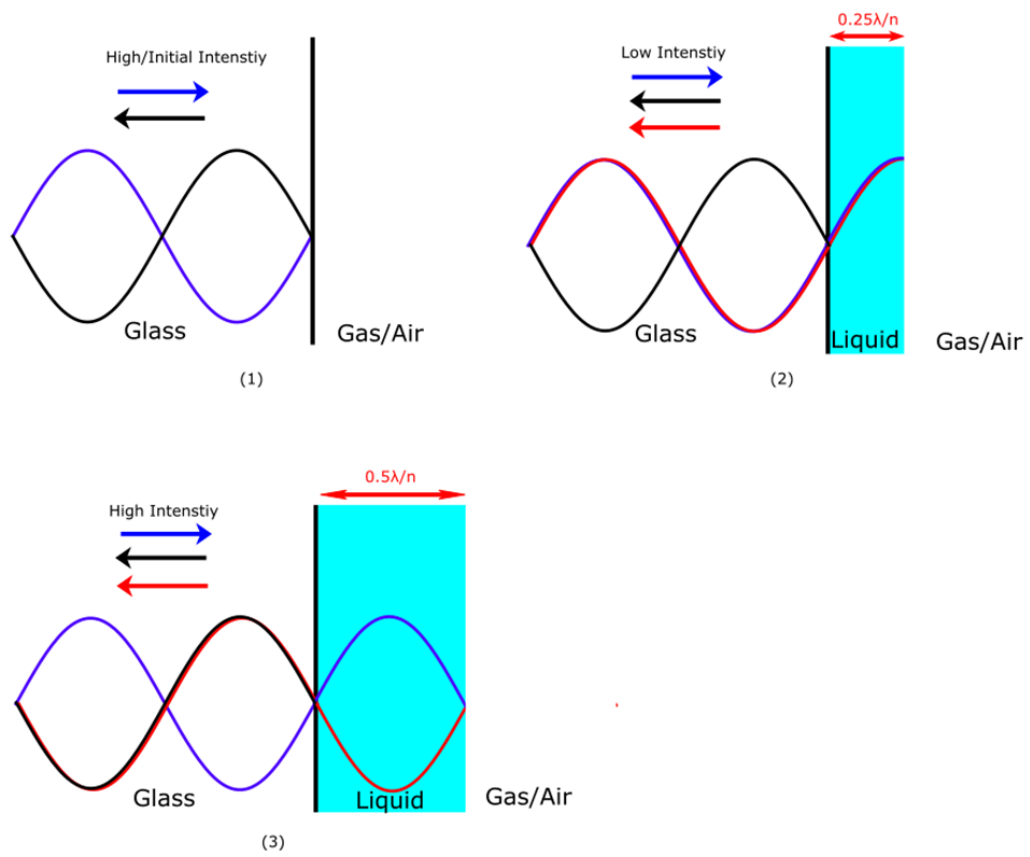
FIGURE 2.4: Example of light reflecting for a liquid layer thickness of $0 \cdot \frac{\lambda}{n}$ (1), $0.25 \cdot \frac{\lambda}{n}$ (2) and $0.5 \cdot \frac{\lambda}{n}$ (3)

again be at its maximum. This pattern will go on and oscillate with a layer thickness of half a wavelength divided by the refraction index between every two peaks in intensity captured by the microscope. With this knowledge, the growth rate of the layer can be determined over time. Note that this does not give direct information about the absolute size of the layer, unless there is certainty that the measurement is started precisely at situation (1) in figure 2.4. The average growth of the layer between to peaks in intensity is then given by

$$\frac{\partial h}{\partial t} = \frac{\frac{\lambda_0}{0.5 n_{liquid}}}{P},$$

(2.75)

with λ_0 the wavelength of the light in a vacuum, n_{liquid} the refraction index of the liquid an P the time between two neighbouring peaks in intensity.

Chapter 3

Numerical models

3.1 Properties

$D_{T_{amb},EG} = 1.08 \cdot 10^{-5} m^2/s$ (*Ethylene Glycol database* n.d.)
$D_{T_{amb},Tol} = 0.87 \cdot 10^{-5} m^2/s$ (*Toluene database* n.d.)
Antoine equation coefficients (Yaws, 2015)
Toluene:
$A_{tol} = 7.13657$
$B_{tol} = 1457.2871$
$C_{tol} = 231.827$
Ethylene Glycol:
$A_{EG} = 9.69599$
$B_{EG} = 3145.8596$
$C_{EG} = 264.246$

$h_{n,air} \approx 5 W/(m^2 K)$ (Edge, n.d.)
$L_{EG} = 5 \cdot 10^5 J/kg$ (ToolBox, 2003b)

$\mu_{EG,T=25^oC} = 0.0161 Pa \cdot s$ (ToolBox, 2003a)
$\mu_{EG,T=70^oC} = 0.0038 Pa \cdot s$
$\mu_{Tol,T=25^oC} = 5.5 \cdot 10^{-4} Pa \cdot s$ (Santos et al., 2006)
$\mu_{Tol,T=70^oC} = 3.5 \cdot 10^{-4} Pa \cdot s$

Surface tension:
$\gamma_{EG,T=25^oC} = 0.0477 N/m$ (ToolBox, 2005)
$\frac{\partial \gamma_{EG}}{\partial T} = -0.0890 mN/(m \cdot K)$ (*Surface tension values of some common test liquids for surface energy analysis* 2017)
$\gamma_{Tol,T=25^oC} = 0.028 N/m$ (ToolBox, 2005)

Software

The software used for the numerical models in this chapter is the finite element software of Comsol Multiphysics 5.3a and 5.5a .

3.2 Falling droplet trajectory

The first model concerns the trajectory of ink jetted droplets in a transverse gas stream. The air flow going over a liquid, to accelerate the evaporation process, also

affects the path of a printed droplet on its way to the substrate. In order to investigate this behaviour, two differential equations have to be solved. The geometry of the falling droplet is described in figure 3.1.
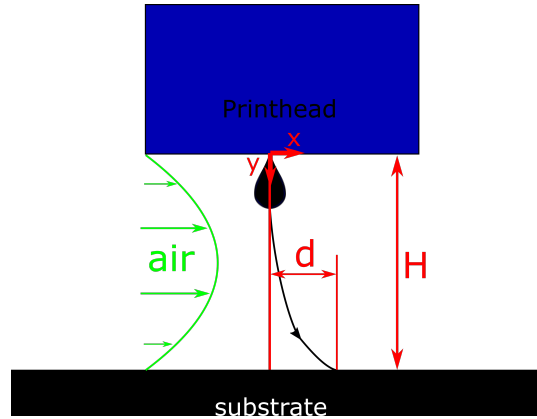
FIGURE 3.1: Geometry of the droplet being jetted by the printhead, with its path from the point where it leaves the printhead, to the point where it its the substrate

The first one is a force balance in the direction of the droplet falling. The forces included here are gravity and the drag force that works in the opposite direction of the falling droplet. Note that for these equations, spherical droplets are assumed, with a uniform density. Another assumption is that $R_{droplet} << H$, so that tracking the middel of the droplet is sufficient for determining when it lands on the substrate. A Stokes Drag for the droplet moving trough the air from section 2.12 is assumed, as the Reynolds number is:

$$R_e = \frac{\rho U L_{char}}{\mu} = \frac{\rho_{air} U_{jet} R_{drop}}{\mu_{air}} = \frac{1.1839 \cdot 6 \cdot 1 \cdot 10^-}{1.85 \cdot 10^{-5}} \approx 3.8 \tag{3.1}$$

, therefore the Stokes drag is still reasonably good for this situation.

$$\frac{d^2 y}{dt^2} = -g - \frac{6\pi \eta_{air} R}{m} \frac{dy}{dt}$$
$$y(t = 0) = 0 \tag{3.2}$$
$$\frac{dy}{dt}(t = 0) = u_{Jet_{y,0}}$$

From the solution of this differential equation, the landing time can be calculated. This landing time is defined as $y(t = t_{landing}) = H$. For the air flow, a Poiseuille flow is assumed, defined by

$$u_x(y) = \left(-\frac{4 U_{max}}{H^2}(y - 0.5H)^2 + U_{max} \right). \tag{3.3}$$

The force balance in the x-direction is then defined as

$$\frac{d^2x}{dt^2} = \frac{6\pi\eta_{air}R}{m}\left(u_x(y(t)) - \frac{dx}{dt}\right)$$
$$x(t = 0) = 0 \tag{3.4}$$
$$\frac{dx}{dt}(t = 0) = u_{Jet_{x,0}} = 0$$

The solution $x(t), y(t)$ gives a trajectory of the droplet, based on size and mass of the droplet, but also the height of the printhead, the velocity of the air and the velocity of jetting.

Bot differential equations are analytically solvable, admittedly complicated. To simplify the reading of the equations,

$$a \equiv \frac{6\pi\eta_{air}R}{m}. \tag{3.5}$$

The solution for the y position, is then

$$y(t) = -\frac{e^{-at}\left(g - e^{at}g + ae^{at}gt + au_{Jet_{y,0}} - ae^{at}u_{Jet_{y,0}}\right)}{a^2} \tag{3.6}$$

For the x position, it is:

$$x(t) = \frac{1}{a^5H^2(g + au_{Jet_{y,0}})^2}e^{-3at}U_{max}\cdot$$

$$\left[e^{at}\left(-2g^4 - 8ag^3u_{Jet_{y,0}} - 12a^2g^2u_{Jet_{y,0}}{}^2 - 8a^3gu_{Jet_{y,0}}{}^3 - 2a^4u_{Jet_{y,0}}{}^4\right)\right.$$

$$+ e^{2at}\left(g^4(-16 + 4a^2t^2)+\right.$$

$$a^4u_{Jet_{y,0}}{}^3(8aH + 4a^2t^2 - 8u_{Jet_{y,0}} - 8atu_{Jet_{y,0}}) + a^3gu_{Jet_{y,0}}{}^2$$

$$(-32u_{Jet_{y,0}} + a(28H - 24tu_{Jet_{y,0}}) + a^2t(12H + 4tu_{Jet_{y,0}}))+$$

$$ag^3(-48u_{Jet_{y,0}} + a(12H - 8tu_{Jet_{y,0}}) + a^2t(4H + 12tu_{Jet_{y,0}}))+$$

$$a^2g^2u_{Jet_{y,0}}$$

$$\left.(-56u_{Jet_{y,0}} + a(32H - 24tu_{Jet_{y,0}}) + a^2t(12H + 12tu_{Jet_{y,0}}))\right)$$

$$e^{3at}\left(g^4(18 - 20at + 8a^2t^2 - 1\frac{1}{3}a^3t^3)+\right.$$

$$a^4u_{Jet_{y,0}}{}^3(-8aH + 4a^2Ht + 10u_{Jet_{y,0}} - 4atu_{Jet_{y,0}})+$$

$$a^3gu_{Jet_{y,0}}{}^2(-2a^3Ht^2 + 40u_{Jet_{y,0}}+$$

$$a(-28H - 24tu_{Jet_{y,0}}) + a^2t(16H + 4tu_{Jet_{y,0}}))+$$

$$a^2g^2u_{Jet_{y,0}}(68u_{Jet_{y,0}} + a(-32H - 56tu_{Jet_{y,0}})+$$

$$a^3t^2(-4H - 1\frac{1}{3}tu_{Jet_{y,0}})a^2t(20H + 16tu_{Jet_{y,0}}))+$$

$$ag^3(56u_{Jet_{y,0}} + a(-12H - 56tu_{Jet_{y,0}})+$$

$$\left.\left.a^3t^2(-2H - 2\frac{2}{3}tu_{Jet_{y,0}}) + a^2t(8H + 20tu_{Jet_{y,0}}))\right)\right] \tag{3.7}$$

The Matlab code used evaluating results is shown in appendix C.

3.3   Heating up liquid in beaker - timescales

3.3.1   Dimensions
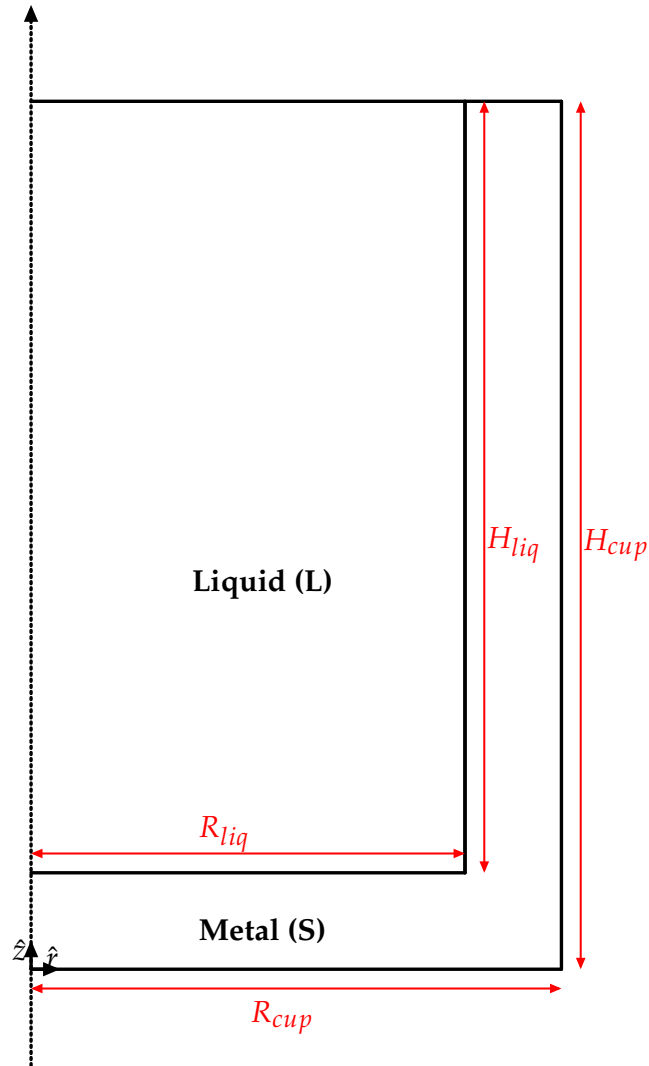
FIGURE 3.2: The geometry metal cup with liquid

The goal of the simulation is to investigate the time scales of the heating process of the liquid. This is done to determine the time it takes in the experiments before a reliable measurement can be done. The metal domain represents the beaker and the liquid domain is the liquid, mostly ethylene glycol or toluene.
The values used in the model are

$R_{cup} = 2.75cm$
$R_{liq} = 2.25cm$
$H_{cup} = 4.5cm$
$H_{liq} = 4cm$

3.3.2 Physics

Liquid equations

- Temperature dependent density (Cengel and Cimbala, 2014)

$$\rho(T) = \frac{\rho_{ref}}{1 + \beta(T - T_{ref})} \tag{3.8}$$

- Incompressible flow, section 2.4.1

$$\frac{\partial \vec{u}}{\partial t} + (\vec{u} \cdot \nabla)\vec{u} - \frac{\mu}{\rho}\nabla^2 \vec{u} = -\nabla \frac{p}{\rho} + \vec{g}, \tag{3.9}$$

$$\rho \nabla \cdot (\vec{u}) = 0. \tag{3.10}$$

- Heat transfer equation, from section 2.2

$$\rho C_p \frac{\partial T}{\partial t} + \rho C_p \vec{u} \cdot \nabla T + \nabla \cdot \vec{q} = Q \tag{3.11}$$

with

$$\vec{q} = -k\nabla T. \tag{3.12}$$

<u>Initial values:</u>

$$\vec{u_0} = 0 \tag{3.13}$$

$$P_0 = P_{amb} \tag{3.14}$$

$$T_0 = T_{amb} \tag{3.15}$$

Metal equations

- Heat transfer equation, from section 2.2

$$\rho C_p \frac{\partial T}{\partial t} + \nabla \cdot \vec{q} = Q \tag{3.16}$$

with

$$\vec{q} = -k\nabla T. \tag{3.17}$$

<u>Initial values:</u>

$$T_0 = T_{amb} \tag{3.18}$$

3.3.3   Boundary conditions
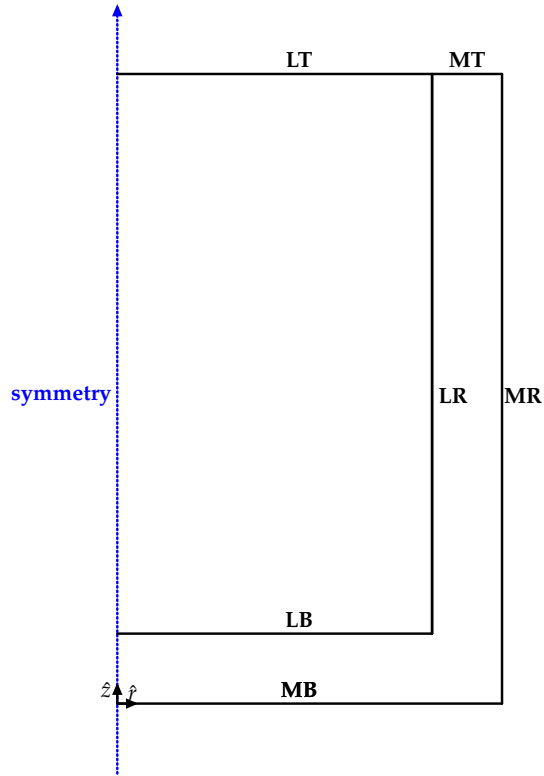
FIGURE 3.3: The boundaries of the model with the metal cup containing liquid, **MB/MR/MT**: Metal bottom/right/top, **LB/LR/LT**: Liquid bottom/right/top.

Boundary condition metal domain

MB, temperature

$$T = 70^{o}C \tag{3.19}$$

MR & **MT**, thermal insulation

$$- \vec{n} \cdot (-k_{metal}\nabla T) = 0 \tag{3.20}$$

Boundary condition liquid domain

LB & **LR**, temperature continuity, wall

$$T_{liq} = T_{metal} \tag{3.21}$$

$$k_{liq}\nabla T_{liq} \cdot \vec{n} = k_{metal}\nabla T_{metal} \cdot \vec{n} \tag{3.22}$$

$$\vec{u} = 0 \tag{3.23}$$

LT, Newtonian cooling, wall

$$q = -h_{n,air}(T_{liq} - T_{amb}) \cdot \vec{n} \tag{3.24}$$

$$\vec{u} = 0 \tag{3.25}$$

3.4 Experiment without external airflow

Symmetry axis
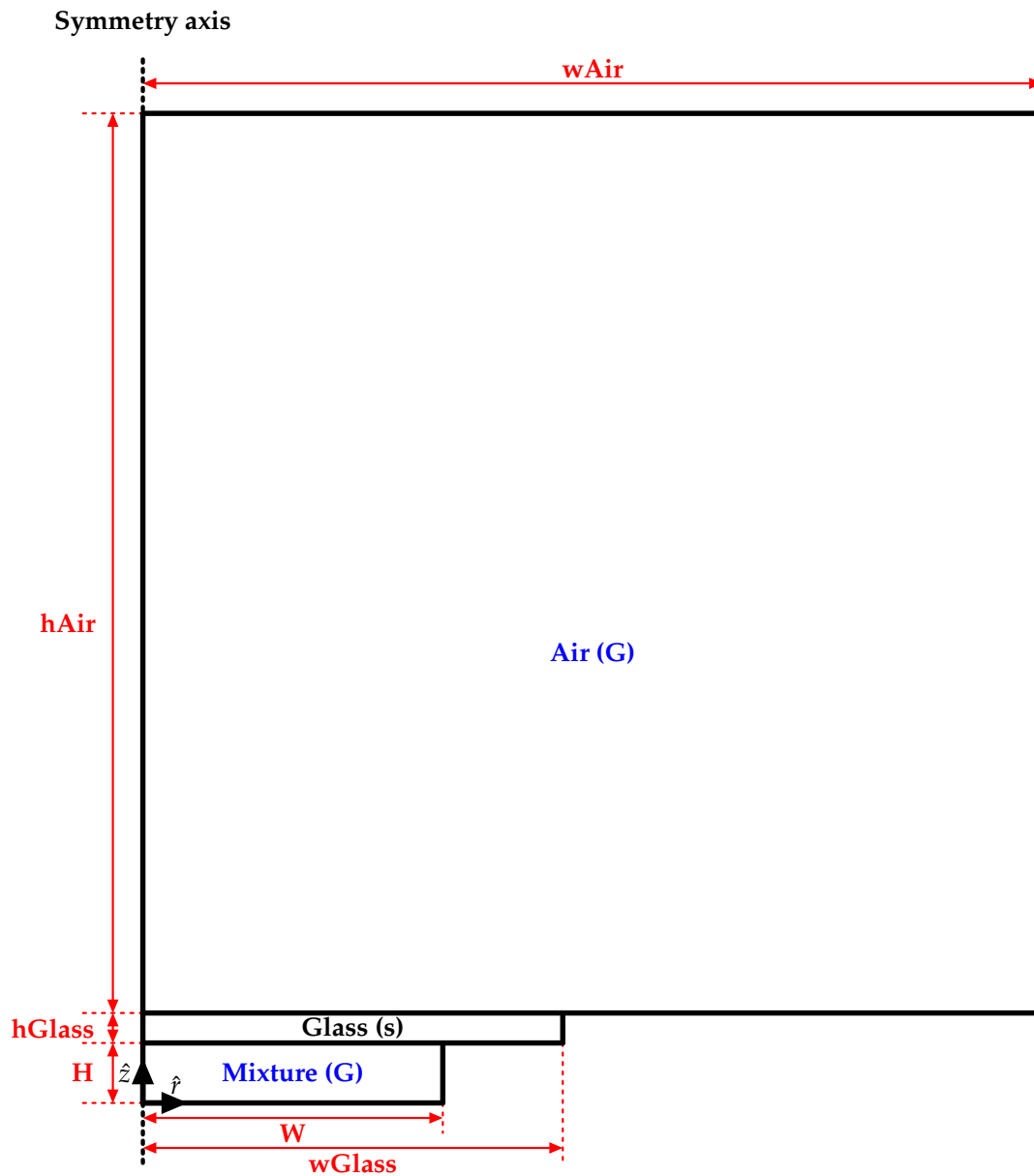
FIGURE 3.4: The geometry of the simulations of the simple experiment

This geometry shows the geometry of the experiment without an external air flow. The experiment was done with an almost filled aluminium beaker of Ethylene Glycol. On top of the beaker there is a glass plate. Note that the simulation doesn't simulate the liquid itself, but only the gas mixture in between the liquid and the glass plate. Furthermore, the air surroundings are also partially taken into account.

3.4.1 Physics domains

Mixture equations

- Compressible flow

$$\rho\frac{\partial\vec{u}}{\partial t} + \rho(\vec{u}\cdot\nabla)\vec{u} = \nabla\cdot\left[-p\vec{I} + \mu_{gas}(\nabla\vec{u} + (\nabla\vec{u})^T) - \frac{2}{3}\mu_{gas}(\nabla\cdot\vec{u})\vec{I}\right] + \vec{F}$$
(3.26)

$$\frac{\partial\rho}{\partial t} + \nabla\cdot(\rho\vec{u}) = 0$$
(3.27)

$$\rho C_{p,gas}\frac{\partial T}{\partial t} + \rho C_{p,gas}\vec{u}\cdot\nabla T + \nabla\cdot\vec{q} = Q + q_0 + Q_p + Q_{vd}$$
(3.28)

$$\vec{q} = -k_{gas}\nabla T$$
(3.29)

$$\rho = \frac{p}{R_s(c,T)T}$$
(3.30)

And after combining equation 2.13 with (Bird and Stewart, 2002) for the heat variables:

$$Q_{vd} = \mu_{gas}\left((\nabla\vec{u} + (\nabla\vec{u})^T)\cdot\frac{2}{3}(\nabla\cdot\vec{u})\vec{I}\right) : \nabla\vec{u}$$
(3.31)

$$Q_p = \alpha_\rho T\left(\frac{\partial p}{\partial t} + \vec{u}\cdot\nabla p\right)$$
(3.32)

$$\alpha_\rho = -\frac{1}{\rho}\left(\frac{\partial\rho}{\partial T}\right)_p$$
(3.33)

- Concentration diffusion and convection

$$\frac{\partial c}{\partial t} + \nabla(-D_{gas}\nabla c) + \vec{u}\nabla c = 0$$
(3.34)

Initial values:

$$T_0(z) = \frac{T_{amb} - T_w}{H}z + T_w$$
(3.35)

$$c_0 = 0$$
(3.36)

$$p_0 = p_{amb}$$
(3.37)

$$\vec{u}_0 = 0$$
(3.38)

Glass equations

- Heat conduction and convection

$$\rho_{glass}C_{p,glass}\frac{\partial T_{glass}}{\partial t} + \nabla(-k_{glass}\nabla T_{glass}) = 0$$
(3.39)

Initial values:

$$T_0 = T_{amb}$$
(3.40)

Air equations

- Heat conduction and convection

$$\rho_{Air}(T)C_{p,Air}\frac{\partial T_{Air}}{\partial t} + \nabla(-k_{Air}\nabla T_{Air}) = 0$$
(3.41)

Initial values:

$$T_0 = T_{amb}$$
(3.42)

Note that heat transfer due to convection in the air is neglected for this model.

3.4.2 Boundary conditions
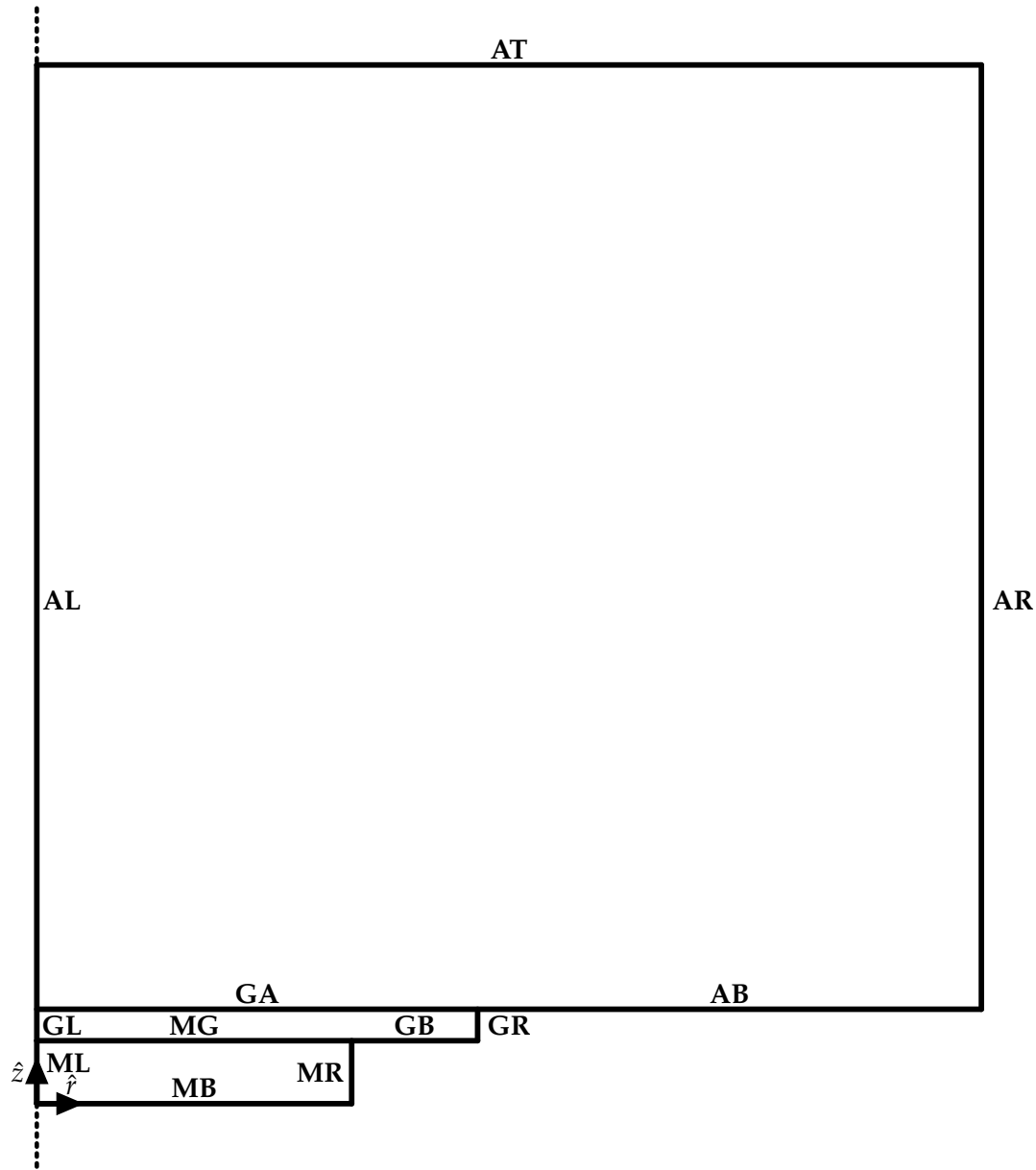
FIGURE 3.5: **MB** = Mixture bottom, **ML/MR** = Mixture left/right, **MG** = Mixture-Gas interface, **GL/GR** = Glass left/right, **GB** = Glass bottom, **GA** = Gas-Air interface, **AB** = Air bottom, **AL/AR** = Air left-/right, **AT** = Air top

Boundary conditions gas mixture domain

MB temperature, concentration, wall

$$T = T_{liq} \tag{3.43}$$

note that T_{liq} is here a constant and not a variable that is solved for in an other domain.

$$c = \frac{cSat(T)}{M_{liq}} \tag{3.44}$$

$$\vec{u} = 0 \tag{3.45}$$

ML and MR thermal insulation, no concentration flux, wall

$$\vec{n} \cdot (-k_{mix}\nabla T + \rho C_{p,mix}T\vec{u}) = 0 \tag{3.46}$$

$$\vec{n} \cdot (-D_{gas}\nabla c + c\vec{u}) = 0 \tag{3.47}$$

$$\vec{u} = 0 \tag{3.48}$$

MG heat flux, concentration, wall

$$T_{mix} = T_{glass} \tag{3.49}$$

$$-k_{mix}\nabla T_{mix} = -k_{glass}\nabla T_{glass} \tag{3.50}$$

$$c = \frac{cSat(T)}{M_{liq}} \tag{3.51}$$

$$\vec{u} = 0 \tag{3.52}$$

Boundary conditions glass domain

MG heat flux

$$T_{mix} = T_{glass} \tag{3.53}$$

$$-k_{mix}\nabla T_{mix} = -k_{glass}\nabla T_{glass} - \frac{\partial c}{\partial z}D_{gas}M_{liq}L_{liq} \tag{3.54}$$

GA heat flux

$$T_{glass} = T_{air} \tag{3.55}$$

$$-k_{glass}\nabla T_{glass} = -k_{air}\nabla T_{air} \tag{3.56}$$

GL thermal insulation

$$\vec{n} \cdot (-k_{glass}\nabla T) = 0 \tag{3.57}$$

GB and GR thermal insulation

$$\vec{n} \cdot (-k_{glass}\nabla T) = 0 \tag{3.58}$$

Boundary conditions air domain

GA heat flux

$$T_{glass} = T_{air} \tag{3.59}$$

$$-k_{glass}\nabla T_{glass} = -k_{air}\nabla T_{air} \tag{3.60}$$

AL and AB thermal insulation

$$\vec{n} \cdot (-k_{glass}\nabla T) = 0 \tag{3.61}$$

AT and AR temperature

$$T = T_{amb} \tag{3.62}$$

3.4.3   Expansion model without external airflow

Due to results not matching, the model was eventually expanded. This was done by taken into account the liquid itself and the metal beaker.
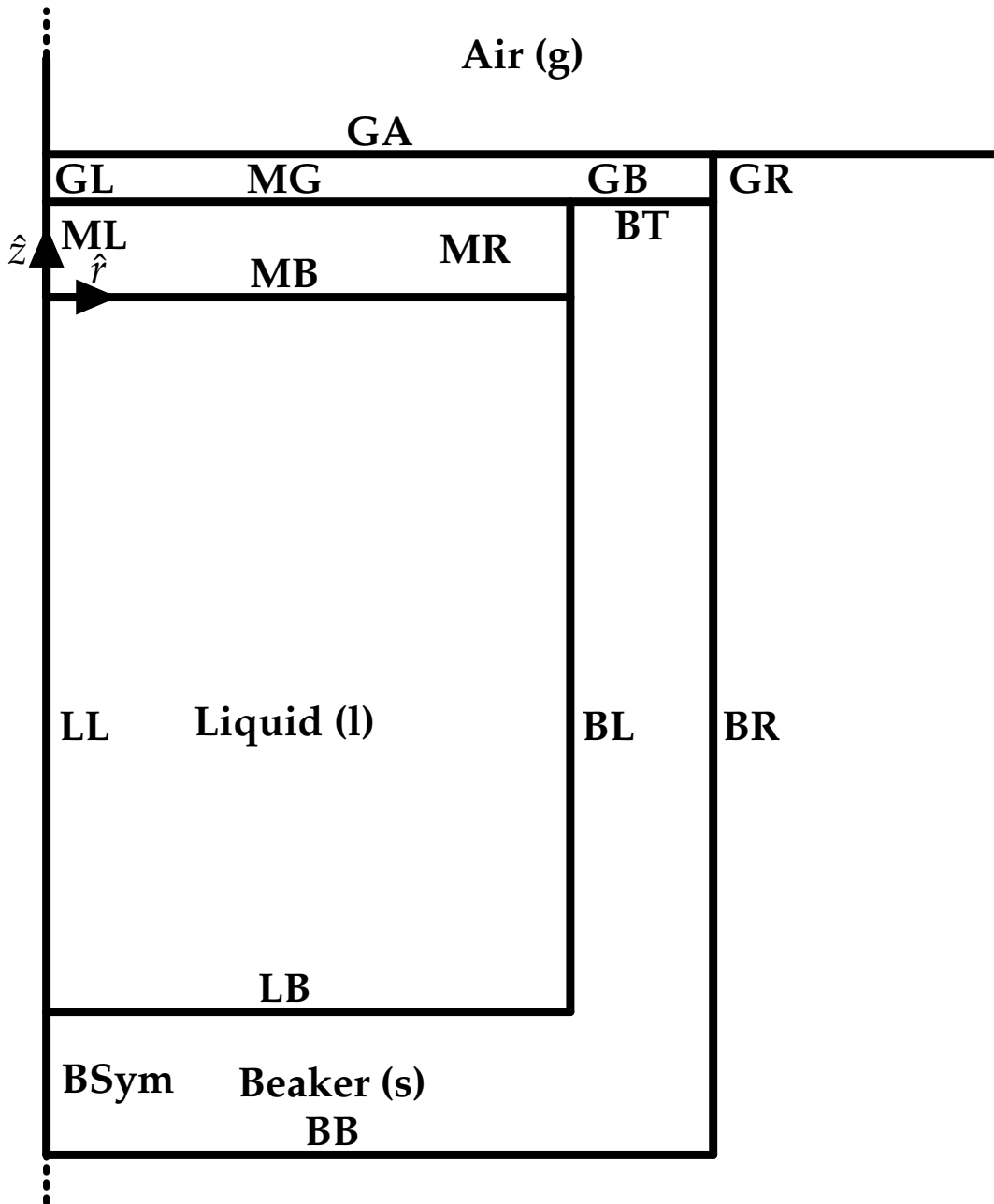
FIGURE 3.6: **MB** = Mixture bottom, **ML/MR** = Mixture left/right, **MG** = Mixture-Gas interface, **GL/GR** = Glass left/right, **GB** = Glass bottom, **GA** = Gas-Air interface, **LL/LB** = Liquid left/bottom, **BL/BR** = Beaker left/right, **BT/BB** = Beaker top/bottom, **BSym** = Beaker boundary on symmetry axis, Air is left out of image, but is simulated

The physics for the liquid and beaker domain are almost copied from section 3.3. Note that the variable T_{liq} was a constant earlier, but is now a variable that is solved for. The contstant temperature is now $T_{HotPlate}$. The differences are in the boundaries adjacent to the boundaries from figure 3.4 and boundary **BR**.

For boundary **BR** a heat flux is set, equal to the newtonian cooling from section 2.2.2. The boundaries **MR** and **BT** have a heat transfer continuity constraint, as described in section 2.2.1.

Boundary **MB** is both for the flow, as well for the heat transfer different from before.

Heat discontinuity due to evaporation:

$$T_{liq} = T_{mixture} \tag{3.63}$$

$$-k_{liq}\nabla T_{liq} = -k_{mixture}\nabla T_{mixture} + \frac{\partial c}{\partial z}D_{gas}M_{liq}L_{liq} \tag{3.64}$$

For the laminar flow, firstly the high temperature dynamic viscosity $\mu_{EG,T=70^oC}$ of Ethylene Glycol is used, as it is assumed that the liquid and the beaker are at the temperature of the hot plate at the moment of measuring.

For the flow boundary setting, Marangoni flow from section 2.4.2 is implemented. Therefore the surface tension is defined as

$$\gamma = \gamma_{EG,T_{ref}} + \frac{\partial\gamma_{EG}}{\partial T}\left(T_{liq} - T_{ref}\right). \tag{3.65}$$

This temperature dependent value of the surface tension will induce flows across the liquid gas interface.

Initial values:
$T_{liq} = T_{beaker} = T_{HotPlate}$
$\vec{u}_{liq} = 0$

3.5 Transition point model

3.5.1 Dimensions
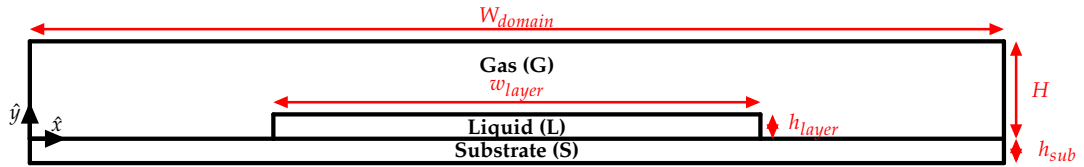
FIGURE 3.7: General setup transition point geometry

The liquid layer is assumed to cover the whole length of the domain. Also the height of the layer is neglected.

$$w_{layer} = W_{domain} \tag{3.66}$$

$$h_{layer} = 0 \tag{3.67}$$

This results in the following domain:
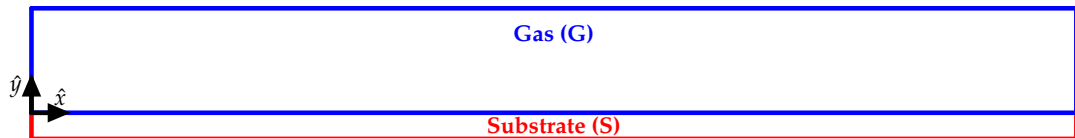
FIGURE 3.8: Geometry of the transition point model simulations

3.5.2 Physics domains

Gas equations

- Compressible flow
  Same as in section 3.4.1, Mixture equations

- Concentration diffusion and convection
  Same as in section 3.4.1, Mixture equations

Initial values:

$$T_0(z) = T_{Nozzle} \tag{3.68}$$

$$c_0 = 0 \tag{3.69}$$

$$p_0 = p_{amb} \tag{3.70}$$

$$\vec{u}_0(y) = \left(-\frac{4U_{max}}{H^2}(y - 0.5H)^2 + U_{max} \right) \cdot \hat{x} \tag{3.71}$$

Substrate equations

- Heat conduction

$$\rho_{sub}C_{p,sub}\frac{\partial T}{\partial t} + \nabla(-k_{sub}\nabla T) + \rho_{sub}C_{p,sub}\vec{u}\nabla T = 0 \tag{3.72}$$

$$\vec{u} = U_{wall} \cdot \hat{x} \tag{3.73}$$

Initial values:

$$T_0 = T_{amb} \tag{3.74}$$

3.5.3 Boundary conditions
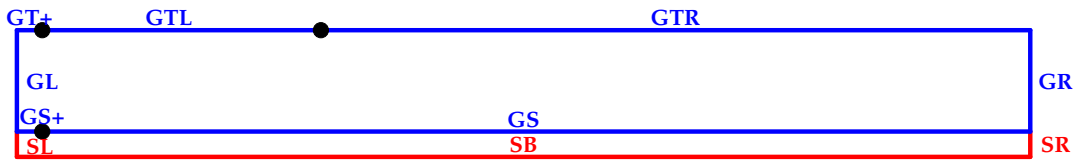
FIGURE 3.9: The adjusted geometry boundaries, **GL/GR** = gas left-/right, **GTL/GTR** = gas top left/right, **GS** = gas-substrate interface, **GT+** = gas top extra, **GS+** = gas-substrate interface extra, **SL/SR** = substrate left/right, **SB** = substrate bottom

Boundary conditions gas domain

GTL Temperature, No concentration flux, Wall

$$T = T_{Nozzle} \tag{3.75}$$

$$\vec{n} \cdot (-D_{gas}\nabla c + c\vec{u}) = 0 \tag{3.76}$$

$$\vec{u} = 0 \tag{3.77}$$

GTR Temperature, Concentration, Wall

$$T = T_{Nozzle} \tag{3.78}$$

$$c = \frac{cSat(T)}{M_{liq}} [mol/m^3] \tag{3.79}$$

$$\vec{u} = 0 \tag{3.80}$$

GL Inlet, concentration

$$T = T_{Inlet} \tag{3.81}$$

$$c = 0 \tag{3.82}$$

$$\vec{u}_0(y) = \left(-\frac{4U_{max}}{H^2}(y - 0.5H)^2 + U_{max} \right) \cdot \hat{x} \tag{3.83}$$

$$p = p_{amb} \tag{3.84}$$

GR Outflow, Outflow concentration

$$\vec{n} \cdot (-D\nabla c) = 0 \tag{3.85}$$

$$\vec{n} \cdot (-k\nabla T) = 0 \tag{3.86}$$

$$p = p_{amb} \tag{3.87}$$

GS heat flux, concentration, wall

$$T_{gas} = T_{sub} \tag{3.88}$$

$$k_{gas}\nabla T_{gas} = k_{sub}\nabla T_{sub} \tag{3.89}$$

$$c = \frac{cSat(T)}{M_{liq}} \tag{3.90}$$

$$\vec{u} = U_{wall} \cdot \hat{x} \tag{3.91}$$

GT+ and GS+ are there to make sure that there are no conflicts in concentration boundaries for Comsol. The inlet has a concentration equal to zero, whereas the full bottom and top of the gas domain has a concentration equal to the, non-zero, saturated concentration. To compensate for this, a small part of the domain has no set concentration, but only a no concentration flux boundary, to function as a transition part from zero concentration to a higher concentration.
GT+ thermal insulation, no concentration flux, wall

$$-\vec{n} \cdot (-k_{gas}\nabla T) = 0 \tag{3.92}$$

$$\vec{n} \cdot (-D_{gas}\nabla c + c\vec{u}) = 0 \tag{3.93}$$

$$\vec{u} = 0 \tag{3.94}$$

GS+ heat flux, no concentration flux, wall

$$T_{gas} = T_{sub} \tag{3.95}$$

$$k_{gas}\nabla T_{gas} = k_{sub}\nabla T_{sub} \tag{3.96}$$

$$\vec{n} \cdot (-D_{gas}\nabla c + c\vec{u}) = 0 \tag{3.97}$$

$$\vec{u} = U_{wall} \cdot \hat{x} \tag{3.98}$$

Boundary conditions substrate domain

SB Temperature

$$T = T_{sub} \tag{3.99}$$

SL and SR thermal insulation

$$-\vec{n} \cdot (-k_{sub}\nabla T) = 0 \tag{3.100}$$

3.6 Transition point model with top air flow

The model used in section 3.5 is an ideal situation, in which the temperature of the top boundary of the gas is kept at a constant temperature. However, this is very hard to realise and will thus not be the case in the transition point experiments. Instead, an extra air flow is used to regulate the temperature of the top boundary. This is taken care for in another model, which is an adaptation of the ideal model of section 3.5.
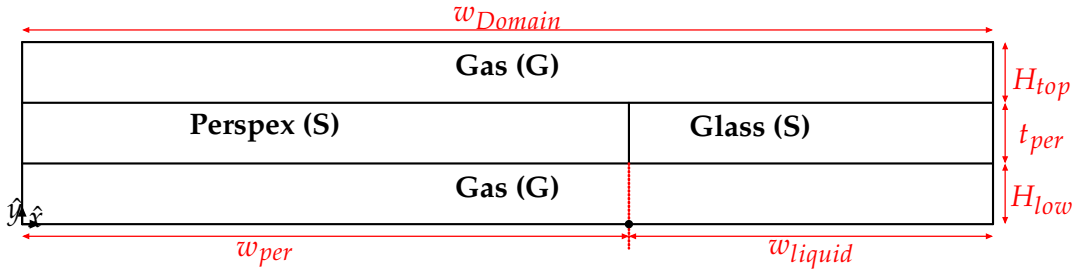
FIGURE 3.10: The geometry of the temperature air flow models

This model has the same gas physics domain as before, only now, underneath it there is not substrate domain. Instead, the bottom of the gas domain just has a temperature constraint,

$$T_{gas,bottom} = T_{sub} \tag{3.101}$$

, which is a constant. This is chosen for, as the substrate is very thin and conductive, meaning simulating for the substrate is computational effort waisted, as almost immediately the whole substrate would at constant temperature.

Perspex
The perspex part of the model simulates the part of the setup that the air at the inlet has to travel trough, before reaching the glass plate on which the condensation is measured. Figures A.2 and A.3 show the inlet part of the controlled temperature gas, and the liquid bath of the setup. It can be seen that the gas that enters the setup, has to travel $4.2cm$ trough the inlet part, and than another $3.75cm$ before it reaches the beginning of the glass, so

$$w_{per} = 7.95cm.$$

The liquid bath is positioned, so that the liquid layer will start directly underneath the beginning of the glass plate. This means that the bottom part can be splitted in 2 parts concentration wise, the left part having the no - flux constrataint, and the right part having a fixed concentration value.

Bottom Left: No-Flux

$$\vec{n} \cdot (-D_{gas}\nabla c + c\vec{u}) = 0 \tag{3.102}$$

Bottom Right: saturated concentration

$$c = \frac{cSat(T)}{M_{liq}} \left[\frac{mol}{m^3} \right] \tag{3.103}$$

Both for the perspex and the glass domain, only heat transfer is solved. This means that both have temperature continuity (section 2.2.1) set for their bottom and top boundaries and their common boundary. The two outer sided, so the left boundary for the perspex and the right one for the glass, have a thermal insulation constraint:

$$-\vec{n} \cdot (-k_{sub}\nabla T) = 0 \tag{3.104}$$

The top flow only solves the heat transfer equation. The bottom boundaries take care of the temperature continuity. The left boundary has a set temperature, equal to the temperature of the air that flowing into the bottom gas domain,
Top gas Left: Temperature

$$T_{Inlet,top} = T_{Inlet,bottom}, \tag{3.105}$$

which will be between 5 and 25 degrees Celsius in most cases.
Top gas Top: Newtonian cooling

$$\vec{q} = -h_n(T - T_{amb}) \cdot \vec{n} \tag{3.106}$$

Top gas Right: Outflow

$$\vec{n} \cdot (-k\nabla T) = 0 \tag{3.107}$$

In the domain, an air flow is assumed, equal to the ideal Poiseuille flow with the maximum velocity equal to the maximum velocity at the inlet of the bottom gas domain. So

$$\vec{u}(y) = \left(-\frac{4U_{max}}{H_{top}^2}((y - t_{per} - H_{low}) - 0.5H_{top})^2 + U_{max} \right) \cdot \hat{x}. \tag{3.108}$$

3.7 Shear-induced displacement of a volatile thin liquid film model

A 1-D simulation is used with length W_{layer}. Only the lubrication equation is used as described in equation 2.66. The gas flow is assumed to be a dry air flow in a channel with height H. Note that this air flow is not simulated. This model is only designed to track the layer height at any point of time.

$$w_{layer}$$

$$\hat{x}$$

FIGURE 3.11

3.7.1 Physics domain

General Form PDE
Initial values:

- $h = t_{layer,0}$

- $\frac{\partial h}{\partial t} = 0$

General Form PDE:

$$\frac{\partial h}{\partial t} + \nabla \cdot \left(\frac{h^2}{2\mu_{liq}} \mu_{gas} u_y - \frac{h^3}{3\mu_{liq}} \frac{\partial P_{lub}}{\partial x} \right) \cdot h_{check} = -EvapRate(x - x_{front}) \cdot h_{check} \tag{3.109}$$

$$u_y(h) = \frac{u_{layer}}{h} \cdot \frac{\mu_{gas}}{\mu_{liq}} \tag{3.110}$$

and from equation 2.65:

$$u_{layer} = \frac{\mu_{gas}}{\mu_{liq}} h \frac{U_{max}}{\frac{1}{2}H + h\frac{\mu_{gas}}{\mu_{liq}}} \tag{3.111}$$

$$P_{lub} = -\gamma_{liq} \frac{\partial^2 h}{\partial x^2} + \rho g h \tag{3.112}$$

$$h_{check} = \begin{cases} 1 & \text{if } h > 100 \cdot 10^{-9} \\ 0 & \text{if } h <= 100 \cdot 10^{-9} \end{cases}$$

Note that h is the height of the liquid layer, whereas H is the height of the channel. This channel is not simulated, but its height is of importance for the velocity at the top of the liquid layer. The function $evapRate(x)$ is a function designed have a large evaporation rate at the beginning of the liquid layer and a lower evaporation rate at the end of the layer. In the real case, with an air flow, the air above the beginning of the liquid is not yet full with vapor, whereas at the end of the liquid there is a lot of liquid in the air. Therefor at the beginning of the layer the evaporation rate is larger than at the end.

$$evapRate(x) = \begin{cases} 0 & \text{if } x < 0 \\ \frac{-0.5Evap}{W_{layer}}x + Evap & \text{if } x <= 0 \end{cases} \tag{3.113}$$

The variable $Evap$ is defined the same way as in equation 2.74. The variable x_{front} is a variable to keep track of the start of the liquid layer and is defined as

$$x_{front} = W_{layer} - \int_0^{W_{layer}} h_{check} dx \tag{3.114}$$

At boundaries, i.e. both ends of the domain, zero flux:

$$-\vec{n} \cdot \left(\frac{h^2}{2\mu_{liq}} \mu_{gas} u_y - \frac{h^3}{3\mu_{liq}} \frac{\partial P_{lub}}{\partial x} \right) = 0 \tag{3.115}$$

Another possibility would have been an outflow kind of boundary condition on the right, to mimic the liquid flowing out of the domain. However, this way makes sure that the moved liquid is still clearly visible in the results as it can not leave the domain.

3.8   Drying liquid layer

The model in this section will be an extension to the one in section 3.5. There the transition point of no condensation to condensation is investigated. However, in that case an infinite liquid layer is assumed, where evaporation is happening all the time. This section will provide a model where this is not assumed. Regarding the model, all the same physics equations and boundary conditions can be assumed. Except for the boundary conditions at the top and bottom boundaries of the gas domain.
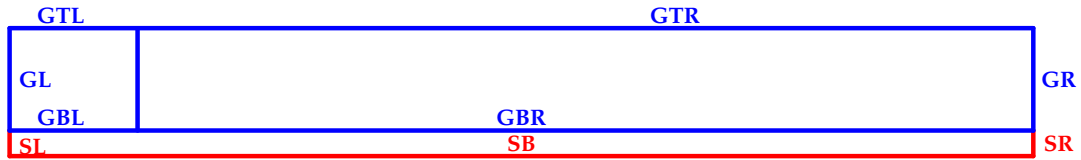
FIGURE 3.12: The adjusted geometry boundaries, **GL**/**GR** = gas left-/right, **GTL**/**GTR** = gas top left/right, **GBL/GBR** = gas-substrate interface left/right, **SL**/**SR** = substrate left/right, **SB** = substrate bottom

3.8.1   Boundary conditions

The top boundary, **GTL & GTR**, have a temperature, no concentration flux and a wall boundary constraint.

$$T = T_{Nozzle} \tag{3.116}$$

$$\vec{n} \cdot (-D_{gas} \nabla c + c\vec{u}) = 0 \tag{3.117}$$

$$\vec{u} = 0 \tag{3.118}$$

GBL is almost the same, except for the temperature constraint, as this boundary establishes the temperature continuity with the substrate, so

$$T_{gas} = T_{sub} \tag{3.119}$$

$$k_{gas} \nabla T_{gas} = k_{sub} \nabla T_{sub} \tag{3.120}$$

The boundary **BGR** is different from the other ones. There there is also a temperature continuity in combination with a no-flow constraint

$$T_{gas} = T_{sub} \tag{3.121}$$

$$k_{gas} \nabla T_{gas} = k_{sub} \nabla T_{sub} \tag{3.122}$$

$$\vec{u} = 0 \tag{3.123}$$

There is also a lubrication equation set for this boundary. This is the same as in section 3.7, only now the $\frac{\partial u}{\partial y}$ term is calculated by the compressible navier stokes equation.

$$\frac{\partial h}{\partial t} + \nabla \cdot \left(\frac{h^2}{2\mu_{liq}} \mu_{gas} \frac{\partial u}{\partial y} - \frac{h^3}{3\mu_{liq}} \frac{\partial P_{lub}}{\partial x} \right) \cdot h_{check} = -\frac{\partial c}{\partial y} D_{gas} \frac{M_{liq}}{\rho_l iq} \cdot h_{check} \tag{3.124}$$

and from equation 2.65:

$$P_{lub} = -\gamma_{liq} \frac{\partial^2 h}{\partial x^2} + \rho_{gas} g h \tag{3.125}$$

But the concentration constraint is a conditional constraint. In the model, the variable $x_{trans,Botttom}$ is defined at **GBR** as

$$x_{trans,Botttom} = \int tresshold_h(h) dx. \tag{3.126}$$

with

$$tresshold_h(h) = \begin{cases} 1 & \text{if } h <= 100 \cdot 10^{-9} \\ 0 & \text{if } h > 100 \cdot 10^{-9} \end{cases}$$

The boundary in between **GBL** and **GBR** is positioned at $x = xPos_{Init}$. The concentration constraint of boundary **GBR** is then defined as

$$\vec{n} \cdot (-D_{gas} \nabla c + c\vec{u}) \cdot c_{check,1}(x) + c \cdot c_{check,2}(x) = 0 \tag{3.127}$$

$$c_{check,1}(x) = \begin{cases} 1 & \text{if } x <= 100 \cdot xPos_{Init} + x_{trans,Botttom} \\ 0 & \text{if } x > 100 \cdot xPos_{Init} + x_{trans,Botttom} \end{cases}$$

$$c_{check,2}(x) = \begin{cases} 1 & \text{if } x < xPos_{Init} + x_{trans,Botttom} \\ 0 & \text{if } x >= xPos_{Init} + x_{trans,Botttom} \end{cases} \tag{3.128}$$

3.8.2 Not working

Despite the effort that was put into the model, it did not work the way it was supposed to work. However, it seems like the logic for the model is not per se wrong, but the software needs a different approach for this simulations. Due to time constraints, it was eventually decided to abandon this model.

3.8.3 Proof of principle

Despite the simulation not working completely, the principle of the drying liquid layer is proven to work in a far more simple model. This simpler model has the geometry shown in figure 3.13.

FIGURE 3.13: The adjusted geometry boundaries, **GL**/**GR** = gas left-/right, **GTL**/**GTR** = gas top left/right, **GBL/GBR** = gas bottom left-/right

In this geometry, no flow is solved for, a Poiseuille flow is asumed, given by

$$u_x(y) = \left(-\frac{4U_{max}}{H^2}(y - 0.5H)^2 + U_{max}\right).$$ (3.129)

, with $U_{max} = 0.009 m/s$ and $H = 4mm$. The heat transfer equation are ignored in the model. The diffusion equations are the same as for the model from figure 3.12, only the saturated concentration is set to a constant, as the temperature is not solved for. That constant is $c_{sat} = 1 mol/m^3$.

The height is tracked by using a similar equation as equation 3.124. Only now this is simplified to

$$\frac{\partial h}{\partial t} + \nabla \cdot \left(-1 \cdot 10^{-10} \nabla h\right) = 100 \frac{\partial c}{\partial y} D \cdot h_{check}$$ (3.130)

,with h the height of the liquid layer, c the concentration and $D = 1 \cdot 10^{-6} m^2/s$ the diffusion coefficient.

Initial values:
Layer thickness at $t = 0s = 20\mu m$

$$c_{t=0} = \begin{cases} c_{sat} & \text{if } x >= x_{front} \\ 0 & \text{if } x < x_{front} \end{cases}$$

Chapter 4

Experimental Setup

The experiments in this report were performed with two main setups.

The first one is a more simple approach, in which a glass plate is put on top of a metallic beaker filled with liquid. This beaker along with the liquid is heated and therefor there will be a temperature difference between the glass and the liquid. This will cause condensation at the bottom side of the glass (the side facing the liquid) which can then be measured with a microscope, using the procedure explained in section 2.14.

The second setup is with an air flow to transfer away the liquid vapor before it has a change to condense on the glass plate. The liquid is again heated to create the temperature difference between the liquid and the glass. However, when longer measurements are done, the whole setup heats up, causing the glass to heat up and thus reducing the temperature difference. To counter this effect, a second air flow is used, which goes over the glass plate, over the non-condensation side of the glass, to keep the temperature of the glass lower. This whole setup will be explained in section 4.2.2.

4.1 Experiment without external air flow

The experiment without external air flow is designed to get an idea of measuring condensation rates using optical interferometry. To do this a metal beaker with a wall thickness of $0.5cm$ on a hot plate is used. The beaker is metal, because of its high thermal conductivity, to make sure all the liquid inside will heat up quickly. Doing the same experiments with a glass beaker resulted in longer times before the liquid reaches the temperature of the hot plate, whereas for a metal beaker, the heat distribution is way faster due to the high thermal conductivity of the metal, as is shown in section 5.2. For the liquid, Ethylene Glycol was used, because of its low toxicity, moderate surface tension and high boiling point. Experiments were also done with water, but the main problem there is the high surface energy. This factor does not stimulate the spreading of the liquid when it is condensed on the glass substrate leading to drop-wise condensation as opposed to the desired film-wise condensation observed with EG. Due to this the forming of an uniform layer is more difficult as the condensed droplets do not want to spread out as much, which will result in a microscopic view of figure 4.1. Ethylene Glycol however, has a much lower surface energy, resulting in a much higher spreading of the liquid when condensed, increasing the changes of a uniform condensation layer.

4.1.1 Cleaning Procedure

Although the simple beaker experiment does not require a lot of complicated steps, the procedure to get the best results is still a time consuming one, as efforts have

shown that a extraordinary clean glass is needed in order to get usable results. A glass that is not cleaned enough will give a non uniform condesation layer, due to filth on the substrate, which will stop the spreading of the liquid. This will result in a high position dependence for the growth of the condensation layer as the liquid that is condensed is held up by dirt on the glass. This results in situations like figures 4.1, 4.2 and 4.3. Whereas in the case of a sufficiently cleaned glass, it looks like figure 4.4.
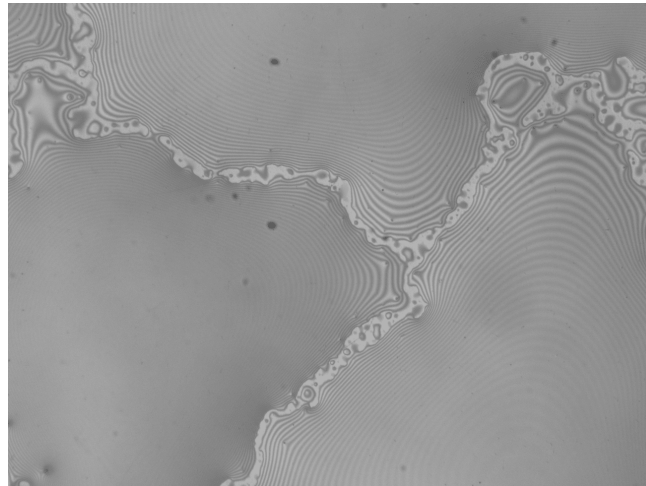
FIGURE 4.1: Microscope view of the glass substrate after 30 seconds, without a clean enough glass and water, which both contribute to a non-uniform layer of condensation.
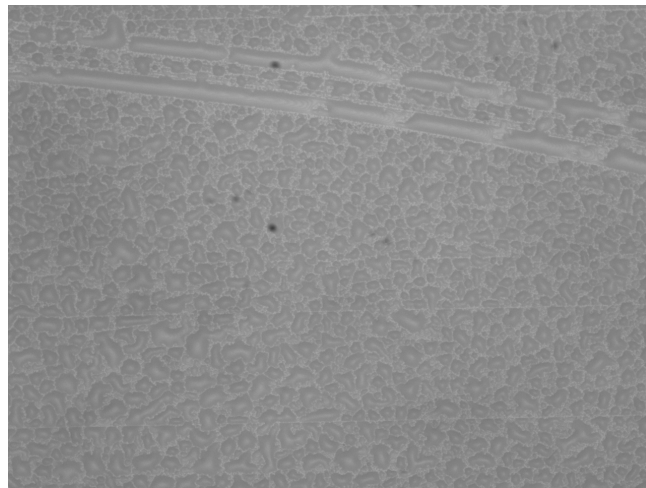
FIGURE 4.2: Microscope view of the glass substrate after 30 seconds, without a clean enough glass and water, which both contribute to a non-uniform layer of condensation.
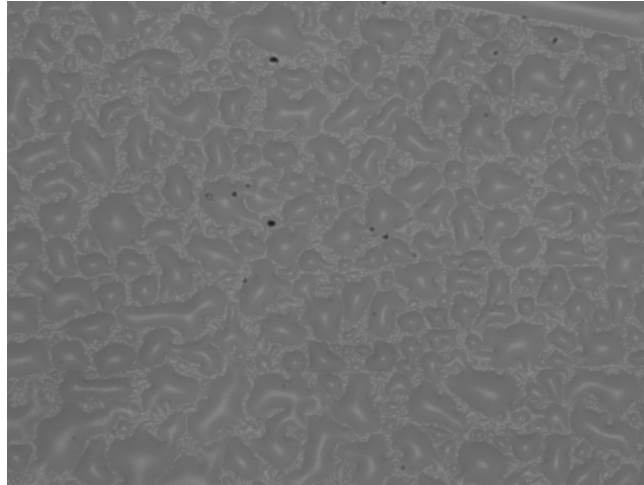
FIGURE 4.3: Microscope view of the glass substrate after 30 seconds, without a clean enough glass and water, which both contribute to a non-uniform layer of condensation.
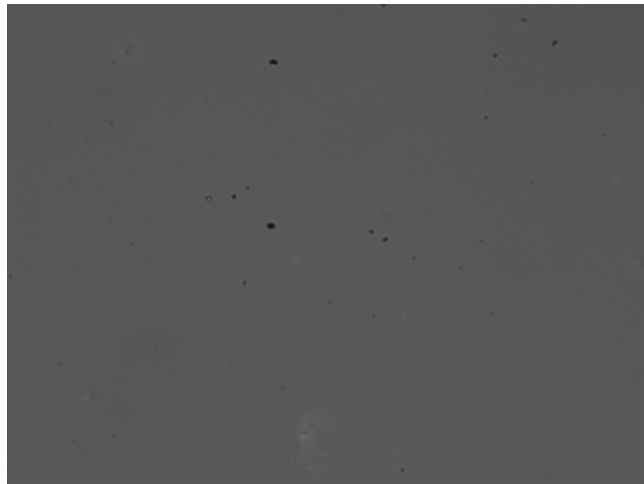
FIGURE 4.4: Microscope view of the glass substrate after 30 seconds, when the glass is cleaned enough for an almost uniform layer of condensation.

So in order to prevent contamination, the glass is thoroughly cleaned before measuring. This is done by cleaning the glass substrate in an ultrasonic bath. In this bath, a larger beaker with ultra pure water and a soap solution is floating. The glass is put in here and cleaned for about 20 minutes. After this the glass is cleaned by some more ultra pure water, before it is dried. The time between the drying and the measurements has to be as short as possible, as dirt can already accumulate on the glass substrate. Another important note is to never touch the glass by hand, but only with a pair of tweezers with an as small as possible surface contact area, to minimally contaminate the substrate. When everything is done correctly, a movie with frames looking like figure 4.4 is obtained, the code from appendix D is used to process the data and get the condensation rate.

4.2   Transition point

4.2.1   Transition point model procedure

The model from section 3.5 is used to calculate the "transition point" from no condensation to condensation at the top boundary of the domain. The full process towards an accurate result consist of two steps. This due to the fact that the point where the condensed layer starts, also affects the the simulation itself. So the calculation to determine where the transition point is, is step one, whereas implementing this information into the model and running another simulation is step 2.

The way to realise these two steps is by starting with stretching the No-Flux boundary (**GTL**) from figure 3.9 over the whole top boundary (with the exeption of the small transition boundary **GT+**). This means that nowhere at the top boundary, the concentration condition is set to the saturated concentration from equation 2.26. During the first simulation the concentration at the top boundary can get higher than the saturated concentration, because of high temperature gradients between the bottom and top of the gas, and the liquid layer on top of the substrate. After the simulation, it is checked where on the top boundary the concentration gets higher than the saturated concentration. The point most to the left where this is true is then defined as the transition point, as condensation would have happened there in the real case. A second simulation is than run with the "transition point" from a Non-flux (**GTL**-boundary) to a set concentration (**GTR**-boundary) exactly at that point.
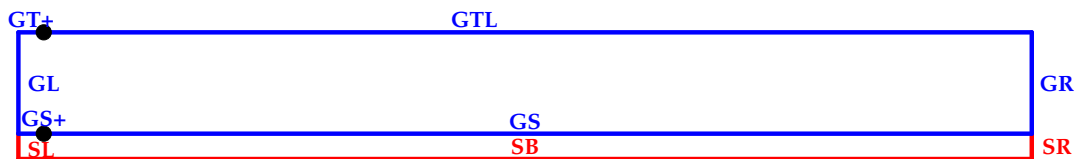
FIGURE 4.5: transition point Model, **Step 1**, Physics in section 3.5, **GL**/**GR** = gas left/right, **GTL**/**GTR** = gas top left/right, **GS** = gas-substrate interface, **GT+** = gas top extra, **GS+** = gas-substrate interface extra, **SL**/**SR** = substrate left/right, **SB** = substrate bottom
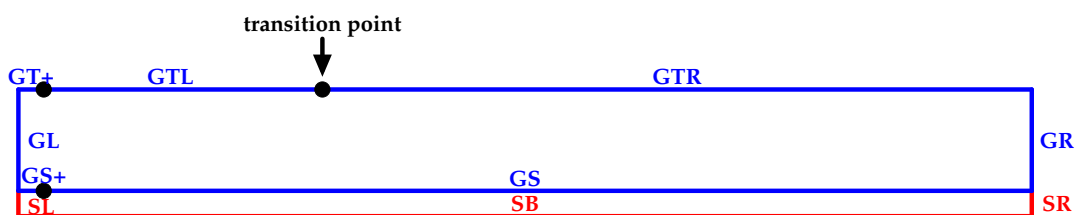
FIGURE 4.6: transition point Model, **Step 2**, Physics in section 3.5, **GL**/**GR** = gas left/right, **GTL**/**GTR** = gas top left/right, **GS** = gas-substrate interface, **GT+** = gas top extra, **GS+** = gas-substrate interface extra, **SL**/**SR** = substrate left/right, **SB** = substrate bottom

4.2.2   Transition point experiment

Figure 4.7 shows a drawing of the simplified setup used to find the transition point between no condensation and condensation.
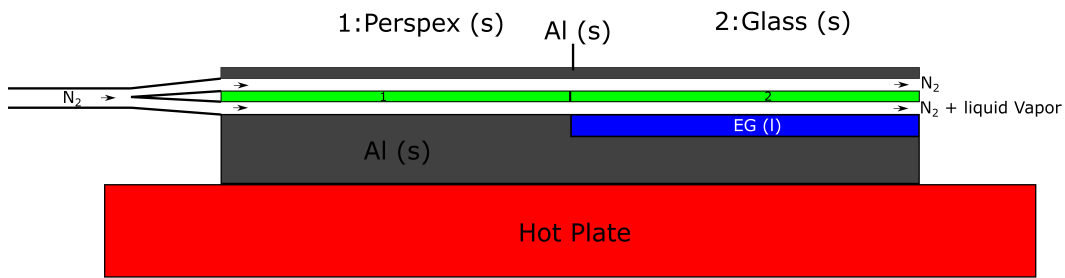
FIGURE 4.7: Simplified drawing of the experimental setup used to find the transition point from no condensation to condensation

Figure **??** and **??** show experimental setup used for the transition point experiments. Section A gives a more detailed schematic overview of the components of the setup.

The glass used for these experiments is also cleaned the way it was described in section 4.1.1.
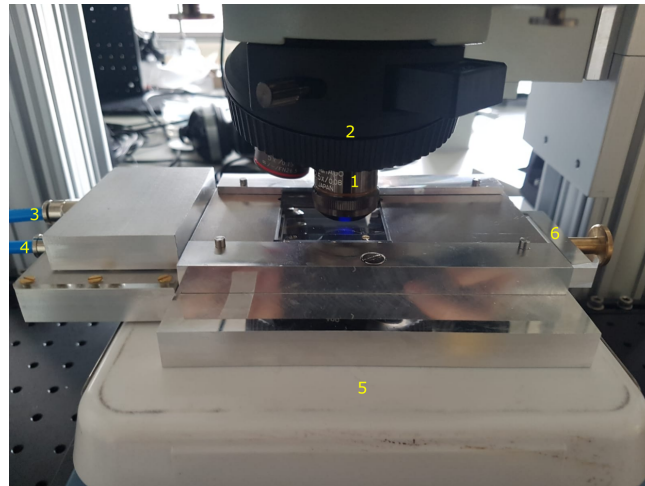
FIGURE 4.8: Experimental setup used for transition point experiments, 1: **Objective**, 2: **Microscope**, 3/4: **controlled temperature nitrogen top/bottom flow**, 5: **Hot plate**, 6: **Removable liquid bath**
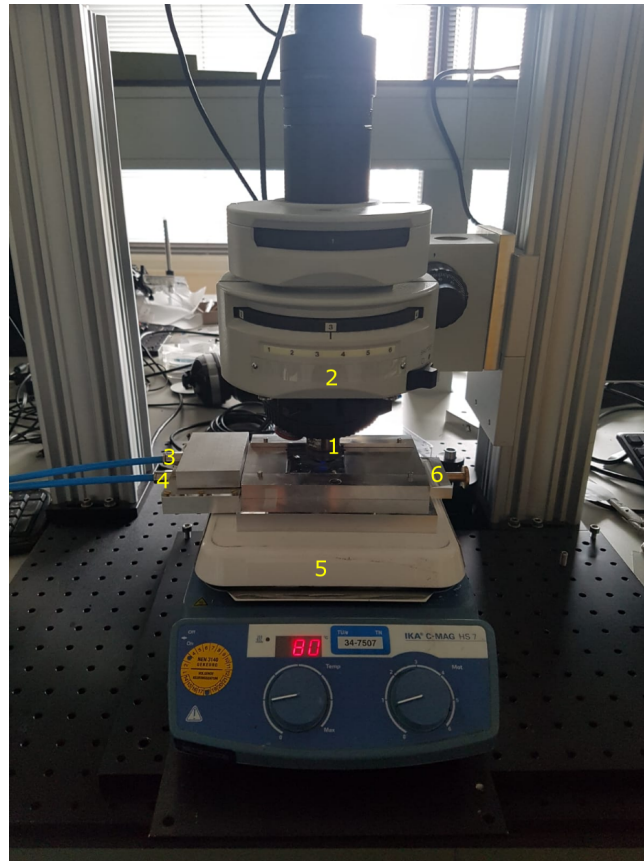
FIGURE 4.9: Experimental setup used for transition point experiments, 1: **Objective**, 2: **Microscope**, 3/4: **controlled temperature nitrogen top/bottom flow**, 5: **Hot plate**, 6: **Removable liquid bath**

The gas used for the flow in the experiments is pure nitrogen. This due to the easy accessibility and also the fact that this is completely non-humid gas. The controlled temperature at the inlet parts of the top and bottom flow, is taken care for by a circulation thermostat. It controls the temperature of a water bath, and circulates this water trough a heat exchanger trough which the gas is flowing before it enter the experimental setup. The water bath cooler is shown in figure 4.10.

FIGURE 4.10: Circulation thermostat that is used to control the temperature of the gas inflow of the experimental setup

4.3 Flow meter

The air flow that goes into the heat exchanger, which is temperature controlled by the water bath thermostat, is measured by an air flow meter. This meter is shown in figure 4.11.

Flow meter
Manufacturer: Bronkhorst High-Tech B.V.
Model Nr: F-112AC-HAD-44-V

This flow meter gives an electronic signal regarding the flow velocity. Therefore another setup is used to translate the voltage to a flow. The other way around, it is also needed to put a voltage on the flow meter, in order to regulate the flow velocity. The velocity measured there is not the maximum air velocity in the setup, which is a variable that is often used in this report. To translate the measured air velocity to the setup air velocity, two steps has to be taken. First, the air flow is seperated into two flows after the measuring point. This means that the air flow is divided by 2. After the air goes into the setup, one has to take in mind the geometry of that setup. The width of the channel that goes over the liquid is *6cm*, this is equal to the end of the inlet part, shown in figure A.2. The height of this channel in the setup is *2mm*. To translate the litre per minute value from the flow meter, to the maximum air velocity used in the report, the code in appendix B is used in Mathematica.
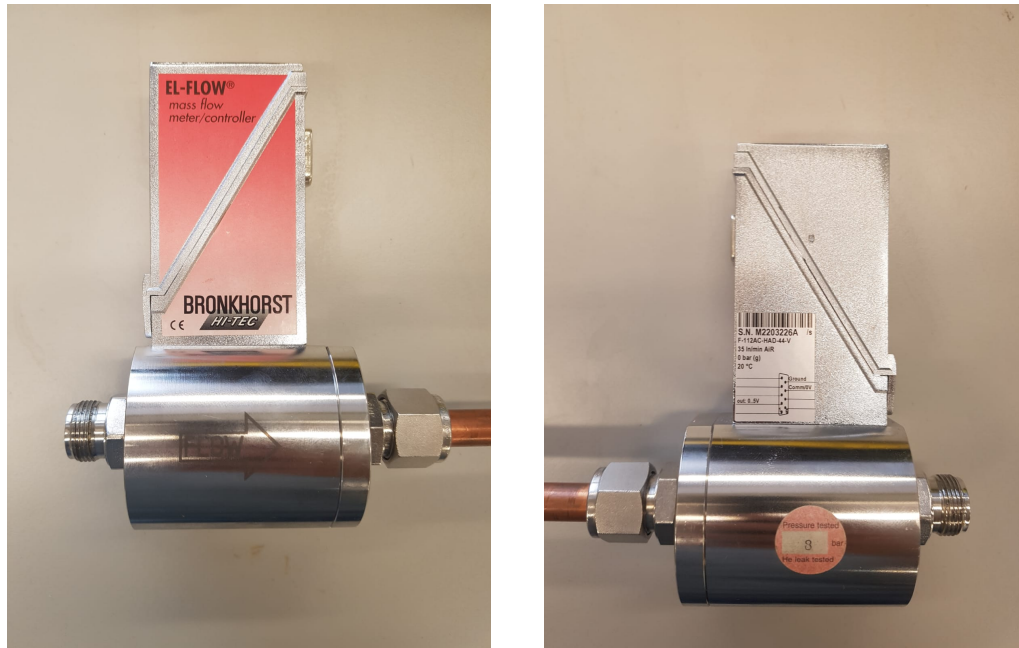
<table>
<tr><td>(A) frontside</td><td>(B) backside</td></tr>
</table>

FIGURE 4.11: Flow meter used to measure air flow velocity

4.4 Microscope

Figure 4.12 shows the reference frame to illustrate the sizes of the microscope pictures in this report.

   Objective: **MPlanApo 2.5x/0,08**
Magnification changer: **1 or 2** (setting 1 or setting 2 in images)
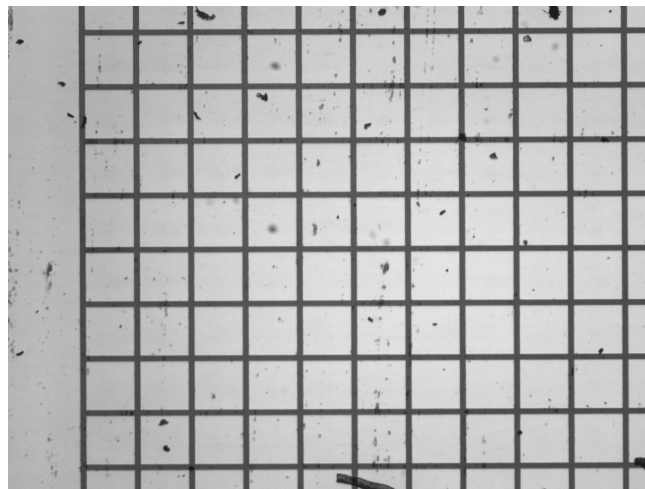
FIGURE 4.12: Microscope view for reference frame, one square grid
has sides with length $200\mu m$. Magnification changer: 1

Chapter 5

Results

5.1 Falling droplet displacements

To investigate the influence of the air flow on the trajectory of a falling droplet, the equations in section 3.2 are used. The liquid that is jetted is assumed to be Ethylene glycol, whereas the jetting velocity in the vertical direction is around $6m/s$ (Chuang, 2017). The droplets that are used are normally $6pL$. The height of the printhead is $1mm$ and the maximum air flow velocity is $1m/s$. Several of these values will be variable at one point, otherwise they will be at the mentioned value. Figure 5.1 shows the trajectory of a jetted droplet.
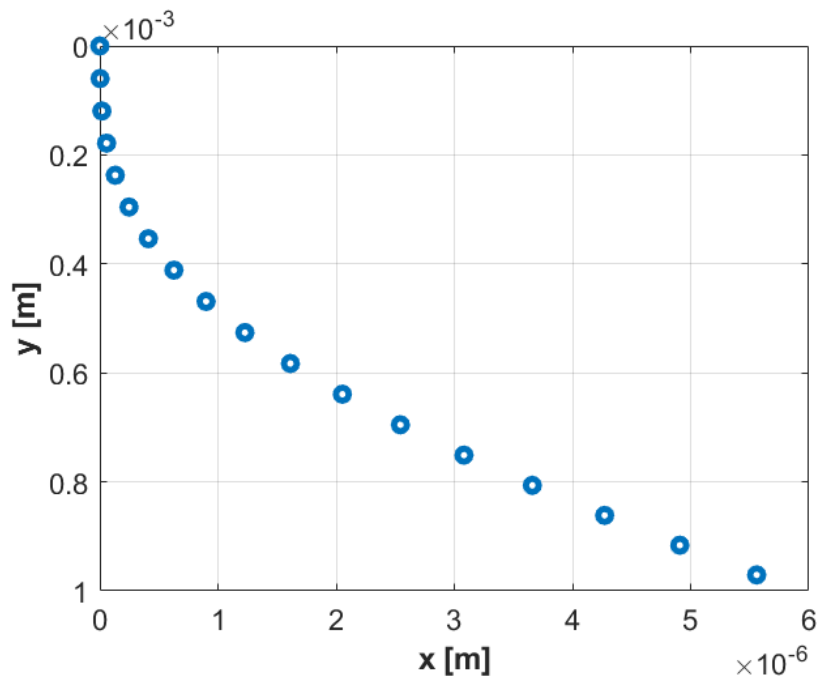
FIGURE 5.1: Trajectory of a droplet being jetted, with $V = 6pL$, $U_{max} = 1 \cdot \hat{x}m/s$, $H = 1mm$, $U_{jet} = 6 \cdot \hat{y}m/s$, $t_{landing} = 1.8s$, $dt = 0.1s$, this is also the time between two positions of the droplet

In the next sections, the influence of several variables on the displacement of the droplet is investigated. Note that the exact results was shown in equations 3.7 and 3.7. However, especially the x component of the solution is quite complicated, so in this chapter a more basic relation is found.

5.1.1   Volume droplet

First the influence of the volume droplet is investigated. Figure 5.2 shows the displacement d from figure 3.1 vs the volume of the droplet.
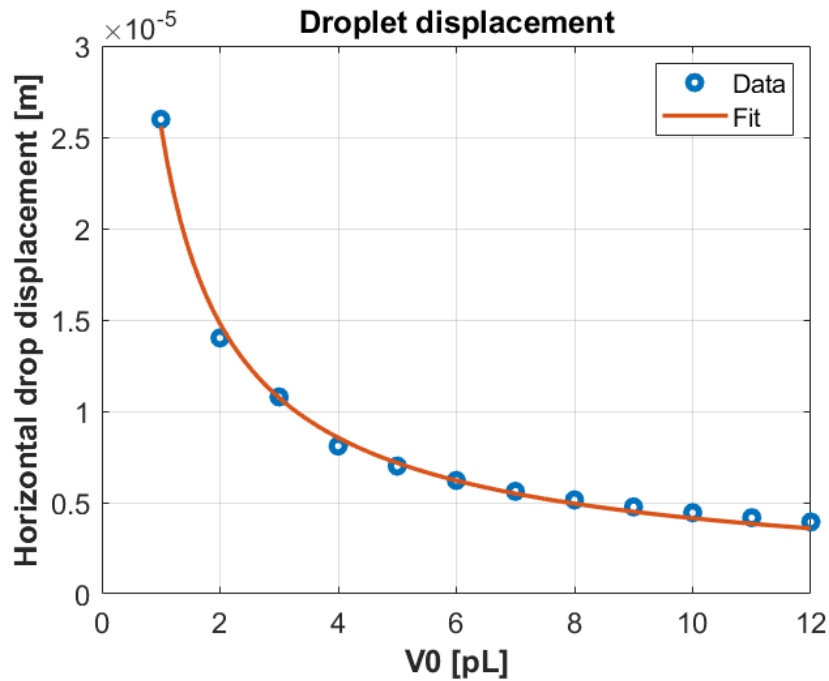
FIGURE 5.2: Displacement 'd' of a jetted droplet vs its volume, with $U_{max} = 1 \cdot \hat{x}m/s$, $H = 1mm$, $U_{jet} = 6 \cdot \hat{y}m/s$, Fit data in table 5.1

Fit function $y = ax^b$		
Variable	Value	Standard error
a	$3.49588 \cdot 10^{-17}$	$1.54204 \cdot 10^{-17}$
b	-0.79098	0.03896

TABLE 5.1: Fit values for fit in figure 5.2

5.1.2   Height printhead

Figure 5.3 shows the influence of the height on the displacement of the droplet when landend in respect to where it was jetted.
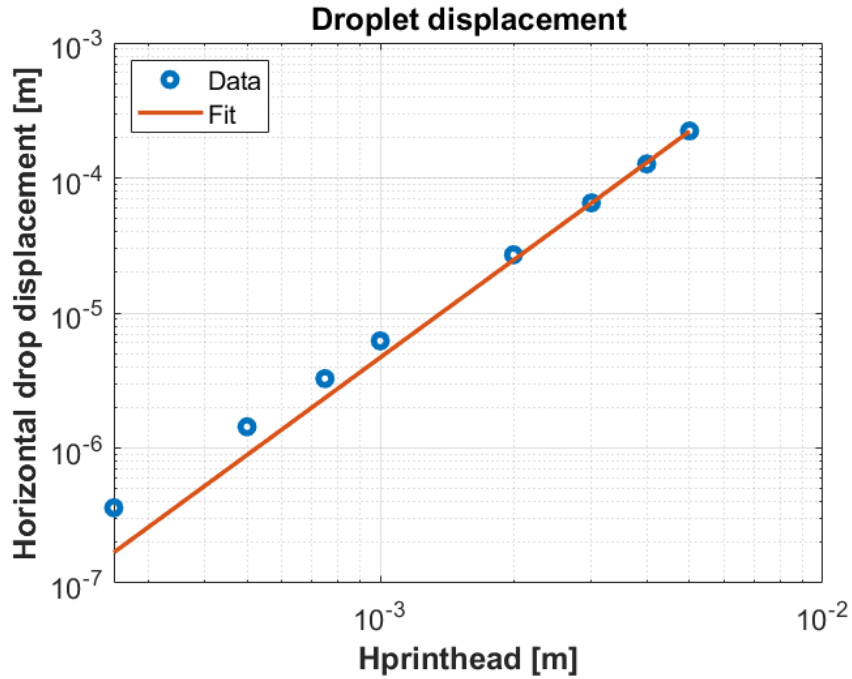
FIGURE 5.3: Loglog plot of the displacement 'd' of a jetted droplet vs height printhead, with $U_{max} = 1 \cdot \hat{x}\,m/s$, $V = 6pL$, $U_{jet} = 6 \cdot \hat{y}\,m/s$, Fit data in table 5.2

Fit function $y = ax^b$		
Variable	Value	Standard error
a	72.61216	16.01012
b	2.39702	0.04222

TABLE 5.2: Fit values for fit in figure 5.3

5.1.3 Air flow velocity

Figure 5.4 shows the influence of the air flow velocity on the displacement of the droplet when landend in respect to where it was jetted. The variable U_{max} is the maximum velocity in the Poiseuille profile flow.
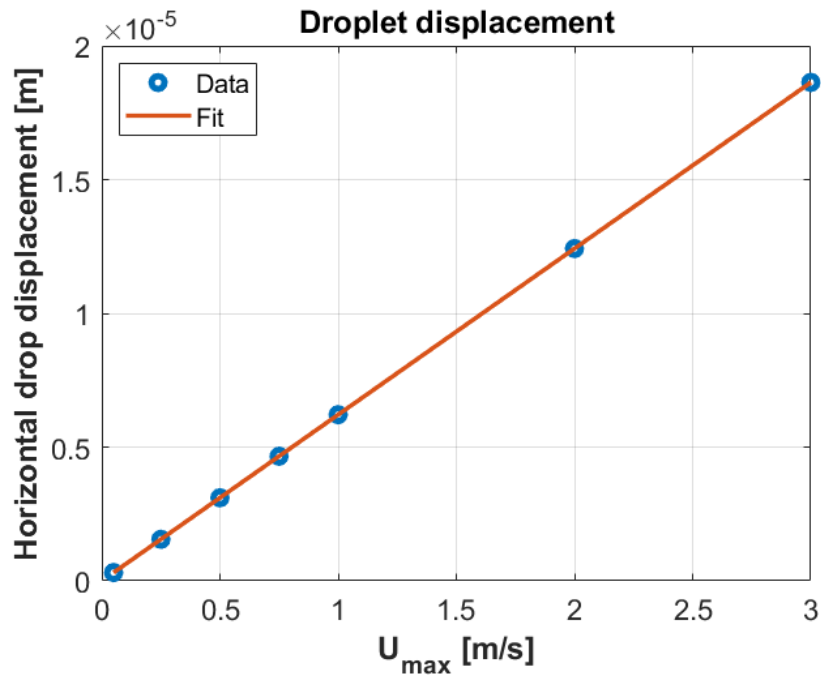
FIGURE 5.4: Displacement 'd' of a jetted droplet vs the maximum air velocity, with $H = 1mm$, $V = 6pL$, $U_{jet} = 6 \cdot \hat{y}m/s$, Fit data in table 5.3

Fit function $y = ax^b$		
Variable	Value	Standard error
a	$6.21140 \cdot 10^{-6}$;	$2.05808 \cdot 10^{-21}$
b	1	$3.52313 \cdot 10^{-16}$

TABLE 5.3: Fit values for fit in figure 5.4

5.1.4   Jet velocity

Figure 5.5 shows how the drop displacement is related to the jetting velocity of the printhead.
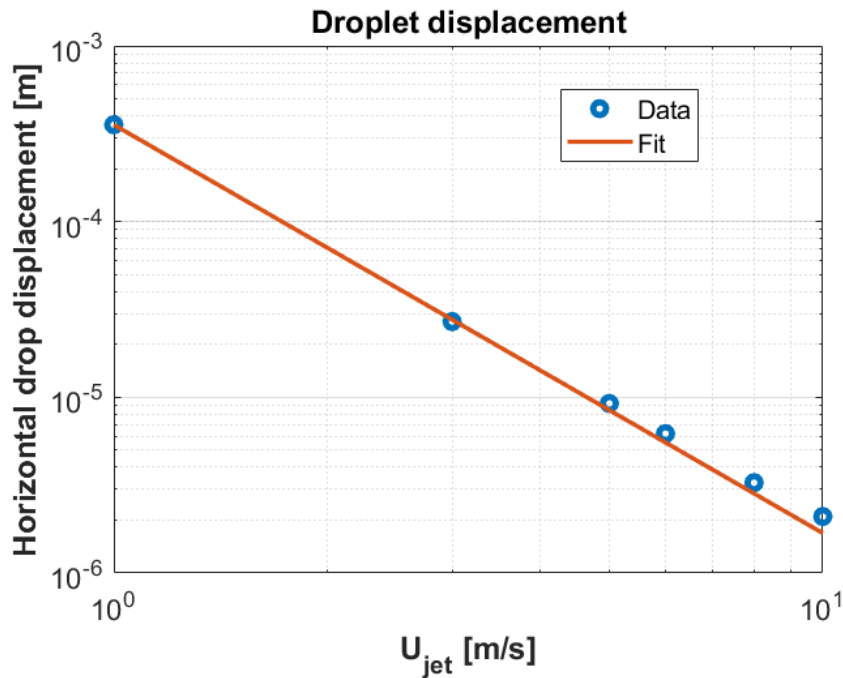
FIGURE 5.5: Loglog plot of the displacement '*d*' of a jetted droplet vs jet velocity, with $H = 1mm$, $V = 6pL$, $U_{max} = 6 \cdot \hat{x}m/s$, Fit data in table 5.4

Fit function $y = ax^b$		
Variable	Value	Standard error
a	$3.55669 \cdot 10^{-4}$;	$6.94012 \cdot 10^{-7}$
b	-2.32404	0.01949

TABLE 5.4: Fit values for fit in figure 5.5

5.2   Heating up liquid in beaker-timescales

The liquid used for the experiment without external airflow was ethylene glycol, to achieve the uniform condensation, which was described in section 4.1. Simulations were done to check the amount of time it takes for a beaker of liquid to heat up to a state in which the temperature can be assumed uniform at the desired value. Figure 5.6 and 5.7 show the temperature of the liquid and the beaker after respectively 60 and 1800 seconds. Figure 5.8 shows the temperature development over time of the centre of the beaker, at the top of the liquid. All figures clearly show that the temperature after a quarter of an hour is more or less constant.
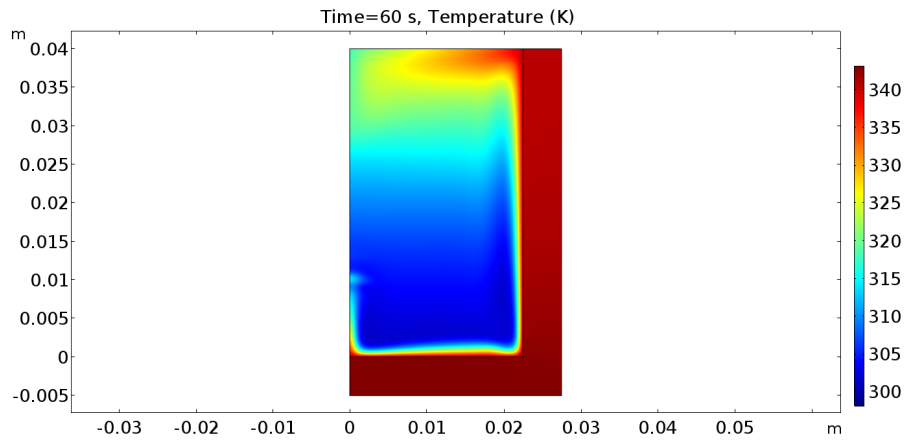
FIGURE 5.6: Temperature of the aluminium beaker and the liquid after 60 seconds, hot plate at $70^o C$
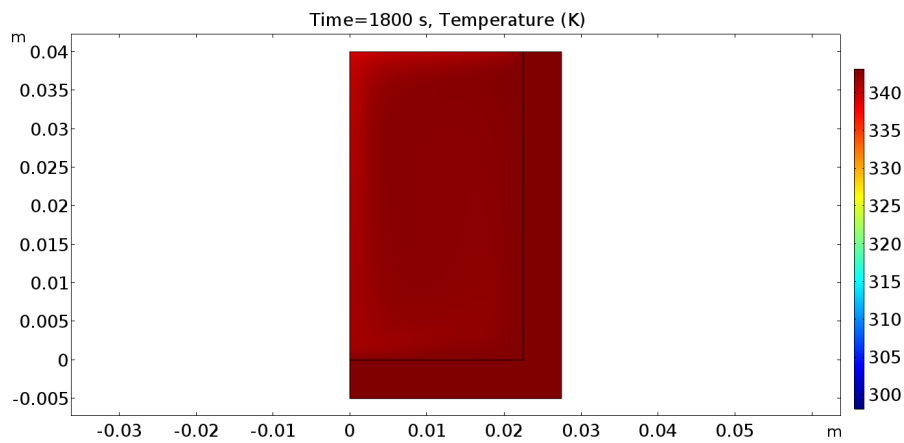
FIGURE 5.7: Temperature of the aluminium beaker and the liquid after 1800 seconds, hot plate at $70^o C$
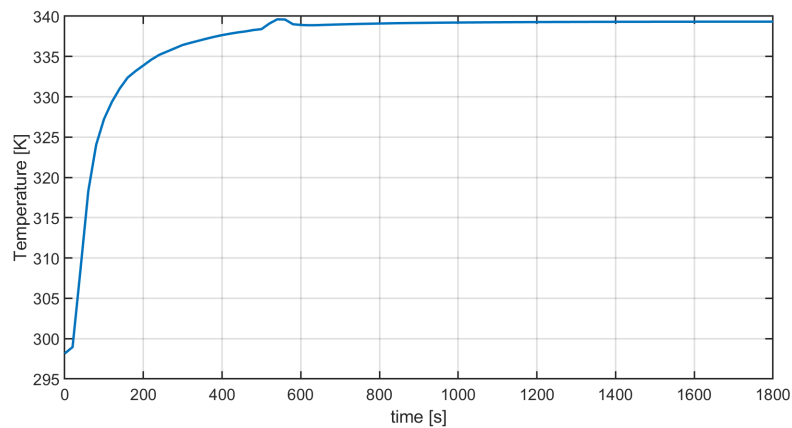
FIGURE 5.8: Temperature at the centre of the metal beaker, at the top of the liquid, plotted over time, hot plate at $70^o C$

5.3 Experiment without external airflow

5.3.1 Model

The model used was the model from section 3.4. Figure 5.9, 5.10 and 5.11 show respectively the temperature, the horizontal velocity and the concentration of EG vapor after 20 seconds of simulating.
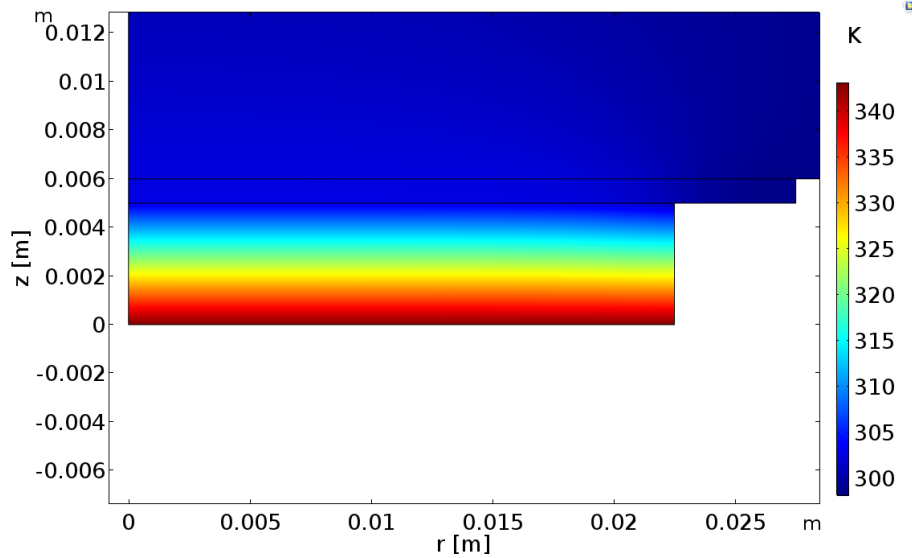
FIGURE 5.9: Temperature at $t = 20s$, with $T_{EG} = 70^oC$ and $H = 5mm$, focussed on gas domain.
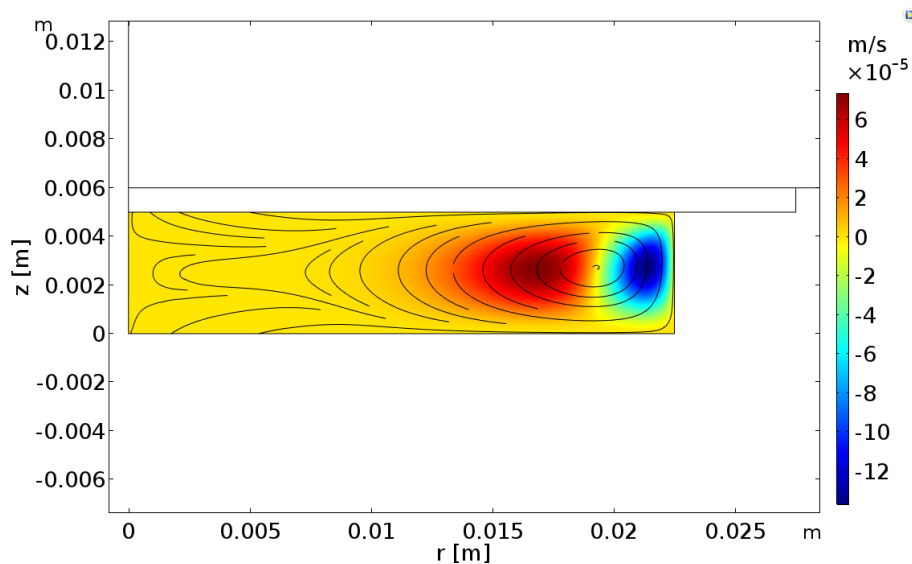
FIGURE 5.10: Horizontal velocity at $t = 20s$, with $T_{EG} = 70^oC$ and $H = 5mm$, focussed on gas domain.
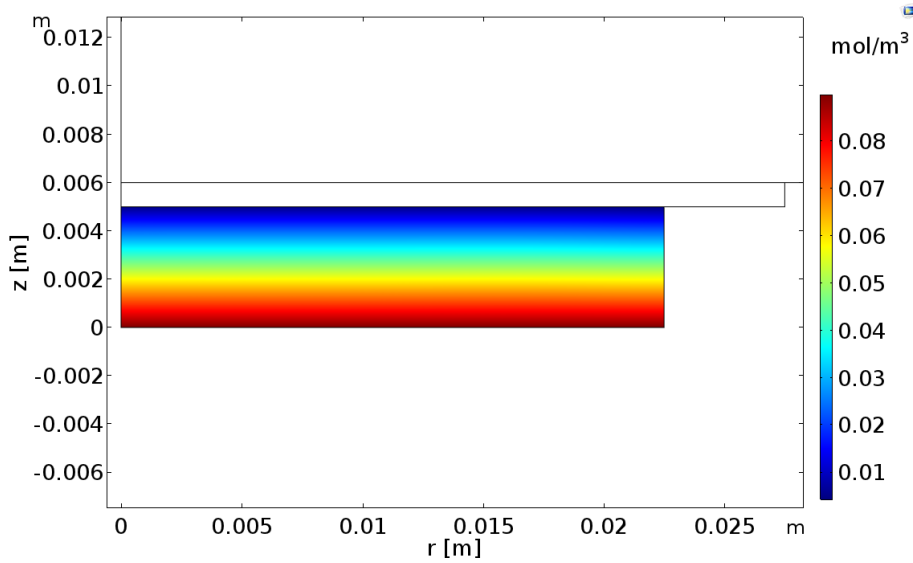
FIGURE 5.11: Concentration of EG vapor at $t = 20s$, with $T_{EG} = 70^o C$ and $H = 5mm$, focussed on gas domain.

Condensation Rate

In order to track the condensation, the condensation rate at the glass, precisely above the centre of the beaker (so $r = 0$) is plotted against the time for several situations in figure 5.12. Note that

$$Condensation Rate = \left| \frac{\partial c}{\partial z} D(T_{gas}) \frac{M_{EG}}{\rho_{EG}} \right| \tag{5.1}$$
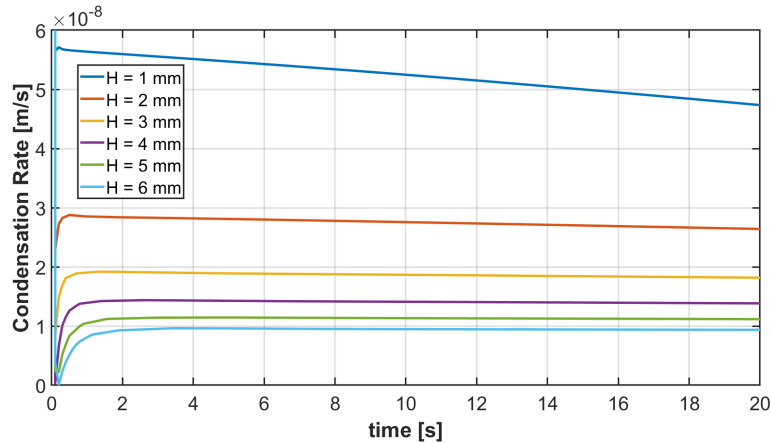
FIGURE 5.12: Condensation rate for several heights plotted against time, $T_{EG} = 70^o C$, zoomed in

It can be seen that the condenstaion rate, with the exception of the $H = 1mm$ case, becomes quite steady after 5 seconds. Therefore, the value for the condensation rate is taken at 5 seconds, in order to compare this to the experimental values. Also because this is the time that it takes before it is possible to measure condensation in the beaker experiments.

For the experiments, the condensation rate is determined the way it is described in section 2.14.

Height vs condensation rate

Figure 5.13 shows the condensation rate plotted agaisnt the height of the gas domain. This is also the distance between the liquid and the glass.
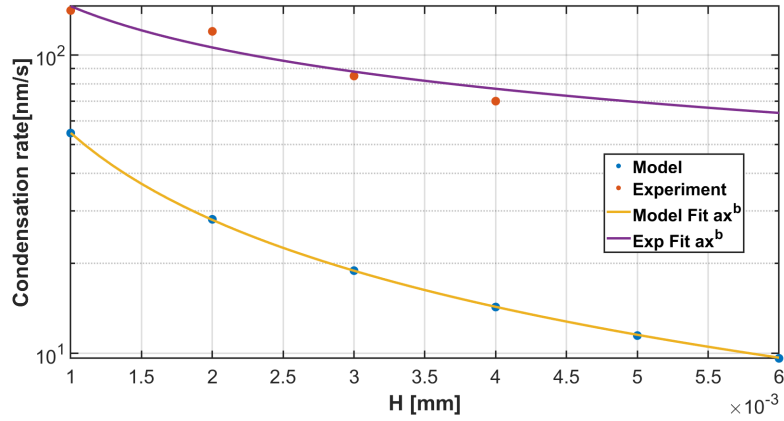
FIGURE 5.13: Condensation rate plotted against the height at $t = 5s$ for model. $T_{EG} = 70^0 C$, Fit data in table 5.5 and 5.6

Fit function $y = ax^b$		
Variable	Value	Standard Error
a	$6.79971 \cdot 10^{-11}$	$9.9895 \cdot 10^{-15}$
b	-0.96861	0.00227

TABLE 5.5: Fit values for Model fit in figure 5.13

Fit function $y = ax^b$		
Variable	Value	Standard error
a	$6.07246 \cdot 10^{-9}$	$4.02694 \cdot 10^{-9}$
b	-0.46008	0.10441

TABLE 5.6: Fit values for Experiment fit in figure 5.13

Temperature vs condensation rate

Figure 5.14 shows the condensation rate plotted agaisnt the initial temperature difference between the liquid and the glass.
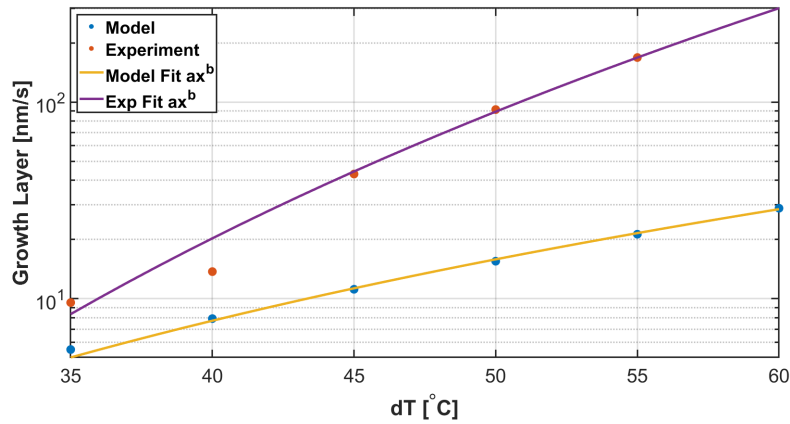
FIGURE 5.14: Condensation rate plotted against the temperature difference between the liquid and the glass at $t = 5s$ for model. $H = 5mm$, Fit data in table 5.7 and 5.8

Fit function $y = ax^b$		
Variable	Value	Standard Error
a	$5.32801 \cdot 10^{-14}$	$1.58778 \cdot 10^{-14}$
b	3.22169	0.07205

TABLE 5.7: Fit values for Model fit in figure 5.14

Fit function $y = ax^b$		
Variable	Value	Standard error
a	$4.56918 \cdot 10^{-19}$	$5.50487 \cdot 10^{-19}$
b	6.6459	0.28359

TABLE 5.8: Fit values for Experiment fit in figure 5.14

In an attempt to make the model better agree with the experiment, the model was expanded with the actual liquid and beaker in order to better represent the experiment. Despite the effort that was put into that model, the results did not seem to be realistic in any kind, as velocities quickly turned to values in the order of kilometres per hour and temperatures above 150 degrees Celsius.

5.4 Transition point Model

5.4.1 Model

The model from section 3.5 in combination with the procedure of section 4.2 was used to investigate the position of condensation, also know as the transition point. Figures 5.15, 5.16 and 5.17 show some results of the simulations. The liquid used here is Ethylene glycol. Until mentioned otherwise, these simulations were time dependent, however, it was clear that after 0.1 seconds a steady state seemed to be reached in almost all cases, except for extraordinary ones with low velocities, or long domains.
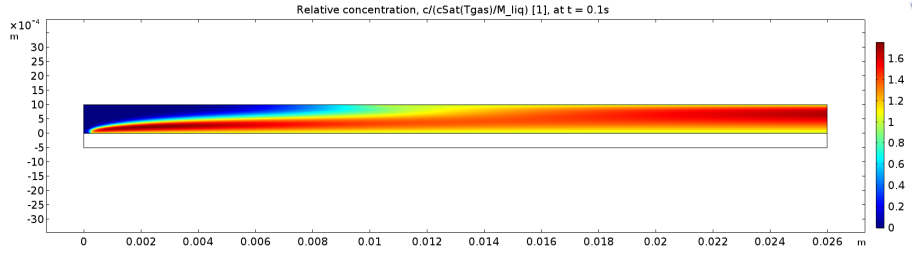
FIGURE 5.15: Relative concentration of EG vapor with respect to saturated concentration c_{Sat} at t=0.1s, $T_{sub} = 70^oC$, $T_{Inlet} = T_{amb}$ and $U_{max,inlet} = 1.5m/s$
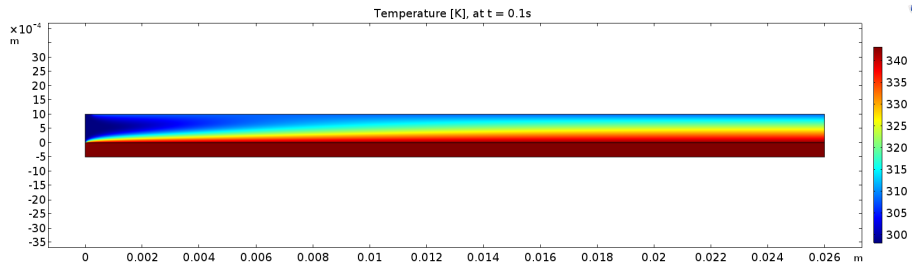
FIGURE 5.16: Temperature at t=0.1s, $T_{sub} = 70^oC$, $T_{Inlet} = T_{amb}$ and $U_{max,inlet} = 1.5m/s$
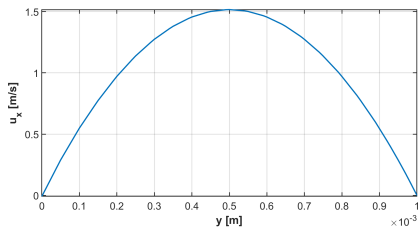
(A) u_x at $x = 0m$ plotted against y
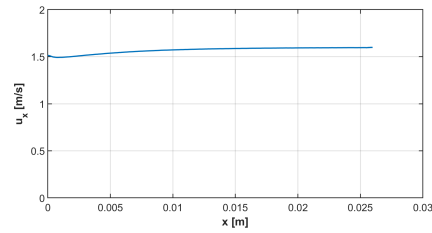
(B) u_x at $y = 0.5 \cdot 10^{-3}m$ plotted against x

FIGURE 5.17: Velocity profile, at t=0.1s, $T_{sub} = 70^oC$, $T_{Inlet} = T_{amb}$ and $U_{max,inlet} = 1.5m/s$

Our goal was to determine the position of the transition point at the top of the domain. As described in section 4.2, this simulation was done in 2 steps. To confirm that the second step, adding the condensation layer, was done correctly, figure 5.18 shows the relative concentration at the top of the domain. An important note regarding figure 5.18 is that the concentration is given in $\left[\frac{mol}{m^3}\right]$, whereas the function $c_{Sat}(T_{gas})$ has units $\left[\frac{kg}{m^3}\right]$.
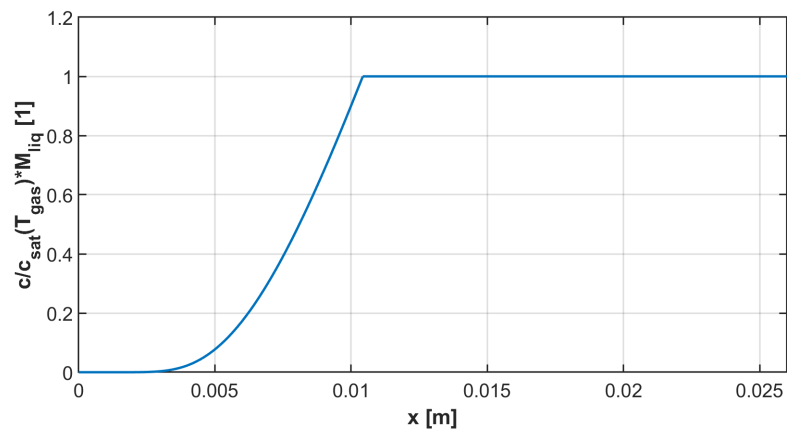
FIGURE 5.18: Relative concentration with respect to saturated concentration c_{Sat} at t=0.1s at y=1mm (Top channel)

It can be seen that the concentration, after the transition point, is set to the saturated concentration, which is constant due to the temperature constraint set in the model. Important however is, that the transition to the saturated concentration happens exactly at the point where the concentration is equal to the saturated concentration.

Height dependency

Ethylene Glycol
Figure 5.19 shows the dependency of the transition point on the channel height.
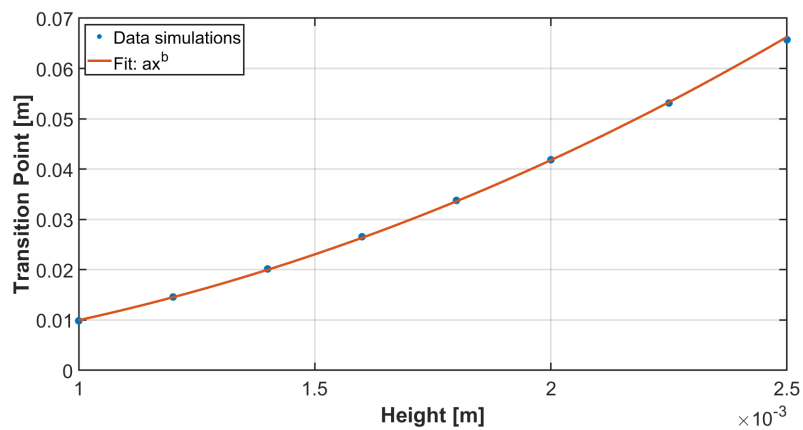
FIGURE 5.19: Transition point vs height, $U_{max,Inlet} = 1.5m/s$, $\Delta T = 35K$, fit data in table 5.9

Fit function $y = ax^b$			
Variable	Value	95% low bound	95% high bound
a	$1.589 \cdot 10^4$	$1.3362 \cdot 10^4$	$1.8409 \cdot 10^4$
b	2.067	2.043	2.092

TABLE 5.9: Fit values for fit in figure 5.19

Equation 2.33 indicated dat the entrance length, here the transition point, is proportional to the height squared. The fit in table 5.9 also shows this, as the exponent is very close to 2.

Toluene

Figure 5.20 shows the dependency of the transition point on the height if toluene is used for the liquid.
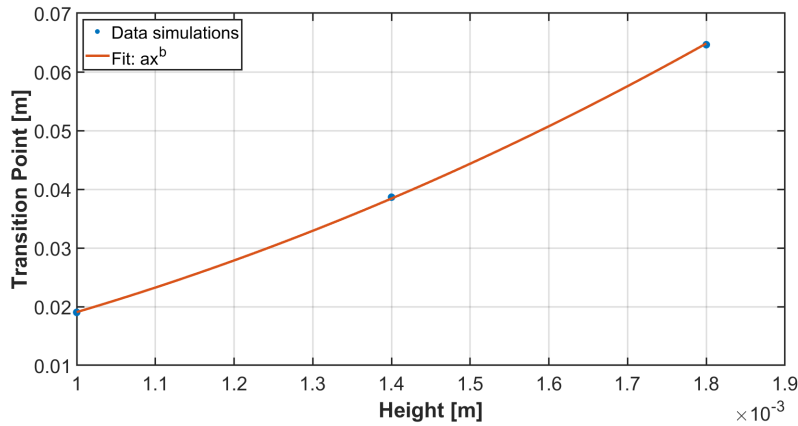
FIGURE 5.20: Transition point vs height, $U_{max,Inlet} = 1.5 m/s$, $\Delta T = 35K$, fit data in table 5.10

Fit function $y = ax^b$			
Variable	Value	95% low bound	95% high bound
a	$3.3651 \cdot 10^4$	$-1.4312 \cdot 10^4$	$8.1614 \cdot 10^4$
b	2.082	1.867	2.298

TABLE 5.10: Fit values for fit in figure 5.20

Velocity dependency

Ethylene Glycol

Figure 5.21 in combination with table 5.11 show the transition point - velocity relation. Not that the velocity is the average velocity over the height of the channel at $x = FP$. This means

$$U_{avg,FP} = \frac{1}{H} \int_0^H u_x dy. \tag{5.2}$$

Equation 2.33 stated that the transition point (entrance length) should be linearly proportional to the velocity. The fit results in table 5.11 show that this indeed looks true.
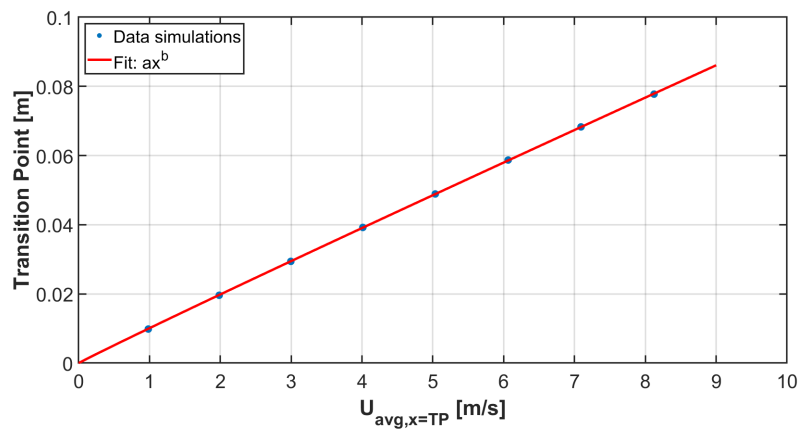
FIGURE 5.21: Transition point vs average velocity at x=FP, $H = 1mm$, $\Delta T = 35K$, fit data in table 5.11

Fit function $y = ax^b$			
Variable	Value	95% low bound	95% high bound
a	0.0101	0.01	0.0102
b	0.9753	0.9699	0.9807

TABLE 5.11: Fit values for fit in figure 5.21

Toluene

Figure 5.22 and table 5.12 show the graph and the fit data regarding the velocity influence on the transition point.
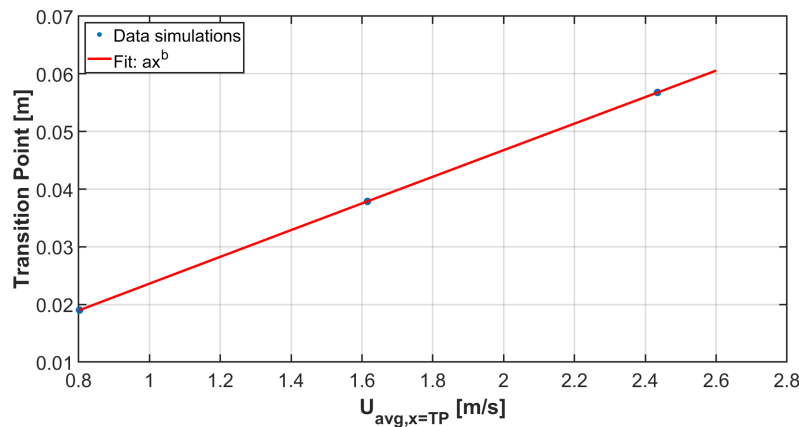
FIGURE 5.22: Transition point vs average velocity at x=FP, $H = 1mm$, $\Delta T = 35K$, fit data in table 5.12

Fit function $y = ax^b$			
Variable	Value	95% low bound	95% high bound
a	0.02362	0.02335	0.02389
b	0.9857	0.9707	1.001

TABLE 5.12: Fit values for fit in figure 5.22

Temperature dependency

Ethylene Glycol

Last dependency is the temperature. Equation 2.33 does not immediately show a clear relation between the temperature and the transition point. However, when filling in all the values in the equation, it is possible to compare the model data with the absolute values that come out of the equation. Figure 5.23 shows the data of the model, the results of equation 2.33 and the fit going through the model data.
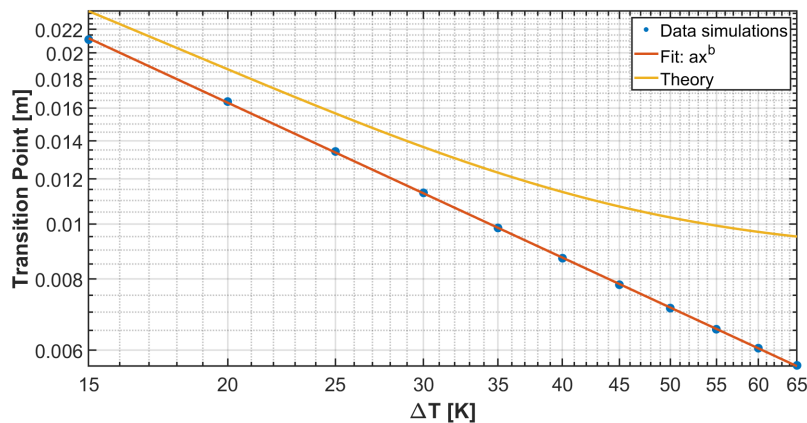
FIGURE 5.23: Transition point vs bottom temperature, $H = 1mm$, $U_{max,Inlet} = 1.5m/s$, fit data in table 5.13

Fit function $y = ax^b$			
Variable	Value	95% low bound	95% high bound
a	0.2468	0.2423	0.2513
b	−0.906	−0.911	−0.9009

TABLE 5.13: Fit values for fit in figure 5.23

Figure 5.23 show that the result of the models are close to equation 2.33. The offset can have different reasons, as a few assumptions were made to construct equation 2.33. However, the overall proportionality between the transition point and the temperature are close to equal. This proportionality is described by the fit going to the data, with values in table 5.13.

Toluene

Figure 5.24 and table 5.14 show the graph and the fit data regarding the temperature influence on the transition point.
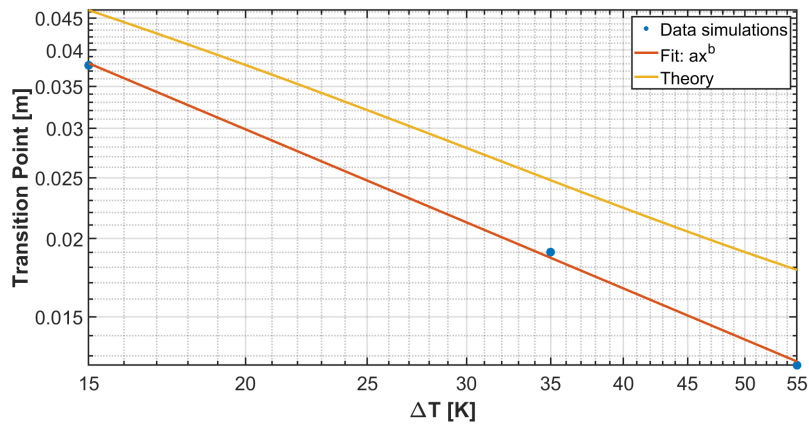
FIGURE 5.24: Transition point vs bottom temperature, $H = 1mm$, $U_{max,Inlet} = 1.5m/s$, fit data in table 5.14

Fit function $y = ax^b$			
Variable	Value	95% low bound	95% high bound
a	0.1433	-0.3157	0.6023
b	-0.8439	-1.198	-0.49

TABLE 5.14: Fit values for fit in figure 5.24

Peclet number

Last to investigate is the dependency on both the height and the velocity of the gas flow. This is combined in the Peclet number from equation 2.36. Figure 5.25 shows the relative transition point, relative to the height, plotted against the Peclet number.

Ethylene Glycol
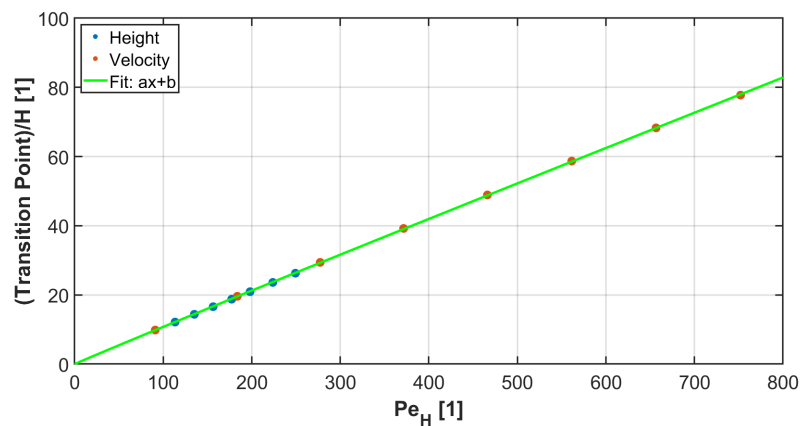
FIGURE 5.25: Relative transition point vs Peclet number, $\Delta T = 35K$, fit data in table 5.15

Fit function $y = ax^b$			
Variable	Value	95% low bound	95% high bound
a	0.1172	0.1145	0.12
b	0.9815	0.9777	0.9853

TABLE 5.15: Fit values for fit in figure 5.25

Equation 2.33 states that the relative transition point ($\frac{FP}{H}$) should be linearly proportional to the Peclet number. This is also shown by the fit data in table 5.15.

Toluene

Figure 5.22 and table 5.12 show the graph and the fit data regarding the Peclet number influence on the transition point.
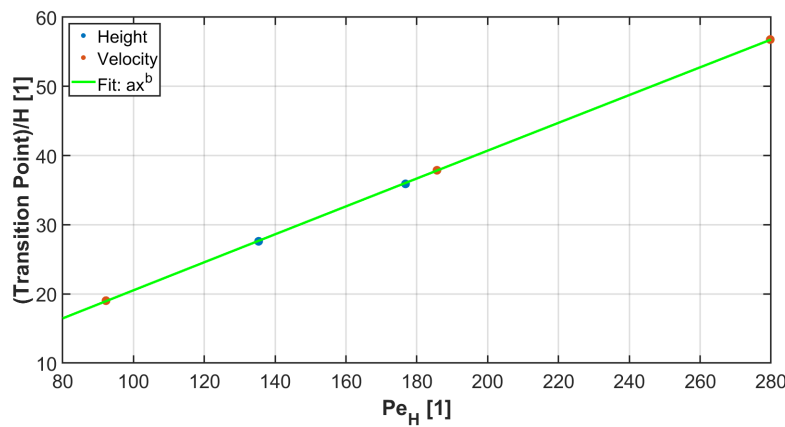
FIGURE 5.26: Relative transition point vs Peclet number, $\Delta T = 35K$, fit data in table 5.16

Fit function $y = ax^b$			
Variable	Value	95% low bound	95% high bound
a	0.217	0.2068	0.2272
b	0.9879	0.9791	0.9968

TABLE 5.16: Fit values for fit in figure 5.26

5.4.2 Experiment

To compare with the real experiment, the model from section 3.6 is used. This was done to have a model more similar to the experimental setup. Figure 5.29 shows the transition point dependency on the maximum gas flow velocity of the experimental setup and the model data. The model data is from a stationary solution, as previously is was noticed that the time dependent simulations became steady after a short while (0.1s). The experimental measurments were also done at a steady state, mostly this was after 15 minutes. Reason for this longer time was the fact that the whole setup heat up due to it being on hot plate. Therefore the results kept changing in the first quarter of an hour before becoming steady.

Important to know is that in order to find the transition point, the whole setup is moved under the microscope. This makes it very hard to see the process of condensation happening from the beginning, as the transition point has to be found after

setting a specific value for the gas flow velocity. After the transition point is found, it could look like roughly two different scenarios. If the transition point is moving away from the start of the liquid layer (retracting), the transition point is very clear, as show in figure 5.27
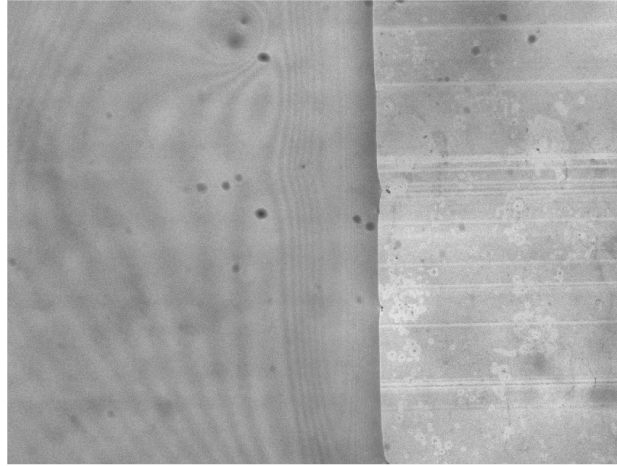
FIGURE 5.27: The transition point moving to the left, clearly a visible and direct distinguish between non-condensation and condensation, note that the gas flow is from right to left and increasing or increased not more than a minute before the picture, Setting 1 for microscope

.

However, if the condensated layer steady for a while, or the transition point is moving toward the beginning of the liquid due to a lower gas velocity, the transition from condensation to non-condensation is far less clear, which is shown in figure 5.28
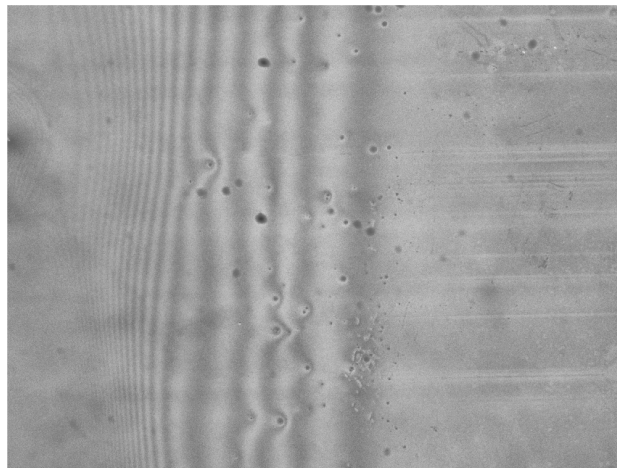
FIGURE 5.28: The transition point a few minutes after changing the gas flow, not clearly a visible and direct distinguish between non-condensation and condensation, note that the gas flow is from right to left steady for a while, Setting 1 for microscope

.
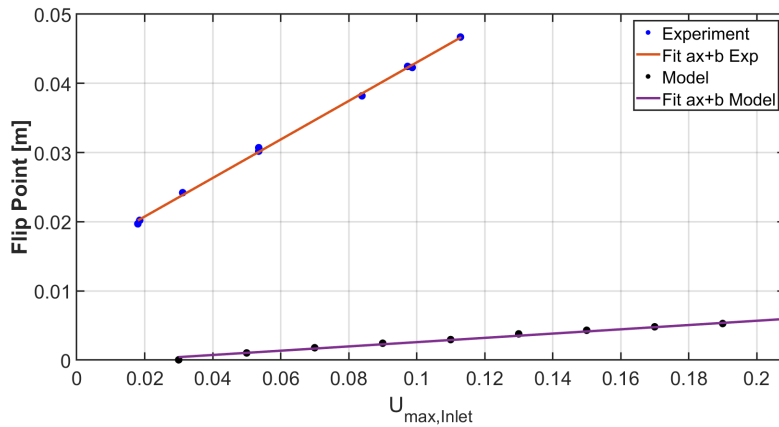
FIGURE 5.29: Relative transition point vs U_{max} at the inlet, $\Delta T = 55K$,
fit data experiment in table 5.17
and model fit data in table 5.18.

Fit function $y = ax + b$			
Variable	Value	95% low bound	95% high bound
a	0.2785	0.2696	0.2874
b	0.01517	0.01454	0.01581

TABLE 5.17: Fit values for Experiment fit in figure 5.29

Fit function $y = ax + b$			
Variable	Value	95% low bound	95% high bound
a	0.03091	0.02801	0.03381
b	-0.0004967	-0.0008823	-0.000111

TABLE 5.18: Fit values for Model fit in figure 5.29

5.5 Shear-induced displacement of a volatile thin liquid film

To test the influence of an air flow going over a liquid layer, in respect to the evaporation of that layer, the numerical model from section 3.7 was used. The Vernooij number is defined as described in equation 2.73.

5.5.1 Layer height

To show how the layer height normally develops, figure 5.30, 5.31 and 5.32 show the height of the liquid layer for different times. The liquid used here was toluene.
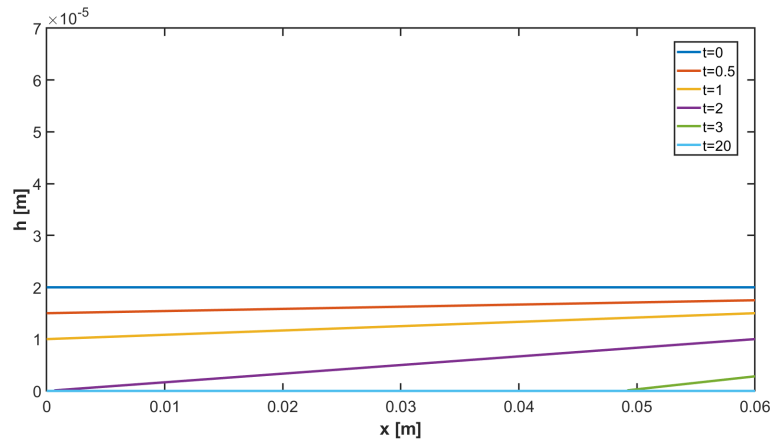
FIGURE 5.30: Height liquid layer at different times. Evap $= 10\mu m/s$,
$H_0 = 20\mu m$, $U_{max} = 0m/s$
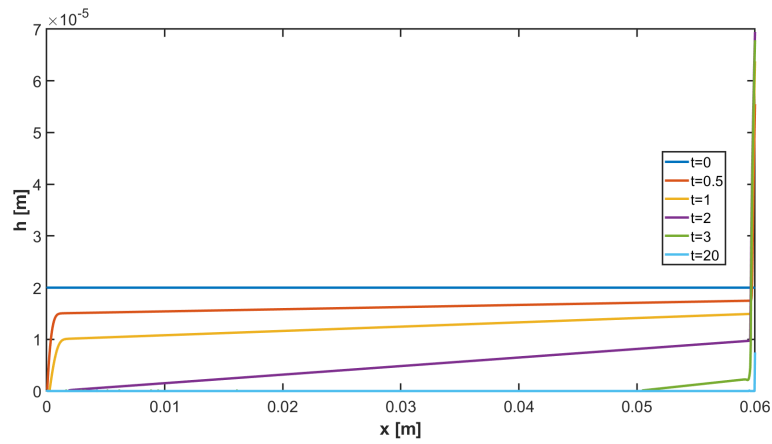
FIGURE 5.31: Height liquid layer at different times. Evap $= 10\mu m/s$,
$H_0 = 20\mu m$, $U_{max} = 1000m/s$

Note that a velocity of $1000m/s$ is not realistic, but it shows how high the air velocity has to be to significantly move the liquid.
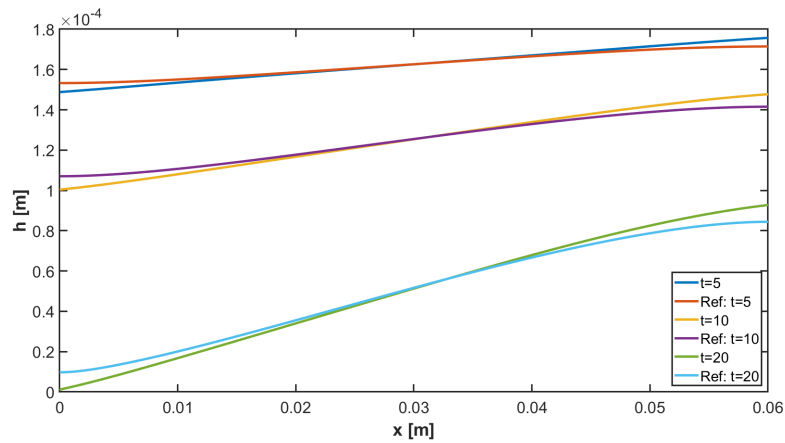
FIGURE 5.32: Height liquid layer at different times. Evap $= 10\mu m/s$,
$H_0 = 200\mu m$, $U_{max} = 10m/s$, Ref: reference with $U_{max} = 0$

Figure 5.30 and 5.31 show the same case, only for 2 greatly different air velocities. It is clear to see that at the beginning of the liquid layer, extra liquid is blown away in the case of a high air velocity. This then stacks up at the end of the layer, as the simulations are set with a no flux at both end of the domain. Figure 5.32 shows both cases in the same graph, only now the height of the liquid is $200\mu m$ and the the maximum air velocity is either 0 or $10m/s$. In this case it is also visible that liquid is taken from the beginning of the layer, and extra liquid is flown to the end of the layer. However, different from the smaller liquid layer, here it seems like the liquid trying to establish a uniform layer due to gravity. This is logical, as due to the larger liquid layer thickness, the timescales are larger with a factor 10. This makes the absolute difference in height between the beginning and the end of the liquid, due evaporation larger and larger. Therefor, eventually, the liquid surplus at the end of the layer will start to make its way to the beginning of the liquid due to gravity.
To make a more qualitative analyse, the following equation is used to investigate the amount of liquid that is moved, with respect to the "no-airflow" case.

$$V_{liq,moved}(t^*) = \frac{\int_0^{W_{layer}} |h(t^*) - h_0(t^*)| \, dx}{2W_{layer}h_0(t=0)}, \tag{5.3}$$

with V_{liq} the moved liquid, $h(t^*)$ the height of the liquid layer at $t = t^*$, with t^* the point in time when the front of the liquid layer is fully evaporated in case of a no-airflow situation. $h_0(t^*)$ is the height of the liquid layer without air flow at $t = t^*$ and W_{layer} the width of the liquid layer.
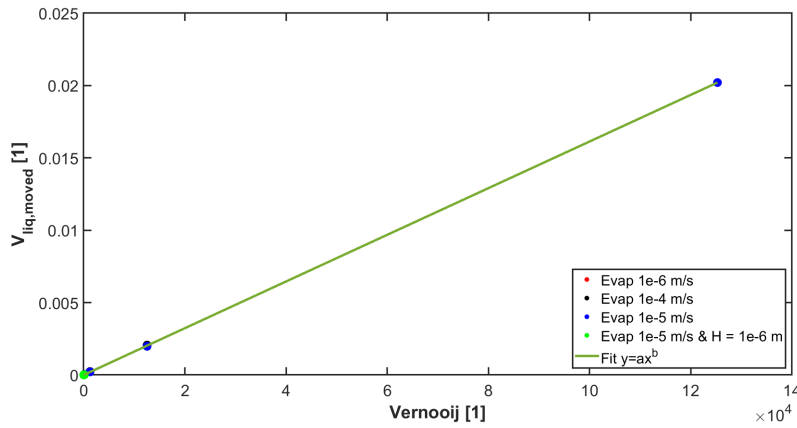
FIGURE 5.33: Moved liquid from equation 5.3 plotted against Vernooij number for toluene. Fit data in table 5.19
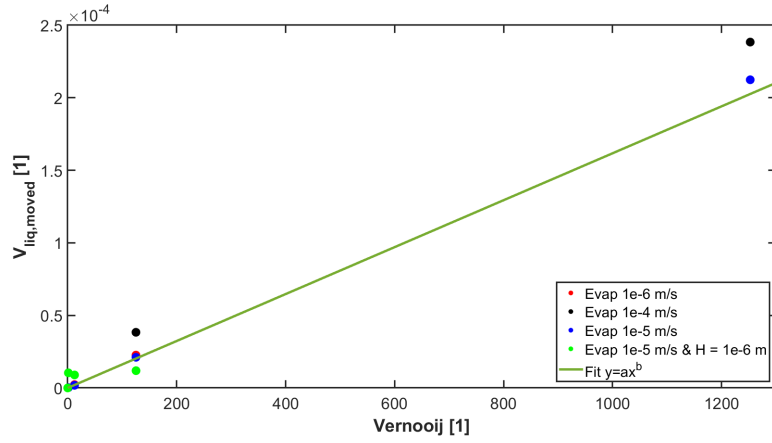
FIGURE 5.34: Moved liquid from equation 5.3 plotted against Vernooij number for toluene. Zoomed in compared to figure 5.33

Tol, Fit function $y = ax^b$		
Variable	Value	Standard error
a	$1.63423 \cdot 10^{-7}$	$5.49436 10^{-9}$
b	0.99889	0.00279

TABLE 5.19: Fit values for fit in figure 5.33
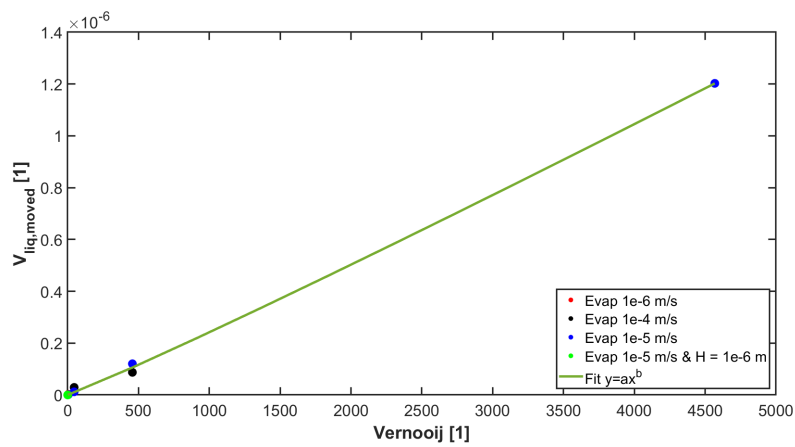
FIGURE 5.35: Moved liquid from equation 5.3 plotted against Vernooij number for EG. Fit data in table 5.20
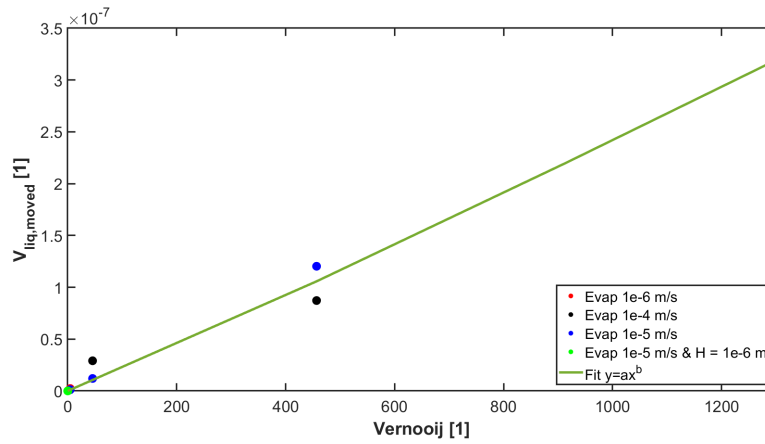
FIGURE 5.36: Moved liquid from equation 5.3 plotted against Vernooij number for EG. Zoomed in compared to figure 5.35

EG, Fit function $y = ax^b$		
Variable	Value	Standard error
a	$1.64506 \cdot 10^{-10}$	$3.35808 \cdot 10^{-11}$
b	1.05578	0.02738

TABLE 5.20: Fit values for fit in figure 5.35

5.6 Drying liquid layer

As mentioned in section 3.8, only a simplified model of the drying liquid layer worked. However, this does show that the principle seems to be right.

(A) $t = 0s$

(B) $t = 1s$

(C) $t = 5s$

(D) $t = 10s$

(E) $t = 20s$
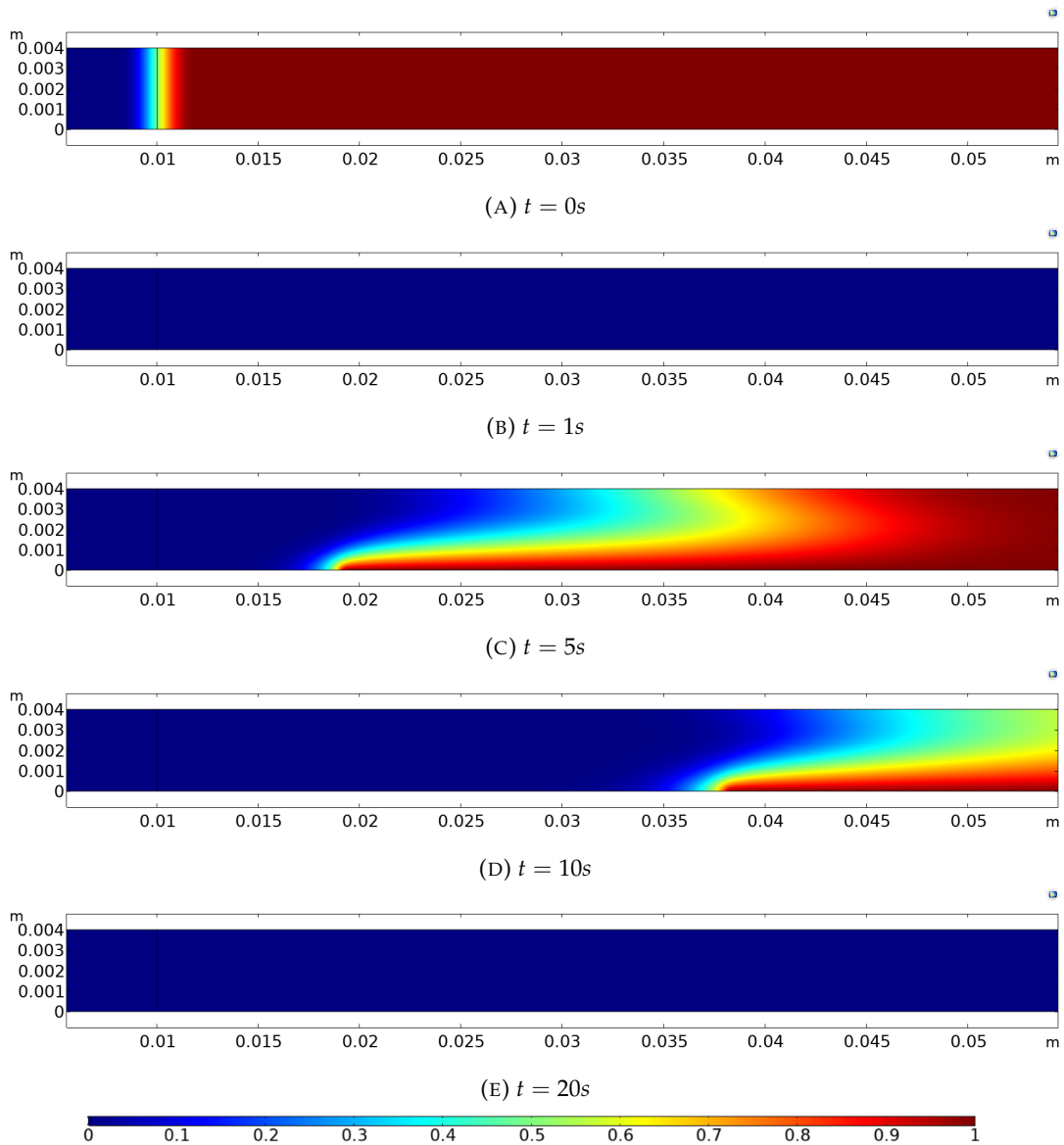
FIGURE 5.37: Concentration surface plot. $U_{max} = 0.009m/s$, $c_{sat} = 1mol/m^3$

Figure 5.38 shows the height at different moments in time to show the development of the liquid layer. Figure 5.39 shows the development of the position of the liquid layer front.
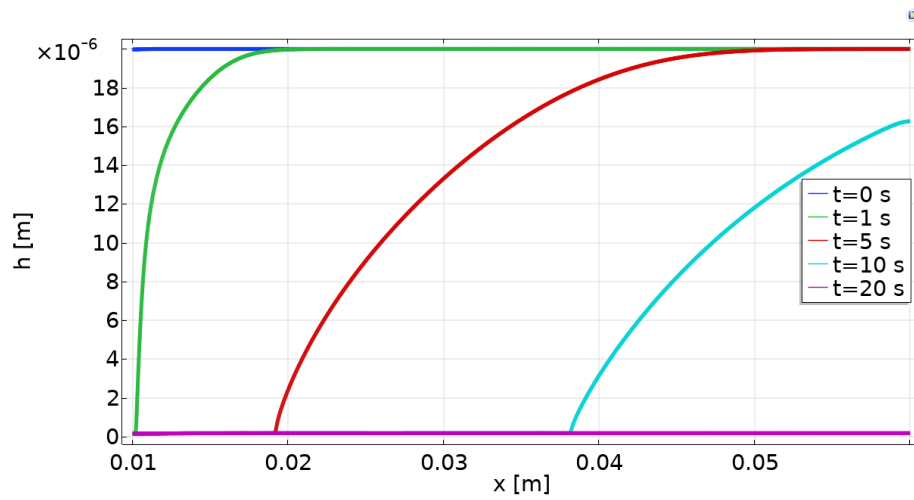
FIGURE 5.38: Height liquid layer at different times, $U_{max} = 0.009 m/s$, $c_{sat} = 1 mol/m^3$
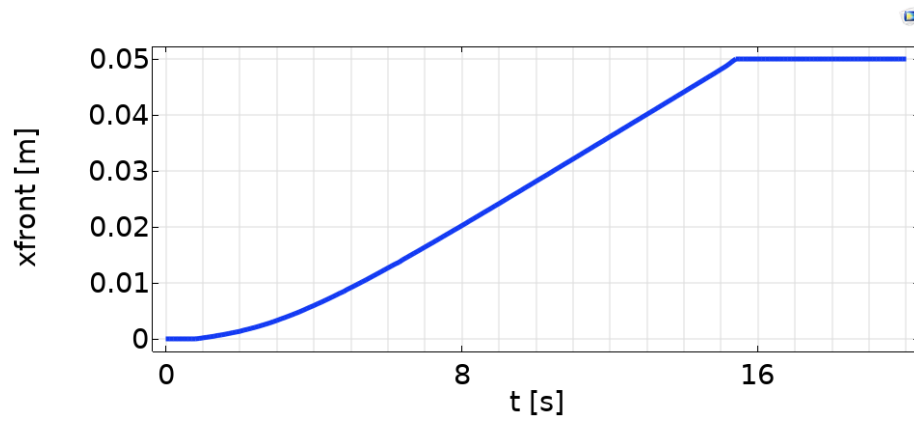
FIGURE 5.39: liquid front over time, $U_{max} = 0.009 m/s$, $c_{sat} = 1 mol/m^3$

Chapter 6

Discussion

6.1 Results

6.1.1 Falling droplet displacement

Table 6.1 shows the relations that were found regarding the horizontal displacement of the droplet at the moment of landing.

Horizontal Displacement $d[m]$	
Variable	Fit function
$V_0[m^3]$	$d = (3 \pm 2) \cdot 10^{-17} V_0^{-0.079 \pm 0.04}$
$H[m]$	$d = (7 \pm 2) \cdot 10^1 H^{2.40 \pm 0.04}$
$U_{max}[m/s]$	$d = 6.21140 \cdot 10^{-6} U_{max}$
$U_{jet}[m/s]$	$d = (3557 \pm 7) \cdot 10^{-7} U_{jet}^{-2.32 \pm 0.02}$

TABLE 6.1: Horizontal droplet displacement relations

Getting a small displacement is key, as the to-be printed structures are also very small. In order to prevent condensation, one can move the printhead further away from the substrate, but table 6.1 shows that this increases the displacement of the droplet a lot. Purely looking at the displacement of the droplet, it is advantageous to choose a faster air flow, as this will not displace the droplet that much, due to its linear relation.
In order to print smaller and detailed structures, small droplets can be desirable. However, it can be seen that small droplets can cause major displacements due to the lack of mass, causing them to get carried by the air flow much further.

6.2 Experiment without external airflow

Table 6.2 and table 6.3 show the found relation between temperature and distance with the condensation rate for the model and the experiments.

Condensation Rate $CR[m/s]$	
Variable	Fit function
H	$CR = (6.800 \pm 0.001) \cdot 10^{-11} H^{-0.969 \pm 0.002}$
$\Delta T[K]$	$CR = (5 \pm 2) \cdot 10^{-14} \Delta T^{3.22 \pm 0.07}$

TABLE 6.2: Condensation Rate from simulations

Condensation Rate $CR[m/s]$	
Variable	Fit function
H	$CR = (6 \pm 4) \cdot 10^{-9} H^{-0.5 \pm 0.1}$
$\Delta T[K]$	$CR = (5 \pm 6) \cdot 10^{-19} \Delta T^{6.6 \pm 0.3}$

TABLE 6.3: Condensation Rate from experiments

The most important thing is the fact that the velocities of the experiment, seem to be significantly larger than those of the model. This was at most times a difference of a factor 10. This difference can be caused by a lot of reason, from which two of them will shortly be elaborated.

- **Non-simulated flows**: Figure 5.10 shows that the velocities in the centre of the beaker are very small. However, at the sides, this velocity get bigger. Although it is still not a large, significant velocity, one can make the relation between this pattern and a Rayleigh–Bénard convection patterns. If such a pattern would be there, it could enhance the condensation strongly. Giving reason for a higher condensation rates in the experiments.

- **Hygroscopicity of Ethylene Glycol**: Another reason could be the fact that ethylene glycol tends to absorb water from its surrounding if left exposed to it. Water tends to evaporate faster than Ethylene Glycol, which could mean more liquid vapor in the air. However, one has to take in mind that this also goes for the condensation. A liquid that quickly evaporates more than it condenses, also has a harder time to condense on a surface, as it needs a very low temperature to tip the balance between evaporation and condensation in favor of condensation.

Apart from the higher condensation rates for the experiments, it is also clear that the relations between height and condensation and between temperature and condensation do not match very nice. For the model, the functions seems to fit quite nice for the height dependence. Also they are not too bad for the temperature dependence as well. However, the fit functions for the experimental values do not seem to match that nice. This is better seen in figure 5.13 and 5.14. This could indicate some other effect which is temperature and height dependent, causing the relations to be more complicated than a power relation. This might indicate that the model used here is not sufficient to estimate the growth of the condense layer.

6.2.1 Transition point

Table 6.4 and table 6.5 show the relations between the transition point and several variables, for ethylene glycol and toluene.

Transition point $TP[m]$, EG	
Variable	Fit function
H	$TP = (1.6 \pm 0.3) \cdot 10^4 H^{2.06 \pm 0.02}$
$U[m/s]$	$TP = (0.0101 \pm 0.0001)U^{0.970 \pm 0.005}$
$\Delta T[K]$	$TP = (0.247 \pm 0.005)\Delta T^{-0.906 \pm 0.005}$
$Pe_H[1]$	$\frac{TP}{H} = (0.117 \pm 0.003)Pe_H^{0.982 \pm 0.004}$

TABLE 6.4: Condensation Rate from experiments

Transition point $TP[m]$, Tol	
Variable	Fit function
H	$TP = (3 \pm 5) \cdot 10^4 H^{2.1 \pm 0.2}$
$U[m/s]$	$TP = (0.0236 \pm 0.0003)U^{0.99 \pm 0.02}$
$\Delta T[K]$	$TP = (0.1 \pm 0.5)\Delta T^{-0.8 \pm 0.4}$
$Pe_H[1]$	$\frac{TP}{H} = (0.22 \pm 0.01)Pe_H^{0.988 \pm 0.009}$

TABLE 6.5: Condensation Rate from experiments

Height

Purely looking at the proportionallity between the height and the transition point, the relations agree with the theoretical relation that stated

$$TP \sim H^2.$$

However, for the toluene the fit does not seem to be a perfect fit, looking at the uncertainty. One should however take in mind that the fit for toluene was made out of only three data points, which largely increases uncertainties. Comparing the two liquids, toluene is better used as liquid, as the transition point is further away from the start of the liquid compared to the ethylene glycol.

Velocity

The air velocity relations in both cases agree with the theory, which states that this should be a linear relation,

$$TP \sim U.$$

Both data sets were fitted with a potential power relation fit. Both turned out with an exponent almost equal to one, indicating a linear relation. Again the toluene is the

liquid with the largest transition point, meaning it is better suited as liquid, purely based on the positioning of the transition point.

Temperature

The temperature relation is harder to compare to the theory, as there is no given relation for it. However, in section 5.4.1 it was clear that the found relations of the fits trough the data looked right and in the same order of size. Again for the toluene the uncertainty is quite big, but these measurement were done with three data points which is hard to fit trough. For both liquids the relation between the temperature and the transition point seems logarithmic, as the double logarithmic plots were linear. However, for larger differences in temperature, the theory did not seems to agree perfectly with this. This can be due to the assumptions made in the derivation of the theory, such as the assumption that a iso-thermal situation was the case, as this is clearly not true.

Peclet number

The found relations between the peclet number and the normalized transition point were very good. Both for ethylene glycol and the toluene the relation turned out to be linear, as expected,

$$\frac{TP}{H} \sim Pe_H$$

Transition point experiment

Table 6.6 shows the found relations between the transition point and the maximum air velocity.

Transition point $TP[m]$, **EG**		
	Variable	Fit function
Experiment	$U[m/s]$	$TP = (0.279 \pm 0.008)U + (0.0152 \pm 0.0006)$
Model	$U[m/s]$	$TP = (0.031 \pm 0.003)U + (-0.0005 \pm 0.0004)$

TABLE 6.6: Condensation Rate from experiments

Starting with a positive note on the results found, regarding the transition point behaviour as an effect of air velocity, is the fact that both the experiment and the model give a linear relation between the two. Note that for this part of the transition point experiments, a slightly different model was used, but this does not seem to affect the linear dependency. It has to be said that the fit function in this case was already linear, but the low uncertainties indicate that the linear relation holds. Moving on, beside the linearity, the results are not that good. The values of the transition point are far from each other, when comparing results to simulation. The model transition point is far smaller, meaning condensation will happens much earlier in the domain in comparison to the experiment. This is contrary to the conclusion that was made after section 6.2, where it was seen that the condensation rate seemed to be lower in the model than in the experiment.
A possible (part of the) explanation would be the heating up of the setup. In the model, the glass does not heat up that much, as all the heat transfer has to come

from the substrate, trough the air. However, in the setup, all part are connected with metal holder and screws. They obviously transfer heat very easily due to the high thermal conductivity of metals. This can cause the setup to be heating up much faster. Even with this heating, one should take in mind that the metal is not touching the glass directly, as the glass plate is hold in place by a perspex plate. Therefore the heating of the setup will make some difference, but probably not enough to cause the large factor 10 difference in the transition point formulas from table 6.6.

Another area to look into is the gas flow coming into the setup. Even though the gas is cooled by a heat exchanger which is kept at a constant temperature, there is still some length of tube in-between the heat exchanger and the setup. In the time it takes the gas to travel trough from the heat exchanger to the setup, the temperature can vary due to heat exchange with its surrounding. When this gas heat ups (meaning it gets closer to room temperature), it can not cool the glass plate as much as in the model is assumed, meaning the temperature difference is smaller. However, this would then indicate a lower condensation rate, meaning a larger transition point, which would be closer to the experimental value of the transition point.

One other remark that has to be made about the experimental setup is the flow regulator. In front of the flow meter, there is a valve to control the gas flow rate. However, the used valves were not steady, meaning that if the air flow was set to a certain value, after a while the flow rate would become lower. This was not much, but given the small displacements between the transition points, it prevented a good measurement to investigate the temperature influence on the transition point position. In order to have a reliable measurement investigating the temperature distance, the velocity should be kept at the same value, this was not possible due to the declining gas velocity. Also, the valve was so sensitive to movement, it was nearly impossible to set the air flow at a certain specific value.

6.2.2 Shear-induced displacement of a volatile thin liquid film

Table 6.7 shows the relation found between the normalized volume of moved liquid and the Vernooij number. The normalized volume of moved liquid was defined in equation 5.3, whereas the Vernooij number was defined in equation 2.73.

Normalized volume of moved liquid $V[1]$		
Liquid	Variable	Fit function
Tol	$Vernooij[1]$	$V[1] = (1.63 \pm 0.005) \cdot 10^{-7} Vernooij^{0.999 \pm 0.003}$
EG	$Vernooij[1]$	$V[1] = (1.6 \pm 0.3) \cdot 10^{-10} Vernooij^{1.06 \pm 0.03}$

TABLE 6.7: Normalized volume of moved liquid

The relation between the Vernooij number and the normalized volume of moved liquid turned out to be linear for both cases, given the fact that the power fit gives an exponent close to 1. However, it was seen that this results works great for larger Vernooij numbers, but for small Vernooij numbers it seemed less likely that the volume of moved liquid is an effect of only the gas flow velocity and the evaporation rate as data points are further apart in that region. Especially for thick liquid layers, gravity seemed to be playing a role as the liquid tries to establish a uniform layer height during. The big difference between the two used liquids is that for ethylene glycol, the air flow has a much smaller effect on the layer height than in the case of

toluene. A good explanation for this is the higher viscosity of ethylene glycol. The viscosity of ethylene glycol is a factor 20 larger, this means the liquid is harder to move around by an external air flow, resulting in less volume moved.

6.2.3   Drying liquid layer

As said earlier, the model did not work the way it was supposed to do. However, the results for the more simplified model are promising. It is clear to see that the liquid layer front moves to the right as the layer evaporates until the point that the layer height is equal to zero. In combination with solving the temperature equation, this could eventually lead to a more realistic model in which it is also possible to check the concentration at the top of the boundary, where the condensation is happening.

6.3   Suggestions/Improvements experiments

6.3.1   Experiment without external airflow

The following suggestions could be made to improve the experimental setup without external air flow designed to investigate the condensation rate.

- Use different sizes of beakers, in order to prevent/estimate the Rayleigh–Bénard convection

- Use fresh Ethylene glycol without absorbed water.

- To make the model agree better, another effort has to be made to expand the model with the beaker itself and the liquid. This makes it possibles to check if a possible Marangoni flow transfers liquid vapor to the glass more quickly, resulting in a higher condensation rate.

6.3.2   Transition point experiment

The following suggestions could be made to improve the experimental setup used to find the transition point in a certain situation.

- Prevent metal from connection bottom setup to top setup. Top setup indicates everything above the perspex plate that separatess the bottom from the top part.

- Measure temperature incoming gas flow

- Better controllable valve for the incoming gas flow

- More steady valve for the incoming gas flow

- Measure temperature glass plate (plate on whcih condensation is happening) to better specify temperature effects

If the above suggestions work and a more repeatable and reliable process can be created, it is also very interesting to look at the condensation rate,close to the transition point. Also the liquid layer profile could than be investigate more due to the fact that one would know were to look from the beginning, instead of searching for the transition point.

6.3.3 Shear-induced displacement of a volatile thin liquid film

It can also be an interesting, maybe less time consuming idea to design an experiment to track the height of a liquid layer in the presence of a gas flow going over the liquid. This experiment can than be used to validate the models in this report.

Chapter 7

Conclusion

This report focussed on several parts of the inkjet printing process which could influence the condensation in the vicinity of a highly evaporating liquid layer. To prevent condensation at unwanted places three main variables were investigated, being the temperature difference between the evaporating liquid layer and its surrounding, the distance between liquid layer and place of condensation and the velocity of the gas flow that is used to transfer liquid vapor out of the system before it can condense.

Even before the jetted liquid has touched the surface, the mentioned parameters are already of importance for the path of the droplet to its landig spot on the surface. It was seen that the volume of the droplet and the height of the printhead both had a power relation with the horizontal displacement of the droplet. Whereas the relation of the maximum gas velocity with the displacement was linear. This could indicate that using a higher maximum gas velocity has the smallest effect on displacement of the droplet, taken into account that high precision is wanted to obtain smaller printed structures.

In order to measure condensation, the experiment without the external air flow was used to investigate measuring abilities. It turned out that the condensation is nicely measurable, however the results did not match the results from the simulations. Several reasons for this were given, being the hygroscopic nature of the used ethylene glycol with water, or Rayleigh-Bernard convection pattern, which was not taken into account in the simulation. However, both does not seem to be the whole reason, as the relation between temperature and condensation, as well as the relation between distance and condensation were quite different for model and experiment.

The models used to calculated the transition point, the point where non-condensation transitions into condensation, worked very well. Both for ethylene glycol and toluene the relations agreed with the earlier found theory, indicating a working principle. However, again in the experiment vastly different results were found. The experimental values for the transition point were larger than the ones for the model, even with an adjusted model to get a model closer to the reality. These larger transition points meant that the condensation was happening further away from the beginning of the liquid, meaning less condensation. A positive note was that despite difference in data, they both showed a clear linear behaviour, which was expected given the theory.

Last physical process that was investigated was the direct effect of a gas flow over a liquid layer on the layer height. In order to make sure that the jetted droplet with its component stays at the right place, one has to make sure that the liquid is not already blown away before the solvent is evaporated. The models used for this show a linear behaviour between the Vernooij constant and the normalized volume of moved liquid. It also turned out that regarding the two used liquids, ethylene glycol is the more suitable one, if the focus is on not moving the liquid before it is evaporated.

Last a suggestion is to design an experiment to check these findings regarding the gas flow velocity and the evaporation velocity.

Appendix A

Transition point experiment setup
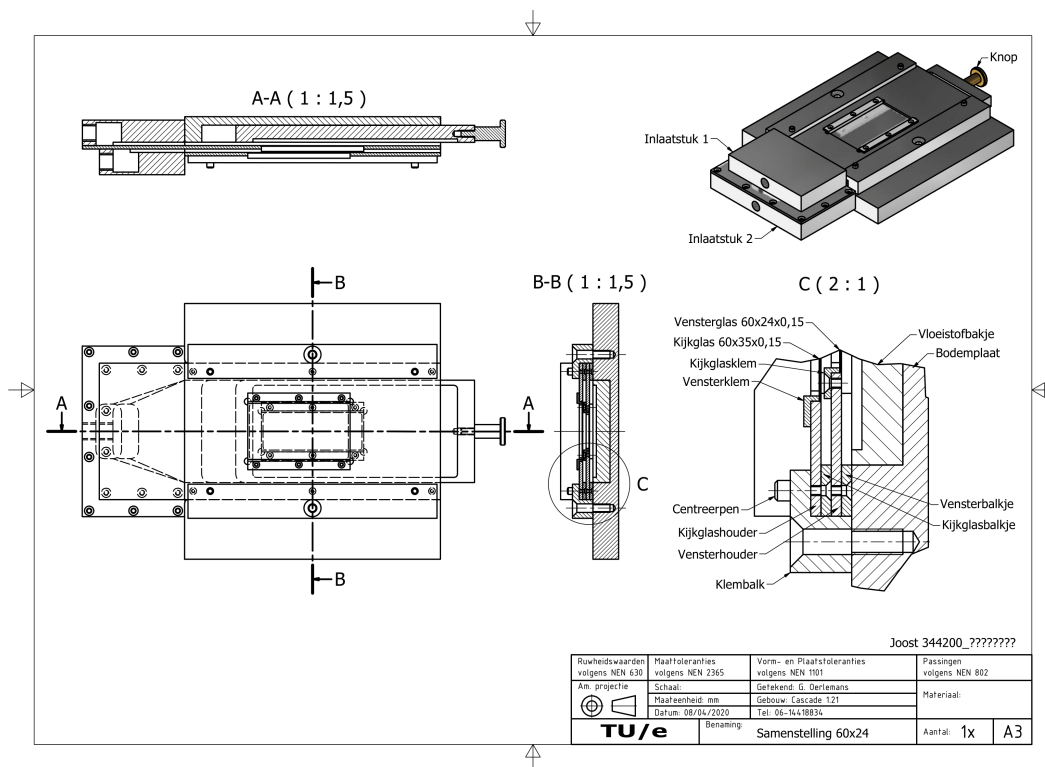
FIGURE A.1: Detailed view of the experimental setup for the transition point experiment
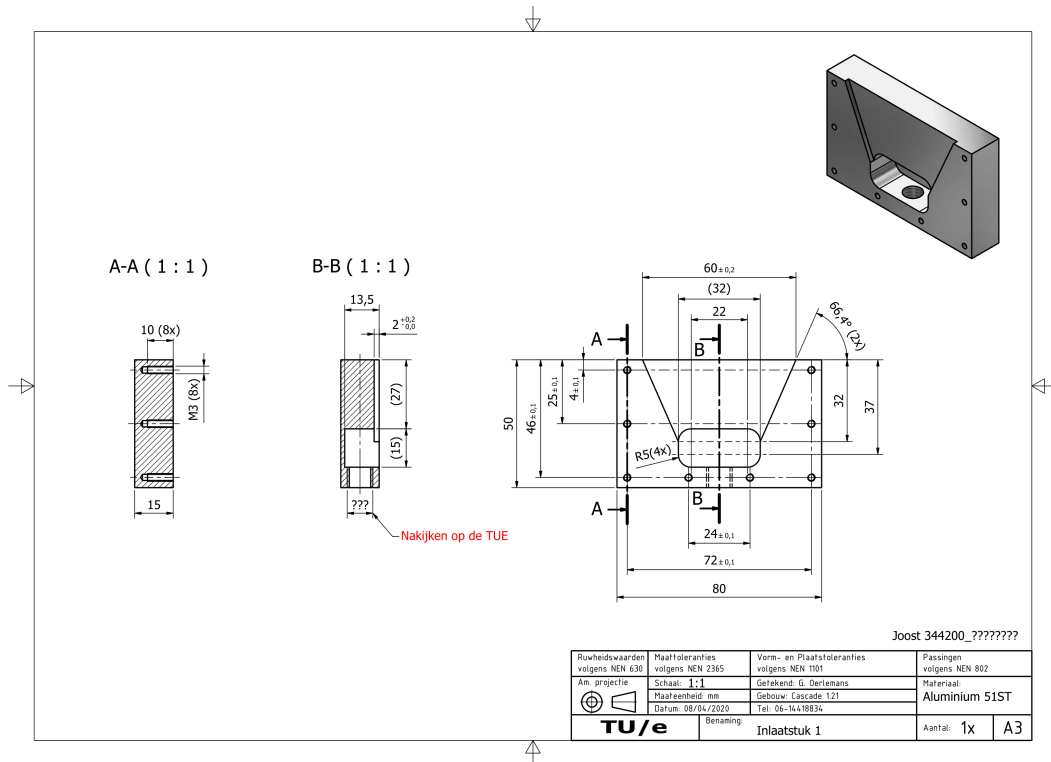
FIGURE A.2: Inlet piece 1 ("inlaatstuk 1") of figure A.1
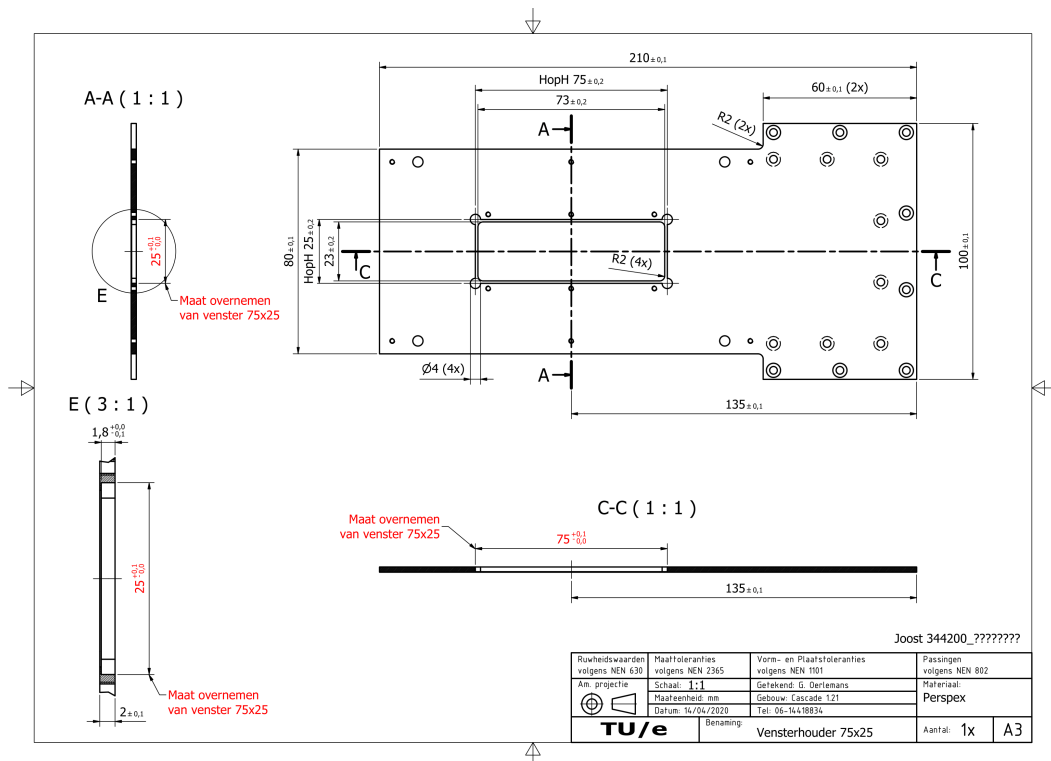
FIGURE A.3: Glass holder ("Vensterhouder") of figure A.1. The glass
plate is the plate on which the condensation is tracked.

Appendix B

LPM to maximum air velocity

```
ClearAll["`*"]
LPM = 2;
H = 2*10^-3;
W = 60*10^-3;
a = 4*U/H^2;
V = -a*(y - 0.5*H)^2 + U
eqn = Integrate[V, {y, 0, H}]/H
sol = Solve[eqn*H*W*1000*60 == LPM/2]
Plot[V /. sol[[1]], {y, 0, H}]
eqn /. sol[[1]]
```

Appendix C

Matlab code trajectory jetted droplet

```matlab
1  cd 'C:'
2  close all
3  clear all
4
5
6  vel_drop_init = [0,-6];        %Initial drop velocity at point
       of jetting
7  eta_air = 1.846*10^-5;         %Dynamic viscosity air
8  eta_EG =          0.0162;         %Dynamic viscosity Ethylene
       glycol
9  eta_liquid = eta_EG;           %Dynamic viscosity used in script
10 labda = eta_liquid/eta_air;    %Ratio dynamic viscosities
11 %R = 10e-06;                    %Radius spherical droplet
12 rho = 1110;                    %Density liquid
13
14 g = 9.81;                      %Gravitational acceleration
15 H = 1*10^-3;                   %Heigth printhead
16 %AirFlowMax = 1;               %Maximum air flow velocity (centre
        poiseuille
17 %flow)
18 saveOn = 0;                    %Posibility to save
19
20 StokesDrag = 0;                %Use normal stokes drag (
       otherwise advance)
21 IndexTotal = 1;
22
23 %Possible combinations of variables:
24 %Ujet = [0,-1,-2,-3,-4,-5];
25 UAirmax = [0.1, 0.25,0.5,0.75,1, 2, 3];
26 %Hprinthead = [0.25e-3, 0.5e-3, 0.75e-3, 1e-3, 2e-3, 3e-3, 4e
       -3, 5e-3];
27 %mDrop = [1e-12, 10e-12, 20e-12, 40e-12, 40e-11, 40e-10];
28 %RDrop = [10e-7, 5e-6, 10e-6, 5e-6, 10e-5, 10e-4];
29 %mDrop = [20e-12];
30 %V0   = (1e-12:1e-12:12e-12)/1000;
31 V0 = 6e-12/1000;
32 R0 = (3/4/pi*V0).^(1/3);       %Radius droplet
```

```matlab
33
34 %test1 = variable that is investigated , AirFlowMax in this
        case
35 for test1 = UAirmax
36
37 %R = test1 ;
38 m = 4/3* pi *R^3* rho ;
39 %H = test1 ;
40 AirFlowMax = test1 ;
41 syms y ( t ) ;
42
43 Dy = diff ( y , t ,1 ) ;
44 Dy2 = diff ( y , t ,2 ) ;
45
46 if StokesDrag == 1
47     ode = Dy2 == −g − 6* pi * eta_air *R*Dy/m;
48 else
49     ode = Dy2 == −g − 4* pi * eta_air *R*Dy/m*(3* labda +2)/(2*(
          labda +1)) ;
50 end
51 cond1 = y (0) == 0;
52 cond2 = Dy(0) == vel_drop_init (2) ;
53 conds = [ cond1 cond2 ];
54
55 ySol ( t ) = dsolve (ode , conds ) ;      %Solution vertical force
        balance differential equation
56
57 Landed = 0;
58 dt = 1e −5;                    %Time step for solution
59 t_end = 5;
60
61 %Search for time where droplet landed :
62 i =1;
63 while (Landed ~= 1 && i <=t_end/dt+1)
64     if (abs ( ySol (( i −1)* dt )) > H && Landed == 0)
65         landingTime = (i −1)* dt ;
66         Landed = 1;
67         indexLanded = i ;
68     end
69     i = i +1;
70 end
71 if (i <15)
72     Landed = 0;
73     dt = dt /10;
74     i =1;
75     while (Landed ~= 1 && i <=t_end/dt+1)
76         if (abs ( ySol (( i −1)* dt )) >= H)
77             landingTime = (i −1)* dt ;
78             Landed = 1;
79             indexLanded = i ;
80         end
```

```
81          i = i +1;
82        end
83  elseif (i >1000)                %If it takes too long (too much
         data) then increase time step
84      Landed = 0;
85      dt = dt *10;
86      i =1;
87      while (Landed ~= 1 && i <=t_end/dt +1)
88          if (abs(ySol((i−1)*dt)) > H && Landed == 0)
89              landingTime = (i −1)* dt ;
90              Landed = 1;
91              indexLanded = i ;
92          end
93          i = i +1;
94      end
95  end
96
97  %{
98  %Check y position vs time :
99  H_line (1: i )=−H;
100 figure %
101 plot(time (1:end) ,posY (1:end) ,time (1:end) ,H_line (1:end))
102 title ('Y position versus time ')
103
104 xlabel ('time ')
105 ylabel ('y')
106 legend ('position droplet ', 'substrate ')
107 %}
108 %
       _____

109
110 syms AirFlow (y );
111 AirFlow (y) = −4*AirFlowMax /(H^2)*(−y −0.5*H)^2+AirFlowMax ; %
        Air flow profile
112
113 %{
114 %Check air flow profile :
115 figure %
116 fplot (AirFlow (y ) ,[−H,0] , 'LineWidth ',2)
117 title ('Air flow profile ', 'FontWeight ', 'bold ')
118 xlabel ('Heigth (y) / H [−]', 'FontSize ',13, 'FontWeight ', 'bold '
       )
119 ylabel ('Air velocity / U_{max} [−]', 'FontSize ',13, 'FontWeight
       ', 'bold ')
120 %}
121
122 syms x( t );
123
124 Dx = diff(x ,t ,1) ;
125 Dx2 = diff(x ,t ,2) ;
```

```matlab
126
127 if StokesDrag == 1
128     ode = Dx2 == 6*pi*eta_air*R/m*(AirFlow(ySol)-Dx);
129 else
130     ode = Dx2 == 4*pi*eta_air*R/m*(AirFlow(ySol)-Dx)*(3*labda
            +2)/(2*(labda+1));
131 end
132 cond1 = x(0) == 0;
133 cond2 = Dx(0) == vel_drop_init(1);
134 conds = [cond1 cond2];
135
136 xSol(t) = dsolve(ode,conds);        %Solve horizontal
        differential equation
137
138 for i = 1:indexLanded %Save coordinates until landing time
139     timeNew(i) = (i-1)*dt;
140     posX(i) = xSol((i-1)*dt);
141     TotalPosX(3,IndexTotal) = double(posX(i));
142     posYNew(i) = abs(ySol((i-1)*dt));
143     TotalPosY(3,IndexTotal) = double(posYNew(i));
144 end
145
146 Displacement(IndexTotal) = double(posX(end)); %horizontal
        displacement landing vs beginning
147 H_lineNew(1:i)=-H;
148
149
150
151 figure %
152 scatter(posX,posYNew, 'LineWidth', 3)
153 ylim([0 H]);
154 titlestr = sprintf('Droplet trajectory, landingtime = %d s,
        dt = %d, V0 = %d', landingTime,dt,m/rho);
155 %title(titlestr,'FontWeight','bold')
156 xlabel('x [m]','FontSize',13,'FontWeight','bold')
157 ylabel('y [m]','FontSize',13,'FontWeight','bold')
158 ax = gca;
159 ax.FontSize = 13;
160 grid on;
161 box on;
162 set(gca, 'YDir','reverse')
163
164
165 xVelSol = diff(xSol,t,1);
166 for i = 1:landingTime/dt
167     velX(i) = double(xVelSol((i-1)*dt));
168 end
169
170 %figure %
171 %plot(timeNew(1:end),velX(1:end))
172 Size = max(size(posX));
```

```
173
174 TotalPosX(1,IndexTotal) = double(test1);
175 TotalPosY(1,IndexTotal) = double(test1);
176 TotalPosX(2,IndexTotal) = double(landingTime);
177 TotalPosY(2,IndexTotal) = double(landingTime);
178 TotalPosX(3,IndexTotal) = round(indexLanded);
179 TotalPosY(3,IndexTotal) = round(indexLanded);
180
181 IndexTotal = IndexTotal+1;
182 clearvars xSol ySol posX posYNew;
183 end
184
185 Legend = [];
186 nrLoops = max(size(TotalPosX(1,:)));
187
188
189 fitfunction = '(x^a)*b';
190 myfittype = fittype(fitfunction ,...
191     'dependent',{'y'},'independent',{'x'},...
192     'coefficients',{'a', 'b'});
193
194 options = fitoptions('Method','NonlinearLeastSquares', 'Lower
        ',[-Inf -Inf]', 'Upper', [Inf Inf], 'StartPoint',[1 0]);
195 [myfit, Goodness] = fit(UAirmax', Displacement',myfittype,
        options);
196 UAirmaxFit = min(UAirmax):(max(UAirmax)-min(UAirmax))/100:max
        (UAirmax);
197
198 a = 1;
199 b= 6.21140e-6;
200
201 figure %
202 scatter(UAirmax,Displacement, 'LineWidth', 3);
203 hold on;
204 plot(UAirmaxFit,b*UAirmaxFit.^(a), 'LineWidth',2);
205 hold off
206 titlestr = sprintf('Droplet displacement');
207 title(titlestr,'FontWeight','bold')
208 xlabel('U_{max} [m/s]','FontSize',13,'FontWeight','bold')
209 ylabel('Horizontal drop displacement [m]','FontSize',13,'
        FontWeight','bold')
210 legend({'Data','Fit'},'location','northwest')
211 ax = gca;
212 ax.FontSize = 13;
213
214 grid on;
215 box on;
```

Appendix D

Condensation rate from movie frames measurements without external air flow

```
1  clear all;
2  close all;
3
4  Dir = 'F:\22_09_2020\Movie 8';  %Folder where movie frames
       are stored
5  cd(Dir);
6
7  powerSize =1; %Either fitting with sin or sin^2 (so 1 or 2)
8  range =8;     %For the peak finding method, how many  frames
       apart can it look for another peak in intensity.
9  RefractionIndex = 1.43;
10 FPS = 15;   %Frames per second
11 WaveLength = 470 * 10^-9;   %wavelength used light
12
13 first = 100032; %First frame NOTE: name your frames number,
       increasing 1 per frame
14 last = 100228;   %Last frame
15 step = 1;        %Step between frames
16 save = 1;        %Save fitted intensity curves in same folder
17 Video =1;        %Make video of frames in same folder
18
19 %video writer:
20 if Video
21     Pos = strfind(Dir,'\');
22     VideoName = strcat('Movie_',num2str(first),'_to_',num2str
           (last),'.avi'); %name video
23     video = VideoWriter(VideoName); %create the video object
24     open(video); %open the file for writing
25
26     for ii=first:last %where N is the number of images
27       I = imread(strcat(num2str(ii),'.BMP')); %read the next
             image
28       writeVideo(video,I); %write the image to file
29     end
30
```

```matlab
31       close(video); %close the file
32 end
33
34 %coordinates of measurement point in frame
35 x=[600,700,100,73,1200,1199 330 930 550];
36 y=[450,600,202,800,900,30 339 723 123];
37
38 Intensity = zeros(max(size(x)),round((last-first)/step)+1);
39
40 if (size(x,1) ~= size(y,1) || size(x,2) ~= size(y,2))
41     error('x and y has to be of the same sizes');
42 end
43
44
45 findPosition = 1;   %show frame with coordinates of
       measurement points
46 if findPosition
47     TestIm = imread(strcat(num2str(first),'.BMP'));
48     imshow(TestIm);
49     grid on;
50     hold on;
51     plot(x,y,'g+', 'MarkerSize', 10);
52     for n = 1:max(size(x))
53     text(x(n)+18,y(n),num2str(n),'Color','g');
54     end
55     hold off;
56     if save
57     saveas(gcf,'PositionPoints,png')
58     end
59 end
60
61 diffMaxTimes = zeros(max(size(x)),100);
62 for p = 1:max(size(x))  %loop over different measurement
     points
63
64     Index = 1;
65 for name = first:step:last
66     File = strcat(num2str(name),'.BMP');
67     if isfile(File)
68         Im = imread(File);
69         pause(0.01)
70         Intensity(p,Index) = Im(y(1,p),x(1,p));
71     else
72         disp(strcat('File ', File, ' does not excist'));
73     end
74     Index = Index+1;
75 end
76 figure %
77
78 %Help values for fitting:
79 minC = min(Intensity(p,:));
```

```
80  maxC = max(Intensity(p,:));
81  avgC = (minC+maxC)/2;
82  maxVarC = (maxC-minC)/2+10;
83  minVarC = (maxC-minC)/2.2;
84  testVarC = (maxC-minC)/2;
85
86  X = (1:max(size(Intensity)))*(1/FPS);
87  %Choose fit function
88  if (powerSize == 2)
89      fitfunction = 'a*x+b+c*exp(-f*x)*sin(d*x+e)^2';
90  else
91      fitfunction = 'a*x+b+c*exp(-f*x)*sin(d*x+e)';
92  end
93
94  myfittype = fittype(fitfunction,...
95      'dependent',{'y'},'independent',{'x'},...
96      'coefficients',{'d','a', 'b', 'c','e','f'});
97
98  %Fit boundaries:
99  options = fitoptions('Method','NonlinearLeastSquares', 'Lower
        ',[-Inf -2 minC minVarC -pi 0]', 'Upper', [Inf 2 maxC
        maxVarC pi Inf], 'StartPoint',[1 0 avgC (maxC-minC)/2 0
        0]);
100
101 myfit = fit(X',Intensity(p,:)',myfittype,options)
102
103 a(p) = myfit.a;
104 b(p) = myfit.b;
105 c(p) = myfit.c;
106 d(p) = myfit.d;
107 e(p) = myfit.e;
108 f(p) = myfit.f;
109
110 %Period between peaks in intensity:
111 period(p) = 2*pi/(d(p)*powerSize);
112 %condensation rate:
113 dhdt(p) = abs(0.5*(WaveLength/RefractionIndex)/period(p));
114
115 %Plot intensity and fitted intensity to check NOTE: p=
        measurement point, p1
116 %is plot
117
118 pl(1)=plot(X,Intensity(p,:));
119 hold on;
120 pl(2)=plot(myfit);
121 pl(1).LineWidth = 2;
122 pl(2).LineWidth = 2;
123 hold off;
124 axis([0 max(X) avgC-1.5*(avgC-minC) avgC+1.5*(maxC-avgC)]);
125 legend('Data',strcat('Fit: ',fitfunction))
126 xlabel('time [s]','fontweight','bold');
```

```matlab
127 ylabel('Intensity','fontweight','bold');
128 title(strcat('Intensity vs Time for point ',num2str(p),'
        dhdt=',num2str(dhdt(p))),'fontweight','bold')
129 set(gca,'FontSize',24)
130 set(gca,'linewidth',2)
131 set(gcf, 'Units', 'Normalized', 'OuterPosition', [0.05, 0.05,
        0.9, 0.9]);
132
133 %save graph if wanted:
134 if (save)
135     saveas(gcf,strcat('Intensity_point_',num2str(p),'_Im_',
            num2str(first),'_to_',num2str(last),'.png'))
136 end
137
138
139 %!! Different method of measuring condensation, not as
        accurate, but almost
140 %always works! Principle is based on searching for different
        peaks in
141 %intensity, and not on fitting with sine fucntion
142 temp2 = 1;
143
144 %search around coordinate if there are values of higher
        intensity around
145 %coordinate, if not --> its a peak.
146 for a = range+1:max(size(Intensity(p,:))-range)
147     [maxTemp, indexmax] = max(Intensity(p,a-range:a+range));
148     if (indexmax == range+1)
149         maxTimes(p,temp2) = X(a);
150         if (temp2 ~= 1)
151             diffMaxTimes(p,temp2-1) = maxTimes(p,temp2) -
                    maxTimes(p,temp2-1);
152         end
153         temp2 = temp2 + 1;
154     end
155 end
156 %Variables periodtest and dhdttest are the period and
        condensation speed
157 %found by the not so accurate peak finding method!
158 if (diffMaxTimes(p,1)~=0)
159 avgDiffMaxTimes(p) = mean(nonzeros(diffMaxTimes(p,:)));
160 periodtest(p) = avgDiffMaxTimes(p);
161 dhdttest(p) = 0.5*(WaveLength/RefractionIndex)/periodtest(p)
162 end
163 end
164
165 %Way to store different solution is one excel file:
166 %{
167 points = [{'point 1'}, {'point 2'}, {'point 3'}, {'point 4'},
        {'point 5'}, {'point 6'}];
168 Fitdata = table(a',b',c',d',e','RowNames',points);
```

```
169 Fitdata.Properties.VariableNames = {'a','b','c','d','e'};
170 if (save)
171     Pos = strfind(Dir,'\');
172     FileName = '..\..\Results_dHdt.xlsx';
173     if isfile(FileName)
174         Temp = str2num(Dir(Pos(end)+4:Pos(end)+5));
175         Name = Dir(Pos(end-1)+1:end);
176     else
177         FileName = strcat('..\','..\..\Results_dHdt.xlsx');
178         Temp = str2num(Dir(Pos(end-1)+4:Pos(end-1)+5));
179         Name = Dir(Pos(end-3)+1:end);
180     end
181
182     T = readtable(FileName);
183     index = size(T,1)+1;
184     writetable(Fitdata,strcat('Fitdata_',num2str(first),'_to_
            ',num2str(last),'_EG_',num2str(Temp),'.xls'),'
            WriteRowNames',true)
185     T(index,:)={Name,first,last,Temp,dhdt(1),dhdt(2),dhdt(3),
            dhdt(4),dhdt(5),dhdt(6)};
186
187     writetable(T,FileName);
188 end
189 %}
```

Bibliography

Antoine, C. (1888). "Vapor Pressure: a new relationship between pressure and temperature". In: *Comptes Rendus des Séances de l'Académie des Sciences* 107, pp. 681–684, 778–780, 836–837.

Bergman, Theodore L. et al. (2007). *Fundamentals of Heat and Mass Transfer*. 6th ed. John Wiley & Sons, Inc, p. 493.

Bird, R. Bryan and Warren E. Stewart (2002). *Transport Phenomena*. 2nd ed. John Wiley & Sons, Inc, p. 337.

Carle, Florian et al. (2016). "Contribution of convective transport to evaporation of sessile droplets: Empirical model". In: *International Journal of Thermal Sciences* 101, pp. 35–47.

Cengel, Yunus A. and John M. Cimbala (2014). *Fluid mechanics. Fundamentals and applications*. 3rd ed. McGraw Hill, p. 47.

Chen, Xue et al. (2018). "Determination of Diffusion Coefficient in Droplet Evaporation Experiment Using Response Surface Method". In: *Microgravity Science and Technology* 30, pp. 675–682.

Chuang, Ming Yuan (2017). *Inkjet Printing of Ag Nanoparticles using Dimatix Inkjet Printer, No 2*. Tech. rep. University of Pennsylvania, p. 5.

Dalton, J. (1802). "Essay IV. On the expansion of elastic fluids by heat". In: *Memoirs of the Literary and Philosophical Society of Manchester* 5, pp. 595–602.

Darhuber, Anton (2012). "3NB90 Fysica van Transportverschijnselen, Deel 2". In.

— (2017a). "3MT020 Micro- and Nanouidics Part I". In: p. 55.

— (2017b). "3MT020 Micro- and Nanouidics Part I". In: p. 39.

— (2017c). "3MT020 Micro- and Nanouidics Part I". In: p. 15.

D.J.Acheson (1990). *Elementary Fluid Dynamics*. Oxford University Press, p. 206.

Edge, Engineers (n.d.). *Convective heat transfer coefficient table chart*. `https://www.engineersedge.com/heat_transfer/convective_heat_transfer_coefficients__13378.htm`.

Ethylene Glycol database (n.d.). `https://www.gsi-net.com/en/publications/gsi-chemical-database/single/276-CAS-107211.html`.

Fowles, Grant R. (1975). *Introduction to modern optics*. 2nd ed. Dover Publications, INC., p. 58.

G.K.Batchelor (1967). *An introduction to fluid dynamics*. Cambridge University Press, pp. 142–148.

Leal, L.G. (1992). *Laminar Flow and Convective Transport Processes. Analysis of Transport Phenomena*. Butterworth-Heinemann, pp. 164, 209.

Persaud, Naraine (2005). "Heat of vaporization: Water Encyclopedia (2005)". In: p. 1.

Popov, Yuri O. (2005). "Evaporative deposition patterns: Spatial dimensions of the deposit". In: *PHYSICAL REVIEW* 71, pp. 036313–4.

Santos, Fernando J. V. et al. (2006). "Standard Reference Data for the Viscosity of Toluene". In: *Journal of Physics and Chemical Reference Data* 35.

Socolofsky, Scott A. and Gerhard H. Jirka (2004). "Advective Diffusion Equation, Lecture Notes". In: *https://ceprofs.civil.tamu.edu/ssocolofsky/cven489/downloads/book/ch2.pdf*.

Sommerfield, Arnold (1908). "Ein Beitrag zur hydrodynamischen Erkläerung der turbulenten Flüssigkeitsbewegüngen (A Contribution to Hydrodynamic Explanation of Turbulent Fluid Motions)". In: *International Congress of Mathematicians* 3, pp. 116–124.

Stokes, G.G. (1851). "On the effect of internal friction of fluids on the motion of pendulums. Analysis of Transport Phenomena". In: *Transactions of the Cambridge Philosophical Society* 9, part ii: 8–106.

Surface tension values of some common test liquids for surface energy analysis (2017). `http://www.surface-tension.de/`.

Toluene database (n.d.). `https://www.gsi-net.com/en/publications/gsi-chemical-database/single/515-toluene.html`. Accessed: 2020-10-02.

ToolBox, Engineering (2003a). *Ethylene Glycol Heat-Transfer Fluid*. `https://www.engineeringtoolbox.com/ethylene-glycol-d_146.html`.

— (2003b). *Fluids-Latent Heat of Evaporation*. `https://www.engineeringtoolbox.com/fluids-evaporation-latent-heat-d_147.html`.

— (2005). *Surface Tension*. `https://www.engineeringtoolbox.com/surface-tension-d_962.html`.

Wedershoven, H. M. J. M. (2017). "Active control of solution deposition processes." PhD thesis. Technische Universiteit Eindhoven, pp. 7–11.

Welty, James R. et al. (2008). *Fundamentals of Momentum, Heat, and Mass Transfer*. 5th ed. John Wiley & Sons, Inc, p. 220.

Yaws, Carl L. (2015). *The Yaws Handbook of Vapor Pressure. Antoine Coefficients*. 2nd ed. Gulf Professional.